STATISTICAL STUDY OF SOUND SPEED IN THE INHOMOGENEOUS UPPER OCEAN

James Richard Fitzgerald

NAVAL POSTGRADUATE SCHOOL
Monterey, California

THESIS

STATISTICAL STUDY OF SOUND SPEED
IN THE INHOMOGENEOUS UPPER OCEAN

by

James Richard Fitzgerald

Thesis Advisor: H. Medwin

December 1972

Approved for public release; distribution unlimited.

Statistical Study of Sound Speed
in the Inhomogeneous Upper Ocean

by

James Richard Fitzgerald
Lieutenant Commander, United States Navy
B.S. B.A., University of Florida, 1962

Submitted in partial fulfillment of the
requirements for the degree of

MASTER OF SCIENCE IN ENGINEERING ACOUSTICS

from the
NAVAL POSTGRADUATE SCHOOL
December 1972

ABSTRACT

The statistics of the fluctuations of the in-situ speed of sound in the upper ocean have been studied by analyzing the instantaneous phase difference of the output of two hydrophones separated by one meter for sounds of frequency 15 to 151 kHz. The experiment was conducted at 11 ft in water of depth 60 ft in low sea states at night. Comparison of the speed calculated from the time averaged phase difference, with the speed given by velocimeter or empirical relations, yielded differential speeds which deviate by 1 m/sec to 8 m/sec from the accepted values, for frequencies less than 100 kHz. Correlation and spectral analysis of the sound phase and ocean height fluctuations has shown the close relation between these two parameters. There is strong evidence of the presence and importance of bubbles in all of the results, particularly of a large population resonant in the frequency range 56.3 to 71.1 kHz (radius 50 to 60 microns). Evidence is presented to suggest that bubbles appear at the surface during internal wave activity at lower depths and that for sound frequencies near the bubble resonances the sound phase is strongly modulated by, and in phase with, the ocean wave height.

TABLE OF CONTENTS

ACKNOWLEDGMENTS

The writer wishes to express his gratitude to Professor Herman Medwin, of the Department of Physics and Chemistry, Naval Postgraduate School, for his guidance and assistance in this research work. Special thanks are also due to Mr. William Smith of NPS for his help in the construction and acquisition of equipment, and Dr. John C. Calhoun, formerly of NPS, for his assistance in computer programs 1, 2 and 3.

The writer also wishes to express thanks to the personnel of the U.S. Navy Undersea Research and Development Center for their support.

This thesis serves also as a technical report to Naval Ships systems Command (Code PMS 302) which provided the major part of the financial support for the facilities, technician, and computer services required for this research.

I. INTRODUCTION

The objective of this research was to measure acoustic phase shifts over a one meter path in order to study the statistics of the variation of sound speed with frequency and time in the upper layer of the ocean.

The sources of the dispersion of sound speed are bubbles of various radii. Motion of these bubbles and of other inhomogenieties cause the temporal fluctuations of phase.

Study of the dispersive behavior is important because in the top tens of meters of the ocean, the speed of sound at military frequencies differs both from the value given by velocimeters (which operate in the megahertz range) and that given by the various accepted empirical formulas. Study of the fluctuations is necessary in order to reveal the oceanographic origins and dependencies of the temporal variations in sonar surface duct propagation.

The bubble problem has been treated theoretically by Meyer and Skudrzyk (1950), Devin (1959) and Albers (1960). The experimental study of wind generated bubbles has been conducted in the laboratory by Glotov (1962) and at sea by Buxcey et al (1965) and Medwin (1970). Most recently Rautmann (1971) measured the magnitude of dispersion and fluctuation of sound speed in the surface layer of the ocean.

Change in the speed of sound with frequency in sea water is attributible in general either to molecular relaxation or bubbles since no other frequency dependent mechanisms

are known to exist at the frequencies of this study. The magnitude of the molecular relaxation can be shown to be negligible as compared to the bubble effects (a frequency shift from 20 to 70 kHz results in a Δc of only approximately 0.3 m/sec).

The research was conducted using the U.S. Naval Undersea Research and Development Center (NUC) Oceanographic Research Tower in Mission Bay, San Diego, as a test platform.

II. INSTRUMENTATION

An aluminum pipe frame of height six feet and length twelve feet was used to mount the transducers and hydrophones (Figure 1). To prevent displacement of the hydrophones, the frame wires were put under tension by spring loaded mounts. To minimize reflections from the frame caused by side-lobes of the transducers, the frame was pulse-echo checked; various segments of the frame were covered with acoustic absorbent rubber (SOAB) so that the echo was down 35 dB below the direct signal.

Opposite to the open end of the frame, at the center, and pointing in the X-direction, an USNRD F33 unidirectional transducer was mounted. On the acoustic axis of this transducer, two Atlantic Research LC-10 hydrophones were placed. The first LC-10 was mounted 82.3 cm from the source and the second was mounted 81.3 cm beyond the first.

The transmitting instrumentation (Figure 2) consisted of a General Radio Coherent Decade Frequency Synthesizer, type 1162-A, generating a stable sinusoidal voltage output of two volts rms and variable in frequency. The signal was amplified by a Hewlett Packard Power Amplifier, 467A, to 18 volts rms and then impressed across the transducer.

The receiving instrumentation (Figure 2) consisted of LC-10 #1 with a flat (-108 dB $\pm$ 2 dB re 1 volt/microbar) receiving response from 15 kHz to 150 kHz, and LC-10 #2 with a flat (-110 dB $\pm$ 3 dB re 1 volt/microbar) receiving response from 15 kHz to 150 kHz. The signals were then amplified 30 dB by an NUS

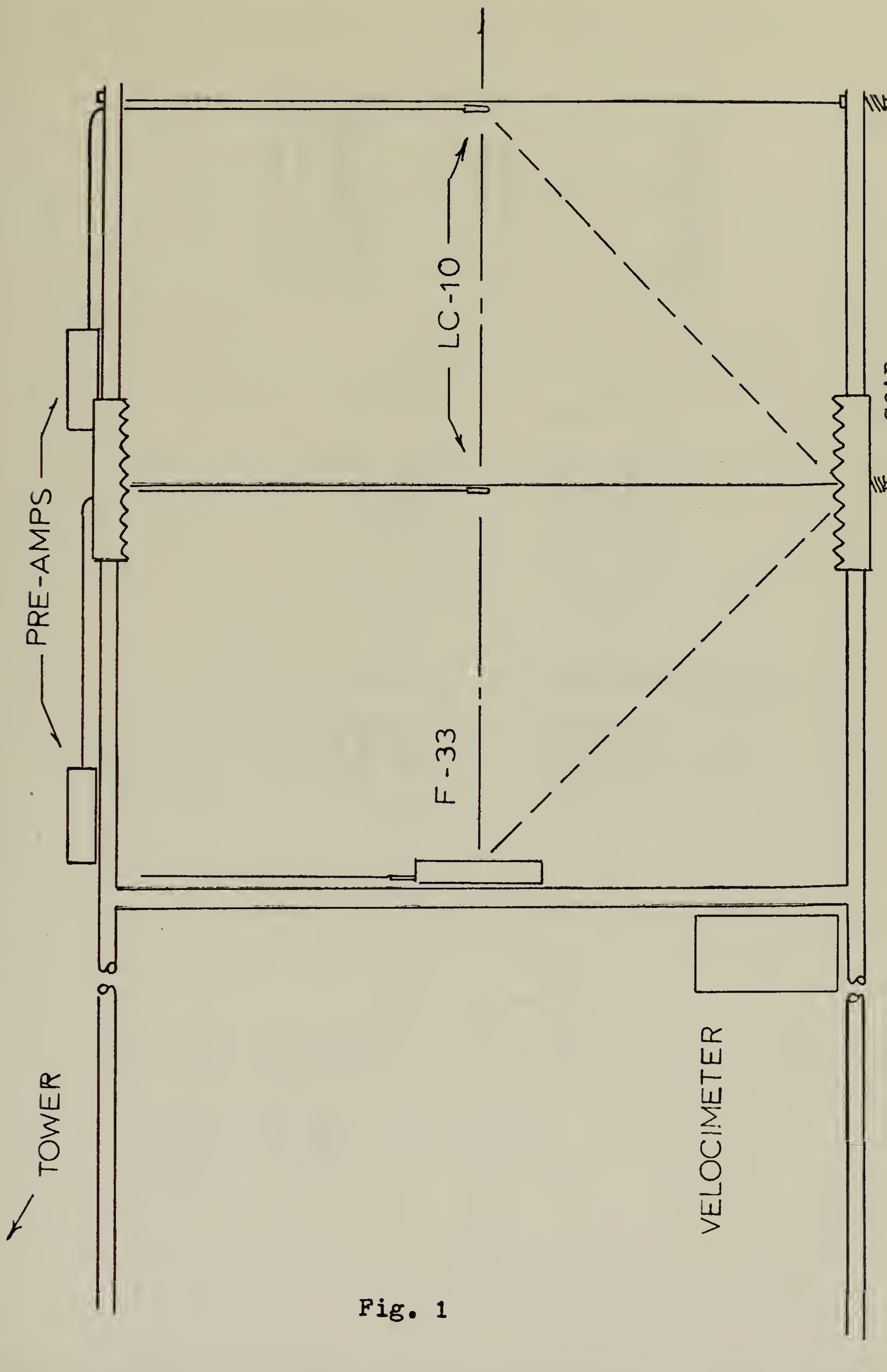

Fig. 1

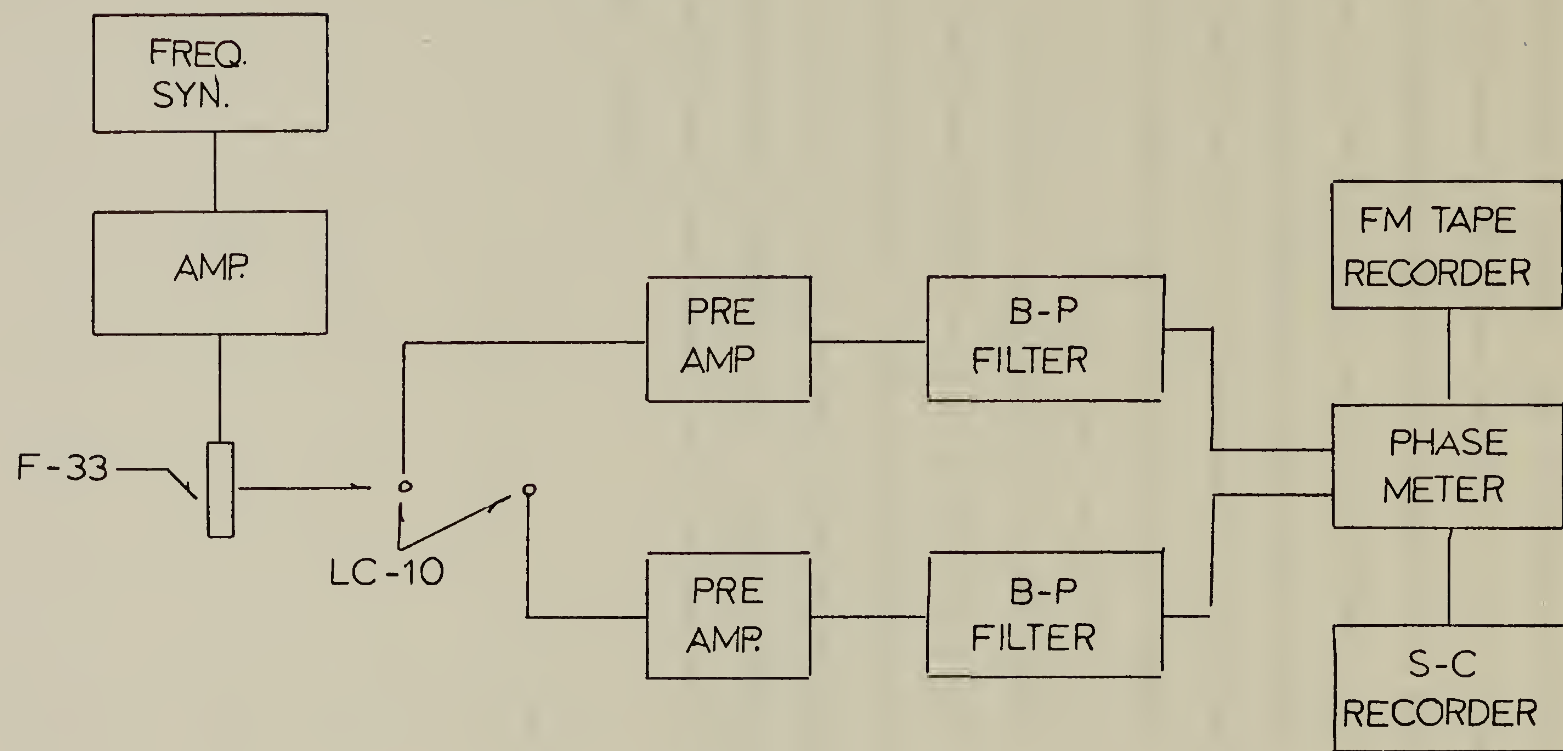
FREQ.
SYN.
AMP.
F-33
LC-10
PRE
AMP
B-P
FILTER
PRE
AMP.
B-P
FILTER
FM TAPE
RECORDER
PHASE
METER
S-C
RECORDER

Fig. 2

pre-amplifier model 2010-030 before passing through 150 feet of waterproof shielded cable. Both signals were then bandpass filtered by a digitally tuned variable Krohn-Hite model 3322 Filter set with the center frequency equal to the transmitted frequency $\pm$ 300 Hz. The filtered signals were then fed into a Dranetz model 305 Phase Meter. The phasemeter measured the phase angle between the two ac voltages at the same frequency and provided a dc voltage output proportional to the difference of the phase angles at 10 mV per degree. The dc voltage was simultaneously FM recorded on a Precision Instrument model 6200, eight track magnetic tape recorder at 3.75 i.p.s. and on a Brush model 220 strip chart recorder, at 10 mV per division and 1 mm per second.

The ocean wave height was measured utilizing the installed NUC Baylor wave height gauge. The wave height gauge was mounted a distance of 6 feet from the acoustic source and at an angle of 60 degrees from the acoustic axis. The dc voltage output was FM recorded with each phase record and simultaneously recorded on the strip chart recorder.

III. OCEANOGRAPHIC COMPONENTS

Field measurements were similtaneously taken to determine the fluctuations of temperature, salinity, water particle velocity and wave height to obtain a better understanding of the acoustic-ocean interaction (theses by CDR J. Gossner, LT M. Whittemore, LT W. Frigge and LT R. Krapole, March 1973).

Unfortunately much of this information is unavailable at this time. However, the time-varying ocean wave height, (NUC Baylor Gauge), the sound velocimeter output, (Ramsey Probe), and temperature (Ramsey Probe) were simultaneously recorded during the phase study. The average value of salinity (33.8 $^{o}/oo$) measured that afternoon was used for the C calulations on the assumption that changes in salinity would have a minimal effect on C.

IV. EXPERIMENTAL SETUP

The frequency of the continuous wave signal applied to the transducer was adjusted by means of the frequency synthesizer until a phase angle of approximately 20 degrees was obtained. This value was selected to prevent the possibility of the phase going negative and changing the integral number of wave lengths between the hydrophones. Since the phase meter compares the signal at input B with respect to the signal at input A, and cannot detect integral numbers of wave lengths difference between the two signals, the displayed phase determines the fractional wave length by which signal B leads signal A. This means an integral number of wave lengths plus a fractional part fits into the separation distance between the two hydrophones. Increasing the frequency will change the phase by 360 degrees or step the integral number of wave lengths by one.

Because it was desired to study the statistics of the speed of sound as a function of frequency over a range most likely to contain resonant bubbles, the frequency range from 15-150 kHz was examined. The 81.3 cm separation between the two hydrophones caused the number of wave lengths within the spacing to be incremented by one approximately every two kHz.

In order to exclude possible errors in the results due to nonstationarity in the medium, it was necessary to examine the total frequency range in as short a period of time as possible. The The frequency range was examined in steps of four kHz, and the

time variable phase difference and wave height were recorded between the hydrophones for four minutes at each frequency.

All the readings were taken within three consecutive hours, from 1900 to 2200 hours on June 5, 1972 at an initial transducer depth of 3.4 meters, and final depth of 2.8 meters. The tide during this period was falling at a rate of 0.5 ft/hr, with low water at approximately 2330.

V. DATA REDUCTION

Thirty-four four minute individual physical records make up the analog recorded sound phase and wave height data. One approach used was to digitize the analog data and use a computer to carry out the statistical and spectral analysis.

The recorded data were digitized using the NPS CDC 5000 and SDS 9300 computers. The initial sampling frequency was 50 Hz giving a Nyquist frequency of 25 Hz. The sampling interval was 0.02 seconds. The 7 track digital tape was then processed to remove spurious signals (Figure 3), scaled, and converted using the IBM 360/67 from 7 track octal to 9 track hexidecimal for use by the IBM 360/67, (computer program 1).

The samples generated, however, by using the 50 Hz sampling rate provided too much data to analyze to the degree of resolution required in any reasonable processing time on the IBM 360. It was then determined to reduce the rate to 6.25 Hz, a sampling interval of 0.16 seconds, and frequency resolution of 0.0244 Hz. This yielded 10 degrees of freedom. This also reduced the amount of each physical record that could be analyzed from 3 minutes 50 seconds to 3 minutes 40 seconds.

A second approach was essential in order to obtain statistics of the average and standard deviation which would be a measure of the microstructure rather than of the microstructure plus the internal wave. To minimize the effect of internal waves each record was analyzed in 30.72 second increments. Each increment

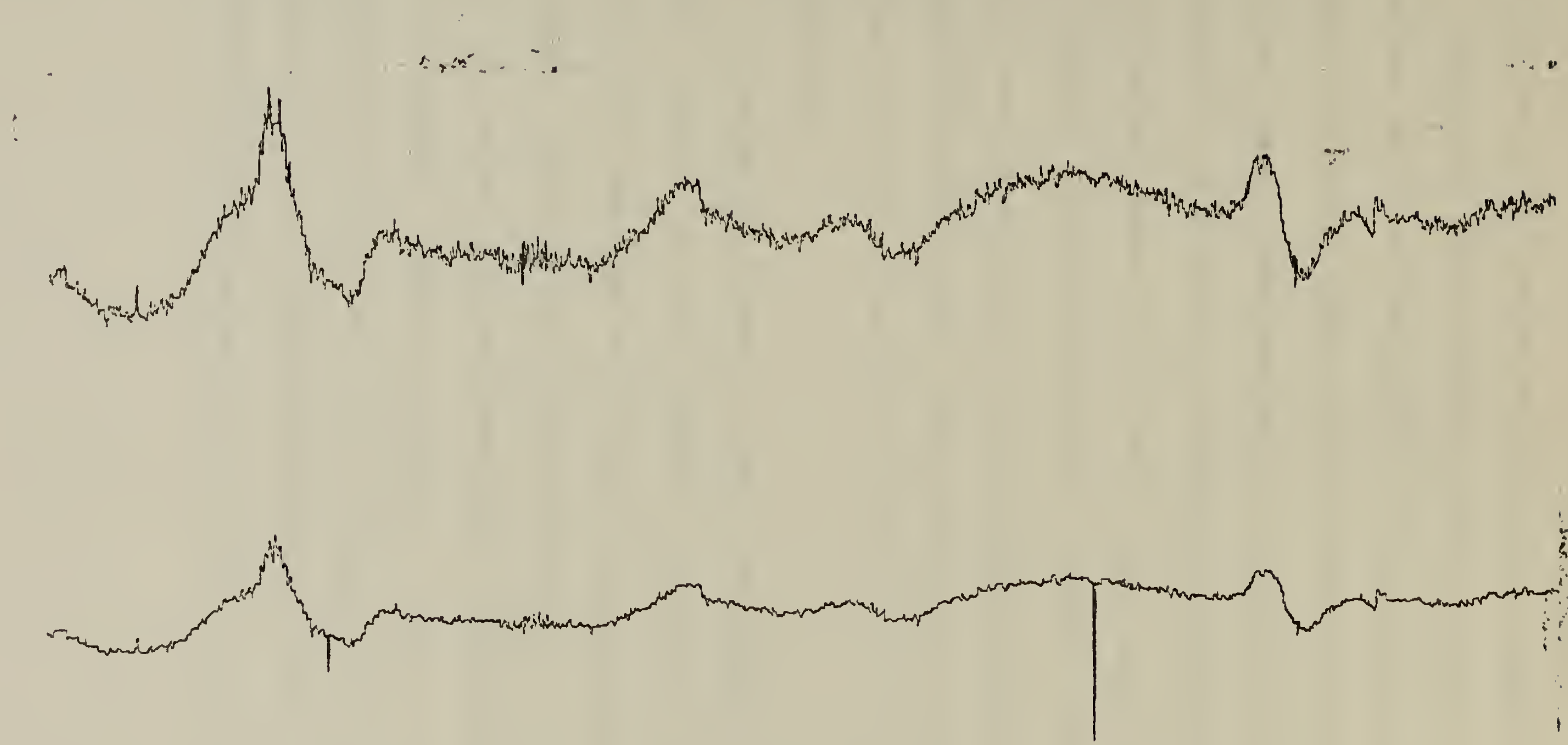

Raw (bottom) and filtered (top) signals (note: Amplitude scales are not equal)

Figure 3

consisted of 1536 samples for which instantaneous values of the velocity of sound were calculated and the means and standard deviation were determined. Similarly the mean value and standard deviation of the phase were computed, (computer program 2).

The speed of the coherent component was also calculated using the mean value of the phase and compared to the mean value of the speed. The point being made is that, if the mean of the entire physical record had been used, the large variance would have been relative to a mean value strongly influenced by the passage of any internal waves and not due to the microstructure of the medium as desired. The mean speed and the mean coherent speed of sound were then compared with the 30 second average values given by a Ramsey Velocimeter and those calculated by empirical formulas using the salinity, depth, and 30 second averages of the temperature.

For selected frequency runs, the temporal autocorrelations and power spectra, in dB re degrees, or dB re cm, of the phase and wave height were computed and plotted using a maximum time lag of 40.96 seconds. The temporal cross-correlation was also computed. From this the cross spectrum, coherence, and cross spectral phase angle were computed, (computer programs 3 and 4). The selected frequencies for which these were calculated were determined by first calculating and plotting the dispersion curve (Figure 4), and then selecting those frequencies of interest from the results.

VI. COMPUTATIONAL METHOD

The computational method for determination of the speed of sound using the phase difference was the same as that used by Rautmann (Dec. 1971) and is included here for information.

Since a continuous wave method was used, the signal received by the first hydrophone can be written as:

$$y_A = a \sin (\omega t)$$

and the signal received by the second hydrophone is:

$$y_B = b \sin (\omega t - kx)$$

where

k = the wave number $= \frac{\omega}{C} = \frac{2\pi f}{C}$

f = the frequency of the applied signal

C = the phase wave velocity

x = the separation between the hydrophones.

Since we compare the two signals with respect to phase by using the digital phase meter we have to find values for which

$$kx = \psi$$

where ψ is the total phase difference between the two signals due to an integral number of wave lengths and a fraction of the wave length. This is written as:

$$kx = (2\pi)n + \phi_r \qquad n = \text{an integer}$$

$$kx = \frac{\omega}{C} x = (2\pi)n + \phi_r \qquad \phi_r \text{ in radians}$$

$$C = \frac{\omega_x}{(2\pi)n + \phi_r} .$$

The final result is:

$$C = \frac{fx}{n + \frac{\emptyset}{360}} \qquad \text{where } \emptyset \text{ is in degrees.}$$

The integer n can be pre-estimated by calculating C from Wilson's equation using the known values of the temperature and salinity.

Therefore the instantaneous speed of sound may be obtained by using the measured frequency separation and whole number of wavelengths at which a residual phase difference is noted.

The value for the speed of sound of the coherent component is defined to be:

$$C_{coh} = \frac{fx}{n + \frac{\langle \emptyset \rangle}{360}} \qquad \text{where } \langle \emptyset \rangle \text{ is the mean value of the phase.}$$

VII. DISPERSION THEORY

The following equation relates bubble size to the speed of of sound and therefore shows the dispersion for a bubble population of unique radius R.

$$C = \left[\frac{1}{C_o} + \frac{3C_o}{2\omega^2} \frac{U(R)dR}{R^2} \frac{\left[\left(\frac{\omega_o}{\omega}\right)^2 - 1\right]}{\left[\left(\frac{\omega_o}{\omega}\right)^2 - 1\right] + \delta^2\left(\frac{\omega_o}{\omega}\right)^2} \right]^{-1}$$

C_o = nondispersive sound speed

ω = sound frequency

$[U(R)dR]$ = fractional air to water volume for the increment between R and R + dR

ω_o = resonant frequency of bubble of radius R

δ = damping constant of bubble of radius R.

A typical dispersion (differential sound speed) curve is shown below. A graph of the variance of C due to a fluctuation of the number of bubbles for a single size bubble as studied by Professor P.C.C. Wang (personal communication) would be M-shaped. In addition, a constant number of bubbles of changing radius (say, due to changing pressure) would create a variance of C which should peak at the mean resonant frequency f_o, as shown by the dashed curve.

A mixed bubble population would have the same equation summed over all of the bubble radii. The various concentrations of bubbles of different resonant frequencies in the ocean would cause combinations of graphs such as shown on the following page. The

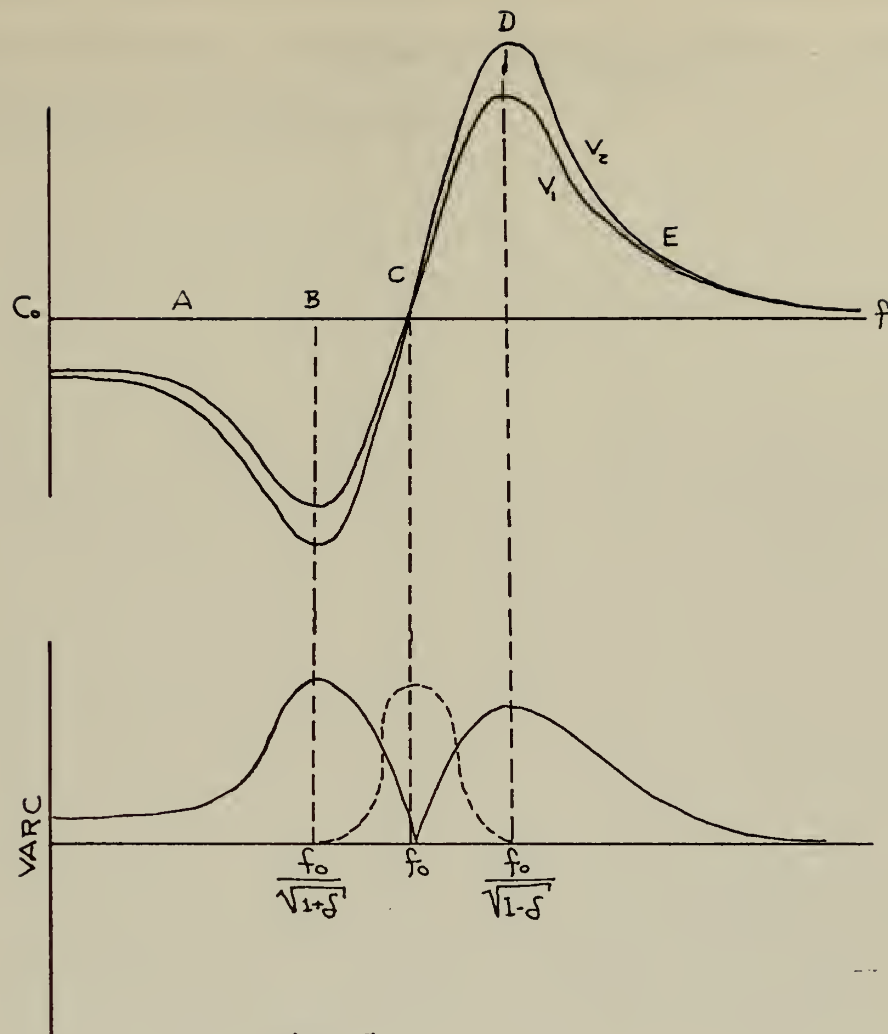

Fig. 5

where f_o = mean resonance frequency of bubble

V_1 = small bubble density

V_2 = large bubble density

δ = damping constant of bubble

Var C = variance of speed of sound due to fluctuation of the number of bubbles

Five distinctive regions of the simple case shown are identified for future use:

Region A: low variance, small negative differential speed

Region B: maximum variance, maximum negative differential speed

Region C: large variance, minimum differential speed

Region D: large variance, maximum positive differential speed

Region E: low variance, small positive differential speed.

differential sound speed and the variance of the sound speed are studied as functions of frequency in order to deduce the bubble concentrations of various sizes.

VIII. EXPERIMENTAL RESULTS

The frequency run was conducted at a depth of 3.4 meters at 1900 decreasing to 2.8 meters by 2200. The run covered a total frequency range of 15 kHz to 151 kHz in steps of approximately 4 kHz.

Continuous direct recordings of temperature and sound velocity were taken throughout the frequency run by a Ramsey Velocimeter. Because of the internal wave presence, Ramsey velocities and temperatures were averaged over 31 second segments for comparison with the speed of sound measured by the phase method in the same interval. During that same interval, calculations of the empirical values of the speed of sound were done using both the generally accepted Wilson's equation [1] and the more recently proposed Leroy's equation [2]. Both methods yielded results within 0.1 m/sec over the range of physical parameters of the experiment (see Table I).

Wilson's equation was used in the following form:

$$\begin{aligned} C = {} & 1449.14000 + 4.57210(T) - 0.04453T^2 - 0.00026T^3 \\ & + 0.00001T^4 + 1.39799(S-35.0) + 0.00169(S-35.0)^2 \\ & + 0.06240 + (S-35.0)(-0.01244T). \end{aligned}$$

Leroy's equation was used in the following form:

$$\begin{aligned} C = {} & 1492.9000 + 3(T-10.0) - 0.00600(T-10.0)^2 - 0.04000 \\ & (T-18.0)^2 + 1.20000(S-35.0) - 0.01000(T-18.0)(S-35.0) \\ & + Z/61.0 + 0.1RHO^2 + 0.00020RHO^2(T-18.0)^2 + 0.10000RHO \\ & (\theta/90.0) + 2.0/(10.0)^7(T)(T-10.0)^4 \end{aligned}$$

where in the equations:

C = speed of sound in meters per second

T = temperature in degrees centigrade

S = salinity in parts per thousand

$D = Z$ = depth in meters

θ = latitude

$RHO = Z/1000.$

The Leroy equation bubble free values were used as the reference for the differential speed of sound curve (Figure 4). The multi-peaked differential sound speed curve suggests several different bubble concentrations of different resonant frequencies. Therefore, the curve was studied and the following frequencies were selected for analysis:

TABLE II: Selected Frequencies

Frequency (kHz)	Reason for Selection
14.79	minimum speed, lowest frequency
18.78	maximum speed, low frequency
26.17	possible zero dispersion frequency
41.32	maximum speed
56.25	possibly near the zero dispersion frequency
63.79	maximum speed
71.13	minimum speed
89.90	minimum speed at higher frequency
112.52	minimum speed at higher frequency
123.72	minimum speed at higher frequency
136.80	minimum speed at higher frequency
146.10	minimum speed at higher frequency

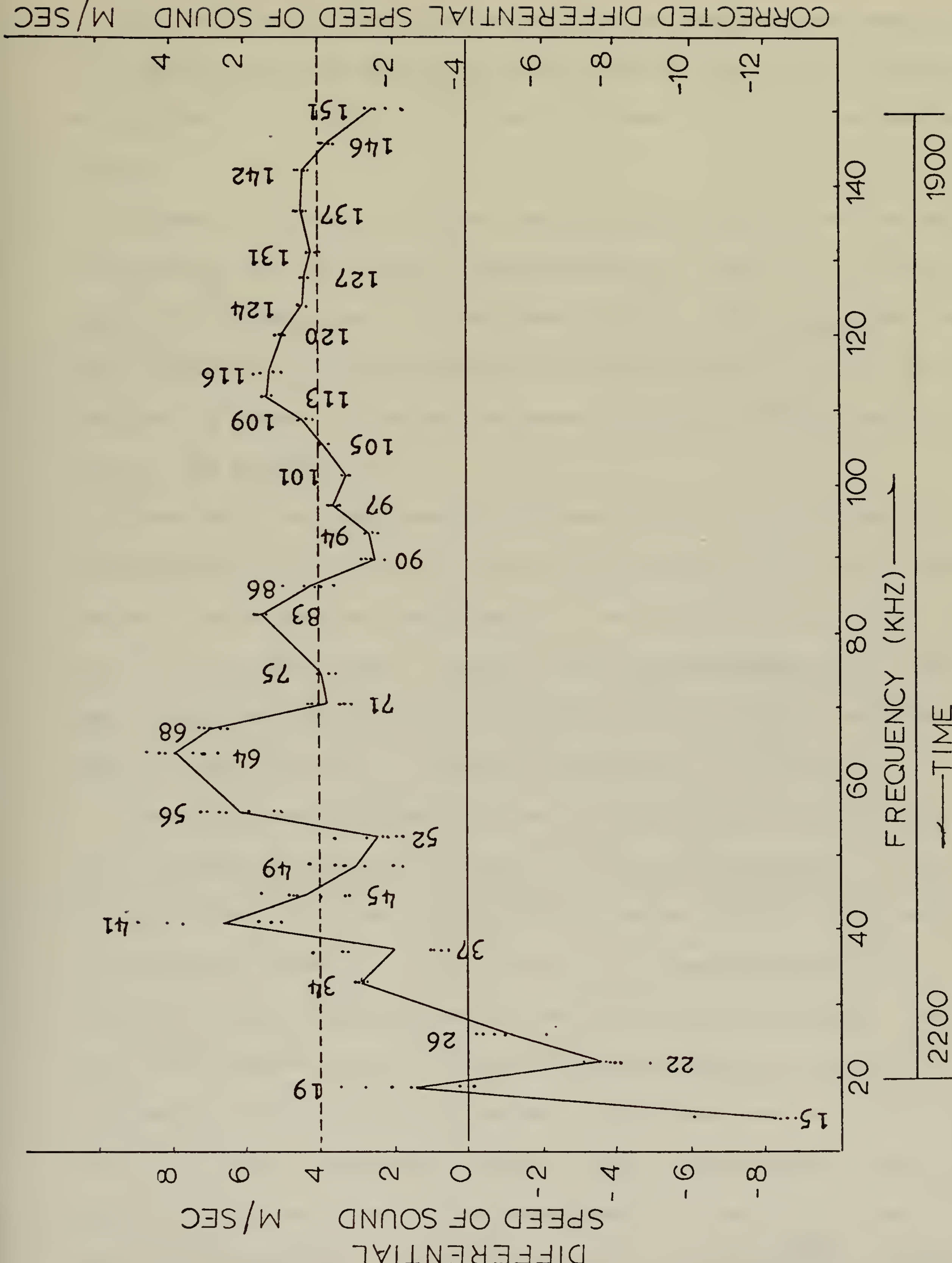
CORRECTED DIFFERENTIAL SPEED OF SOUND M/SEC
DIFFERENTIAL SPEED OF SOUND M/SEC
FREQUENCY (KHZ)
TIME

Fig. 4

A. DIFFERENTIAL SPEED OF SOUND AND VARIANCE OF SOUND SPEED AS A FUNCTION OF FREQUENCY

The variation of the speed of sound with frequency was determined by subtracting the values calculated by Leroy's equation (a function of temperature, salinity, depth and latitude) from the experimental values.

At each frequency a pre-run electrical calibration was conducted to determine the phase error correction due to differential phase shifts in the amplifier and band-pass filters. This correction was then algebraically subtracted from the phase measured during the experiment to obtain the corrected phase difference between the signals at the hydrophones.

There were two other sources of possible corrections that were investigated. The first was motion of the medium, such as an onshore current. In a previous experiment, it was determined that there was no dc flow at this point. However, any correction would have been small and would affect only the absolute values and not the relative values. This correction would be independent of frequency.

The second was measurement error in determining the exact distance between the acoustic centers of the two hydrophones. A measurement error of 2.2 mm would yield a 4 m/sec change in the speed of sound at a frequency of 136.80 kHz. This measurement error would affect only the absolute values of the speed of sound. However, the relative values of the differential speed of sound are of interest, not the absolute values. Therefore this correction is not relevant. The dashed line on Figure 4 illustrates the effect on a 2.2 mm error in the measurement of the distance between the hydrophones. It is believed that this probably is close to the correct absolute value as the speed of sound correction

would be small at high frequency. In theory, the bubble effect becomes negligible as the frequency increases (section VII). As the frequency increases, the speed of sound calculated by the phase method asymptotically approaches the values predicted by the Wilson and Leroy equations. This is also the reason the Ramsey velocimeter values agree with the predicted values. The Ramsey Velocimeter operates in the megahertz range, well above any bubble effects.

The speed of sound values were calculated, and the differential sound speed determined, by subtracting the Leroy's equation values from the phase calculated values.

The values obtained from Leroy's equation were in agreement within $\pm$ 0.1 m/sec of those obtained from Wilson's equation. The Ramsey velocimeter values were within $\pm$ 1 m/sec of both the Leroy and Wilson values. The calculated values from the four methods are included as Table I.

The values are plotted in Figure 4. What are of interest are identifiable bubble concentrations of various size bubbles. The graph is similar to the one presented by Rautmann, based on measurements at the same location in October 21, 1971. Troughs and peaks of speed, presumably bounding a relative zero differential speed and loosely corresponding to the regional identification BCD defined in Figure 5, appear to be present at frequency bands roughly 15-19 kHz, 22-40 kHz, 50-65 kHz, 70-80 kHz, 100-120 kHz. This tenative description will be confronted with other statistical evidence, in sections VIII A and B.

The twelve selected frequencies of Table II. will now be considered in detail:

The frequency 14790 Hz shows a corrected differential sound speed of -12 m/sec. This suggests that this frequency is below the resonant frequency of a large concentration of bubbles. Theory predicts a maximum standard deviation in this frequency range (Region A) caused by bubbles resonant at any higher frequency. The large standard deviation calculated was 1.57 m/sec therefore again suggesting that this frequency is in the range $f < f_o$.

The frequency 18777 Hz shows a corrected differential speed of -2.4 m/sec. If the (-) sign is correct, this would suggest region A of the bulk of bubble population but in region C of a large concentration of resonant bubbles at an f_o less than 18.9 kHz. If this is true, a batch of large bubbles (radius greater than 200 microns has been identified, which could only have come from the bottom, or which perhaps represent biological entities. The large standard deviation of 0.92 m/sec may show that this fluctuation in f_o is indeed taking place.

At 26170 Hz, the corrected differential sound speed is -5.7 m/sec. This may imply region B of a large population of bubbles. The standard deviation is large at 0.84 m/sec.

At 41320 Hz the corrected differential sound speed is +2.6 m/sec. The standard deviation is 0.58 m/sec. This value of the standard deviation implies this frequency is above the resonant frequency of a major bubble concentration.

The 56245 Hz record shows strong evidence of a slowly changing speed of sound, such as for an internal wave. The internal wave inferred from phase information reached a phase trough approximately 40 seconds into the 4 minute record. This resulted in

measured instantaneous phase angles on the order of $\pm$ 13 degrees, at the beginning of the record, to + 25 degrees at the passage of the peak of the wave. During this period, the values of the instantaneous sound speed measured by our phase difference technique decreased 1.7 m/sec while the Ramsey Velocimeter showed no appreciable change. That this is not clearly reflected in Table I is due to the 31 second intervals, chosen in the attempt to eliminate these effects, over which the means and statistics were computed. More will be said about this apparent discrepancy later. The results here seem to indicate evidence of a resonant bubble population. The corrected differential sound speed is + 2 m/sec and the standard deviation is large at 0.55 m/sec. This large value for the standard deviation may mean this frequency is in or near an f_o. As in the 18777 Hz record a small fluctuation in f_o would cause this large σ_c.

The 63790 Hz record has the maximum corrected differential sound speed value of + 3.8 m/sec. The standard deviation is also large, 0.55 m/sec. This may mean that a frequency close to the resonant frequency of a large bubble population.

At 71130 Hz the record shows the largest local value in the standard deviation of the speed, 0.71 m/sec, (Figure 6). If the variance is due to change of number of bubbles it would represent a peak in the standard deviation at $f_o\sqrt{1+\delta}$ or $f_o\sqrt{1-\delta}$. However, if near a concentration of resonant bubbles, whose frequency is changing in Region C, the fluctuations of the surface wave and upper ocean particle velocity may also cause a large variance. It remains then to investigate the correlation functions to interpret

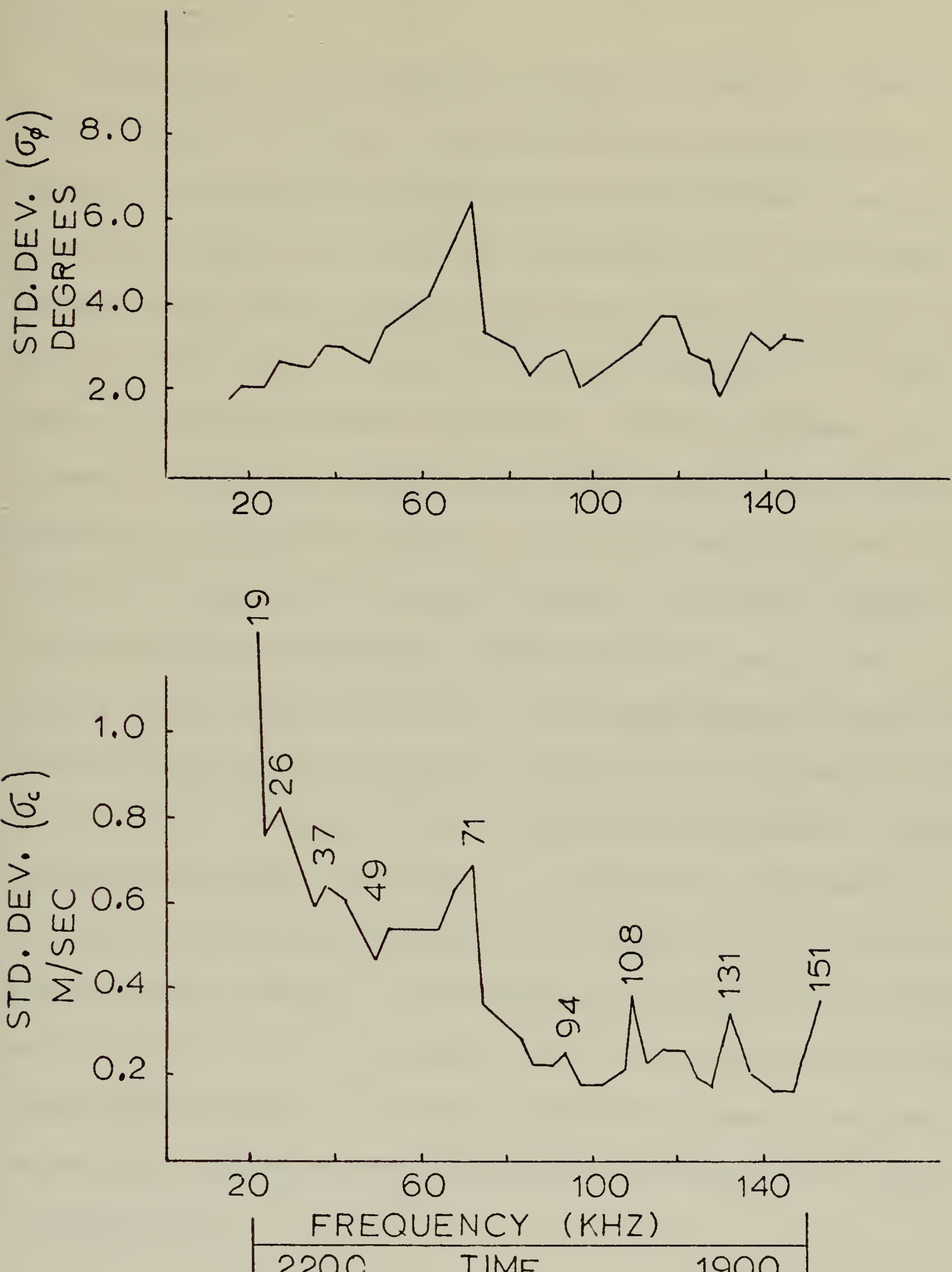

STD. DEV. (σ_ϕ)
DEGREES
8.0
6.0
4.0
2.0
20
60
100
140
STD. DEV. (σ_c)
M/SEC
1.0
0.8
0.6
0.4
0.2
19
26
37
49
71
94
108
131
151
20
60
100
140
FREQUENCY (KHZ)
2200
TIME
1900

Fig. 6

this record. In any event, since $\delta \approx 0.1$, the peak standard deviation at a frequency is within 5% of the resonance of a large bubble population.

At 89900 Hz, the corrected differential speed of sound is down to -1.4 m/sec and a small standard deviation of 0.28 m/sec. This suggests a resonance above 89.9 kHz. The remaining records at 112519 Hz, 123720 Hz, 136800 Hz, and 146100 Hz all have small standard deviations and small corrected differential sound speed values. This would indicate that these frequencies are above the region of any major bubble populations. As the frequency increases, in theory, the sound speed should approach the empirically predicted or velocimeter values. That the speeds are now reasonably constant in the frequency region 130-150 kHz suggests that the sound speed is approaching this asymptote, perhaps with a small error in the 4 m/sec correction. This suggestion, in the case of the sound speed, is supported by the now slowly increasing value of the variance of the phase as the frequency increases from approximately 100 kHz to 150 kHz. An increase proportional to f^2 is predicted by Chernov (equation 141, page 75, Ref. 5), for a medium without bubbles. At frequencies above 100 kHz, it appears that movement of the sea surface has little effect on the sound phase except insofar as the wave induced well correlated particle velocities underwater move temperature inhomogeneities through the sound path.

B. OTHER STATISTICAL ANALYSES

1. Probability Density Functions

Computer program 2 was used to compute the instantaneous values of the speed of sound and to form histograms for each of the 30.72 second intervals. This allowed interpretation of the speed of sound distribution functions. The predominant pattern of the envelopes followed a Gaussian distribution for the lower of the frequencies. This was expected because in the measurements many weak fluctuations in temperature and salinity would cause small random fluctuation.

In studying the distributions of the selected frequencies, a change is observed at frequencies where the probability of resonant bubble populations were noted. At 14790 Hz the distribution is well defined and sharply Gaussian. At 18777 Hz, 26170 Hz, and 41130 Hz, the shape is still that of a Gaussian distribution but now flatter with wider skirts.

At 56145 Hz, the frequency where clear effects of bubbles were noted, the PDF begins to change the shape of its envelope. The envelope now shows two peaks in the distribution of velocities. Because of the presence of the internal wave it is difficult to determine whether this is predominantly due to the wave effects or the proximity of the resonant bubble population.

The envelope at 63790 Hz also shows this double peaked behavior. This may again be due to the sound frequency being in the proximity of the resonance frequency of a major population of bubbles. The passage of these bubbles back and forth through the acoustic path and their size modulation due to the changes in the

hydrostatic pressure as the wave passes over are suggested as the cause of the non-Gaussian PDF. The PDF's at 71130 Hz also display this same behavior.

The PDF behavior above these frequencies is not clear. At 89900 Hz a double peaked envelope appears in 4 of the 7 segments analyzed. At 112519 Hz the distribution again appears Gaussian. In the remaining 3 records studied, the envelope was not consistant, one segment of a record being Gaussian and the next double peaked. It is less likely that bubbles are important here, which suggests that the velocity distributions at higher sound frequencies are the result of influence by internal waves. Because of the relatively diffuse nature of the data from the 84 PDF graphs, they have not been reproduced here.

2. Correlation Analysis

The temporal autocorrelation function is the normalized temporal autocovariance function, normalized by dividing the autocovariance function by the variance, its maximum value at $\tau = 0$. The temporal autocorrelation function is then:

$$R(\tau) = \frac{\langle x(t)x(t+\tau)\rangle}{\sigma_x^2} .$$

The plots of the autocorrelation functions of the phase and wave height are included as Figures 7 - 18.

Similiarly the temporal crosscorrelation function is the normalized temporal crosscovariance function, normalized by dividing the crosscovariance function by the square root of the product of the maximum values of the two signals. The temporal crosscorrelation function is then:

$$R_c(\tau) = \frac{\langle x(t)y(t+\tau)\rangle}{[\sigma_x^2\ \sigma_y^2]^{\frac{1}{2}}}$$

The plots of the crosscorrelation function of the phase with the wave height are included as Figures 19 - 30.

At 14790 Hz (Figure 7) the phase and wave height remain correlated only for approximately the first 3 seconds. The cross-correlation (Figure 19) of the phase with the wave height has a peak to trough value of 0.45, and is good over only a time of approximately 25 seconds. The periodicity of the crosscorrelation, approximately 16 seconds, corresponds to a surface swell and therefore a particle motion through the sound field. The cross-correlation does not peak at $\tau = 0$, which suggests that there is a time lag between those two effects. This time lag could identify transport of bubbles into and out of the sound path and represent the time difference between peak wave height at the wave height probe 6 ft away and the maximum particle velocity of the sound path.

At 18777 Hz (Figure 8) the phase and wave height remain relatively in step. The crosscorrelation (Figure 20) is good for approximately 16 seconds and has a peak to trough value of 0.4. This again suggests a resonant bubble population as implied in the previous discussion of this frequency in Section VIII A.

The 26170 Hz (Figure 9) correlation functions show a phase periodicity on the order of 12 seconds, while the surface wave height periodicity was again 16 seconds. The crosscorrelation (Figure 21) function is not a maximum at $\tau = 0$ but has a high peak to trough value of approximately 0.6.

The 41320 Hz (Figure 10) correlation functions of the phase and wave height are uncorrelated indicating that this

frequency was not at a resonant frequency of a bubble population. The crosscorrelation (Figure 22) has a peak to trough value of only 0.16. There is evidence of good crosscorrelation with an internal wave of periodicity perhaps 200 seconds.

At 56245 Hz (Figure 11) the correlation functions are in step for a time lag up to approximately 28 seconds. Note the peak of crosscorrelation at zero time lag. The crosscorrelation (Figure 23) function has a peak to trough value of 0.6 at the swell average periodicity and also shows the effect of an internal wave. This is strong evidence of a resonant bubble population superimposed on internal wave effects. It was observed previously that the Ramsey Velocimeter showed no evidence of an internal wave at this time. In fact, the phase measurement is so close to the surface, and in the mixed layer, that large temperature changes are not expected. The contradiction can be resolved if it is speculated that bubbles of resonant frequency 56245 Hz were generated in step with the internal wave activity in the thermocline.

The 63790 Hz (Figure 12) record shows a region of bubble concentration is near. The peaks of the phase correlation are mostly in step with the wave height; only the magnitude here differs. However, the phase correlation is not as narrow banded as the wave height and shows some evidence of an internal wave. The wave height displays the same narrow band and magnitude as the previous records. The peak to trough crosscorrelation (Figure 24) value occurs at zero time lag and has now increased to 0.8, the second largest value of the experiment. The double peak in the phase record near 30 seconds shows up here as in the 41320 Hz

functions, and is apparently a component of the sea surface height spectrum. This is verified by observation of the spectrum (Figure 37).

At 71130 Hz (Figure 13) it is found that the temporal correlations of the phase and wave height are of equal narrow band and have the same values at the same lag times. The cross-correlation function (Figure 25) has a peak to trough value of 1 and is in step at $\tau = 0$. This is the strongest evidence that the sound phase is changing in step with the ocean hydrostatic pressure. If the analysis is correct, this means that the phase is increasing and decreasing as the wave height increases and decreases. That is to say, this frequency is at the resonant frequency of a major population of bubbles and the speed is moving up and down the steep portion of the slope of the dispersion curve (Region C) for these prominent bubbles at this frequency.

The correlation functions at 89900 Hz (Figure 14) show that the phase at this frequency is poorly correlated with the wave height. The crosscorrelation function (Figure 26) shows almost no correlation with wave height. There is some evidence of long period correlation with an internal wave. This means that the sound phase is almost undisturbed by the surface wave or the orbital particle motion. This implies this frequency is not near any major resonant bubble population frequencies. Note also the sound phase and surface wave height are no longer in step $\tau = 0$.

The wave height temporal correlation function at 112519 Hz (Figure 15) is particularly simple and that of a narrow band swell. This is a good example of a simple damped cosine auto-correlation function. The phase correlation is poor but shows small peaks

at 7, 12, 19, 28, 32, and possibly 40 seconds. The cross-correlation function (Figure 27) shows very weak correlation between sound phase and wave height. The peak correlation does not occur at $\tau = 0$.

At 123720 Hz (Figure 16) the phase remains correlated with itself longer than the wave height and shows some contribution due to the wave height periodicity at 16 seconds. Additional phase correlation peaks show up at 26 and again possibly 40 seconds. The crosscorrelation (Figure 28) has a relatively strong correlation for approximately 25 seconds. The peak to trough value is 0.65 but it now shows a full 180 degree phase shift between sound phase and wave height. This means that instead of phase increasing with wave height, it decreases. This is interpreted to mean Region E for all bubbles, that is, there are no significant bubbles resonant above this frequency.

In the remaining two records, 136800 Hz (Figure 17) and 146100 Hz, (Figure 18) which were studied for the higher frequency effects, the phase again remains correlated with itself longer than the wave height, that is, it is relatively uninfluenced by wave height. The crosscorrelation has a weak peak to trough value of approximately 0.3. This means again that the phase is relatively undisturbed by the surface waves or that the sound speed is undisturbed by the particle motion. The 136800 Hz phase correlation shows small peaks at 12 and 18 seconds. The 146100 Hz phase correlation shows small peaks at 10 and again at 18 seconds of lag.

The peak-to-trough range of crosscorrelation values (Figures 29, 30) at the swell frequency, constitutes an important

parameter showing the ability of the sound phase to follow the surface wave height (or orbital particle velocity). A curve of this variation with frequency is shown in Figure 31.

3. <u>Spectral Analysis</u>

The power auto-spectral density of the phase and wave height records gives the distribution, in the frequency domain, of average power of the fluctuations vs. frequency. The method used was to compute the autocovariance function and take an FFT and applying a Hamming window. This was done using computer program (3) and yielded plots of phase angle squared and wave height squared vs. frequency in Hz. The frequency resolution is 0.024 Hz. To improve the pictoral representation in amplitude, 10 $\log_{10}$ of the ordinate values was taken so that the power spectrum is a power spectrum level[1] in dB re 1 cm^2.

For all records of the wave height, there is a distinct peak at 0.06 Hz due to the observed ocean swell component, and some smaller peaks up to 0.4 Hz. The peaks up to approximately 0.4 Hz could be due to a smaller wind generated wave superimposed on the larger swell component. The constancy of the spectral characteristics below 0.4 Hz, implies that over the 3 hour duration of the experiment, the ocean was not changing significantly. However, the higher frequencies (above 0.4 Hz) with relatively constant levels are apparently some form of generated noise.

---

[1] An error appears to have slipped into the ordinate of Figures 36, 40, 41, 42. The wave height power levels can be corrected by subtracting 26 dB from these ordinates. The visually observed rms wave height of approximately 2 ft, agrees with this correction.

The phase spectral records are not as consistent as the wave height records. The surface wave component contribution at 0.06 Hz is readily identifiable in all except the 41.3 kHz record. Beyond that, any consistency is not so clear. The phase plots are in relative dB only.

The peak at 0.4 that was observed in all the wave height spectrums was only observed in the lower three frequency phase records analyzed. The 0.4 Hz peak was again probably a surface wave component. In the vicinity of bubble population effects, this frequency could not be identified.

The coherence and cross spectral phase angle is computed (computer program 4) by taking the Fourier Transform of the cross-covariance function and finding the cross-spectral density using a Parzen lag window. This yields a real part; the co-spectrum, and an imaginary part; the quad-spectrum. The magnitude is then the square root of the sum of the squares of the co and quad-spectra. The square of the magnitude is then divided by the product of the individual spectral densities to yield the coherence function. The values so obtained range from -1 to +1. The cross spectral phase angle is found by taking the arctangent of the quotient of the quad-spectrum with the co-spectrum. The maximum values are then $\pm$ 180 degrees. Interpretation of these functions is such that for a high coherence value, a value of the relative phase lead, or lag between the two signals, can be obtained.

An overview shows, that at frequencies above and below the three frequencies studied where a strong possibility of a resonant bubble population existed, the phase and coherence

functions appeared much more confused. In all records, the signals are in phase at low frequencies. For all the maximum phase shifts and zero crossings, the coherence values are very low.

At the bubble frequencies of 56.2, 63.8, and 71.1 kHz, the coherence values are around 0.6 to 0.8 and the two signals are in phase within 30 degrees in the vicinity of the surface wave height frequency. This again underscores the affect of the sea surface wave height at these frequencies.

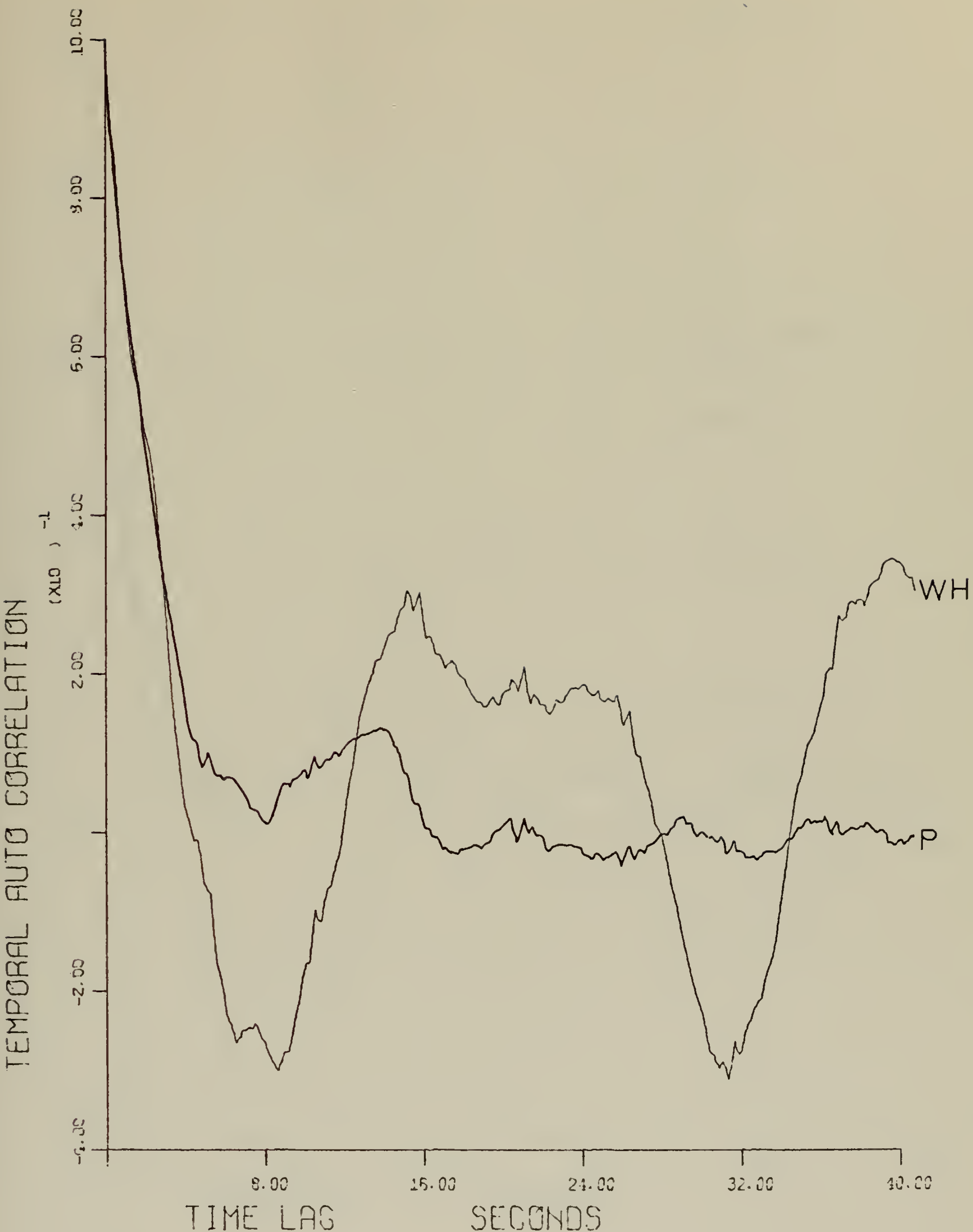

WAVE HEIGHT AND PHASE
FREQUENCY = 14790

Fig. 7

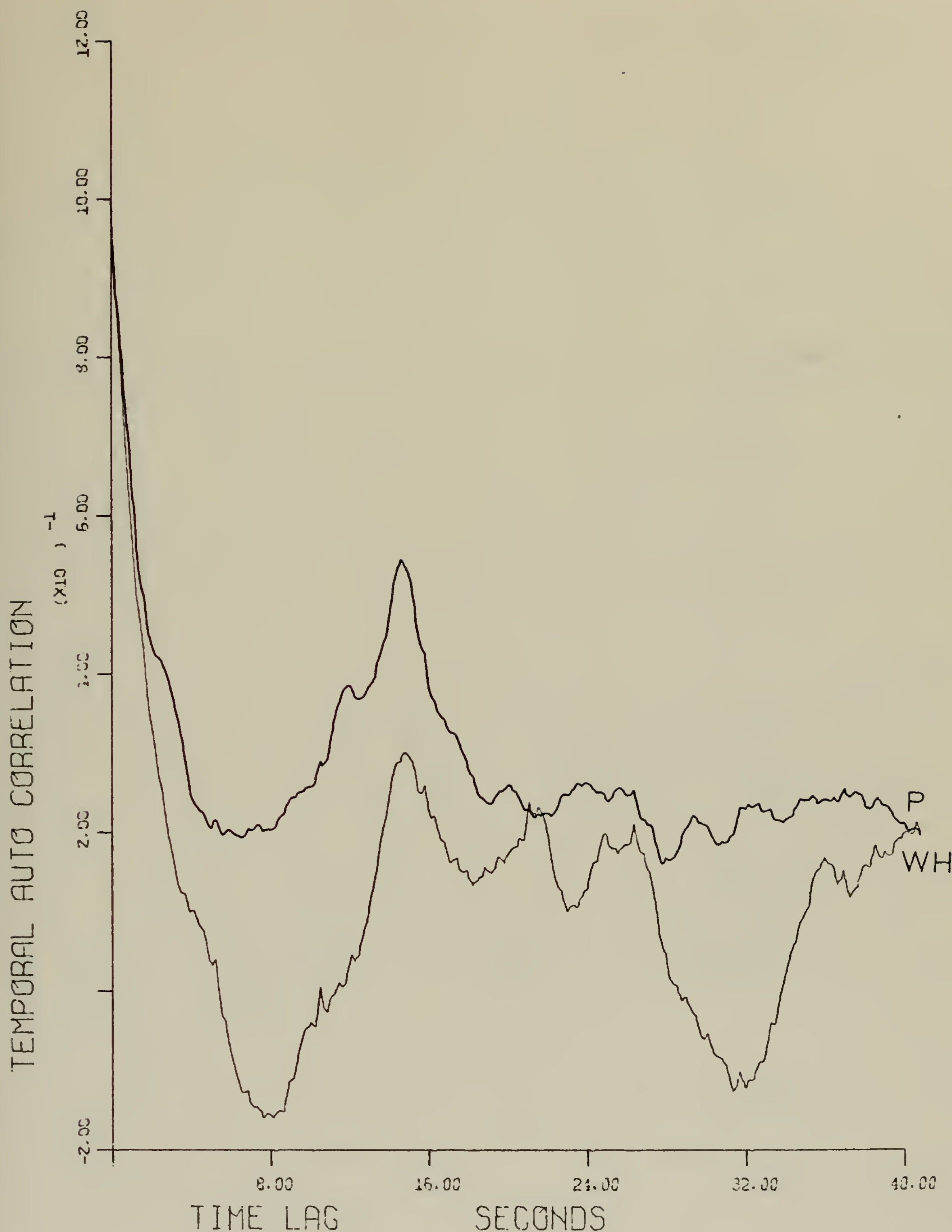

WAVE HEIGHT AND PHASE
FREQUENCY = 18777

Fig. 8

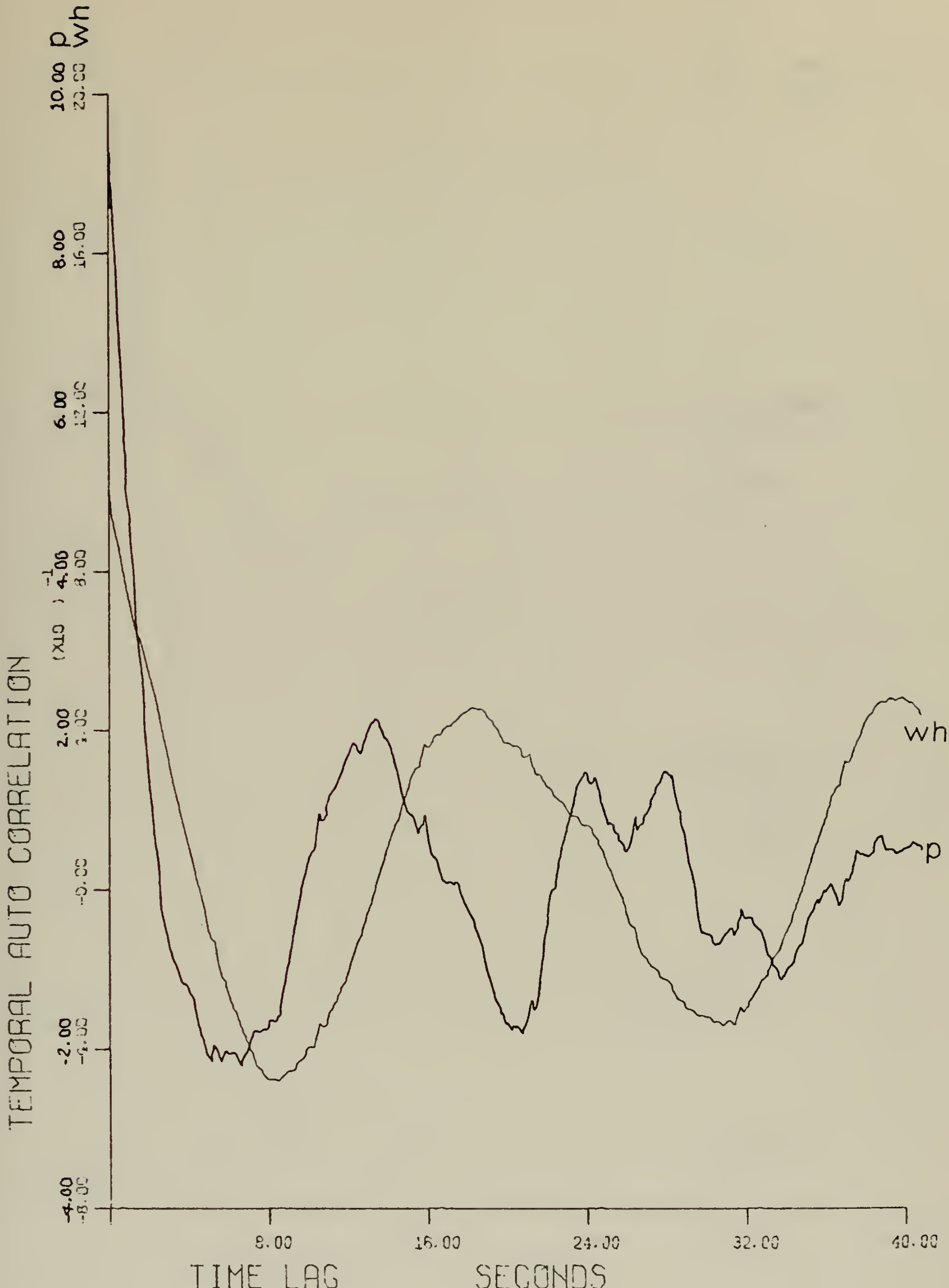

WAVE HEIGHT AND PHASE
FREQUENCY = 26170

Fig. 9

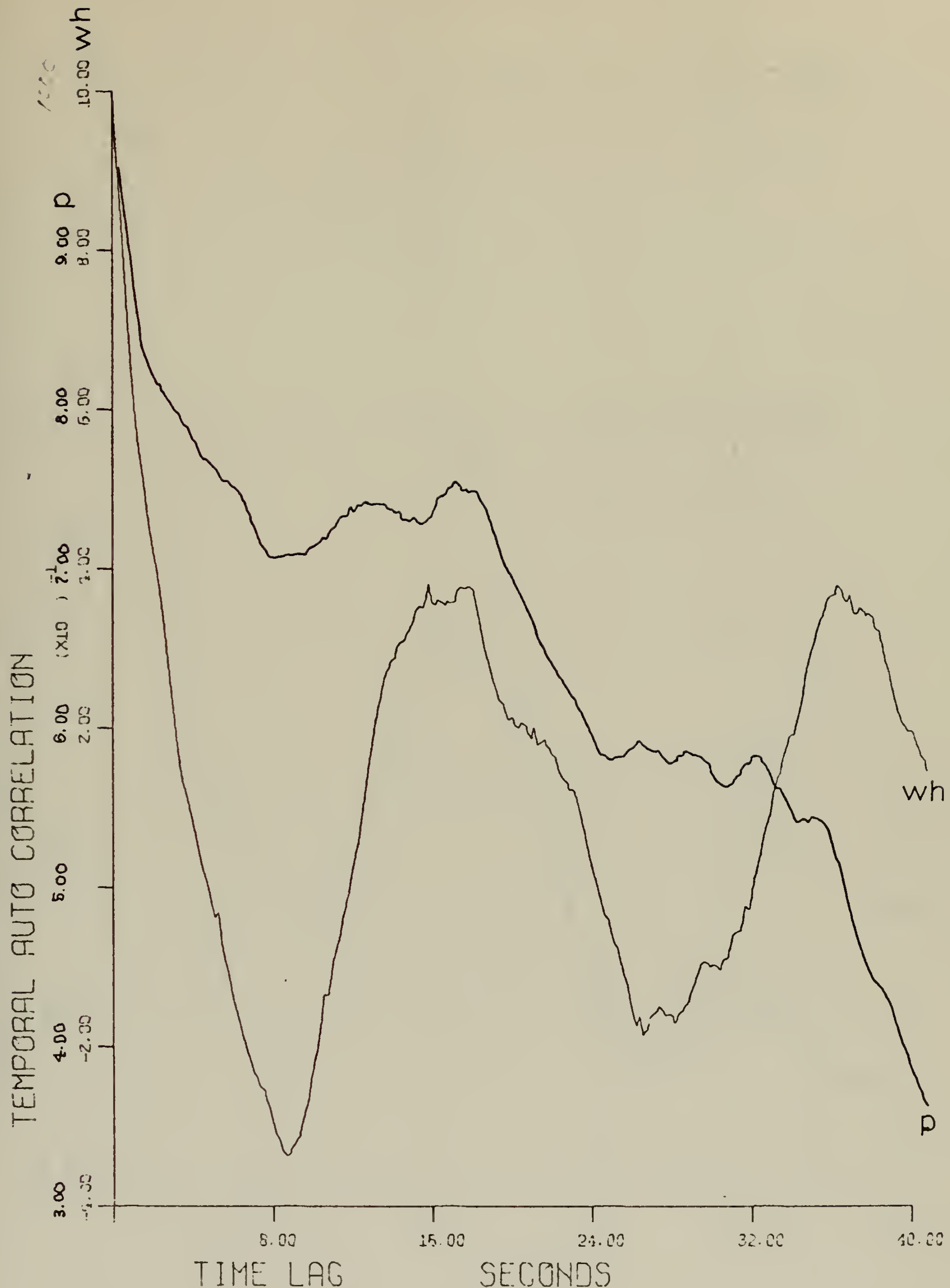

WAVE HEIGHT AND PHASE
FREQUENCY = 41320

Fig. 10

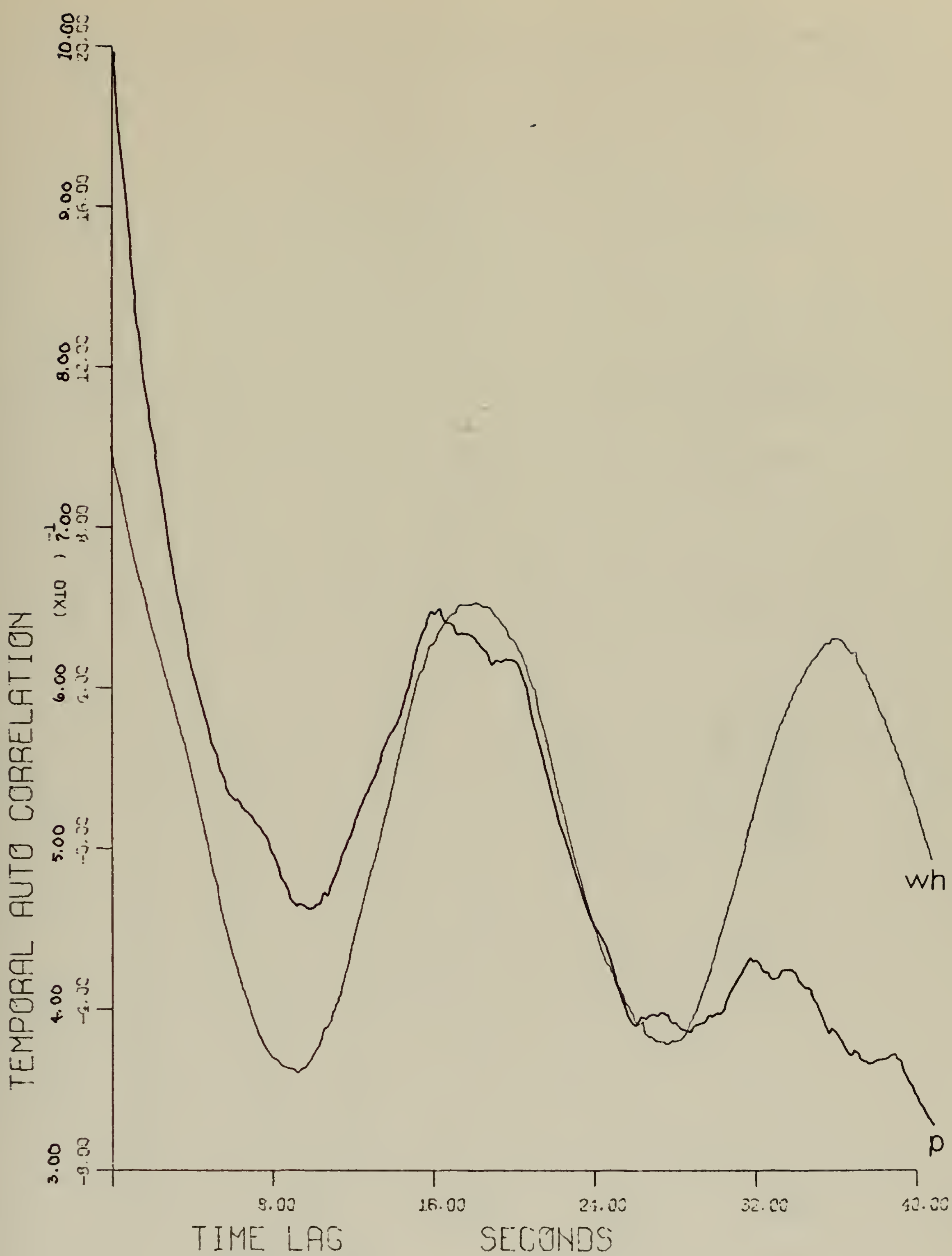

WAVE HEIGHT AND PHASE
FREQUENCY = 56245

Fig. 11

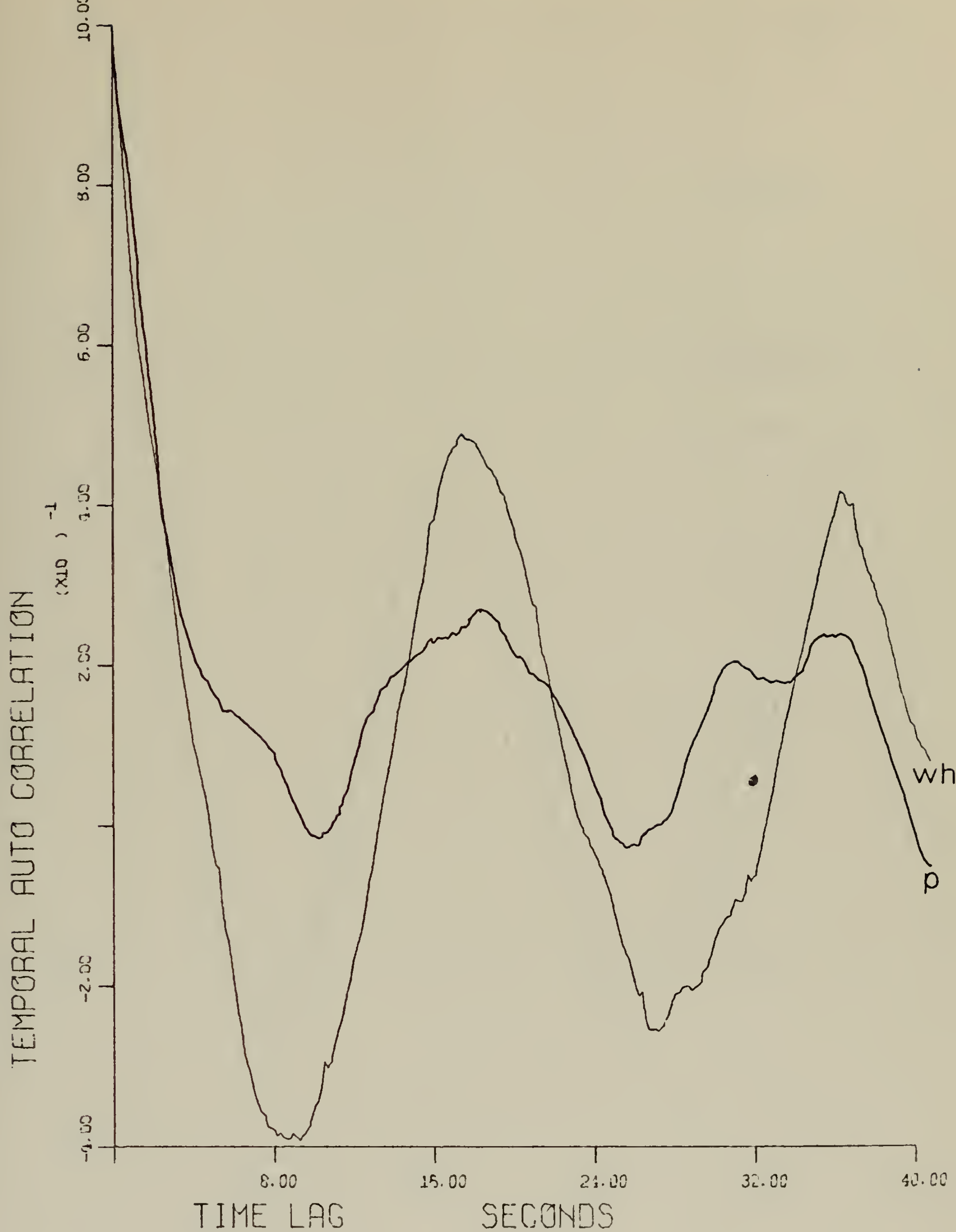

WAVE HEIGHT AND PHASE
FREQUENCY = 63790

Fig. 12

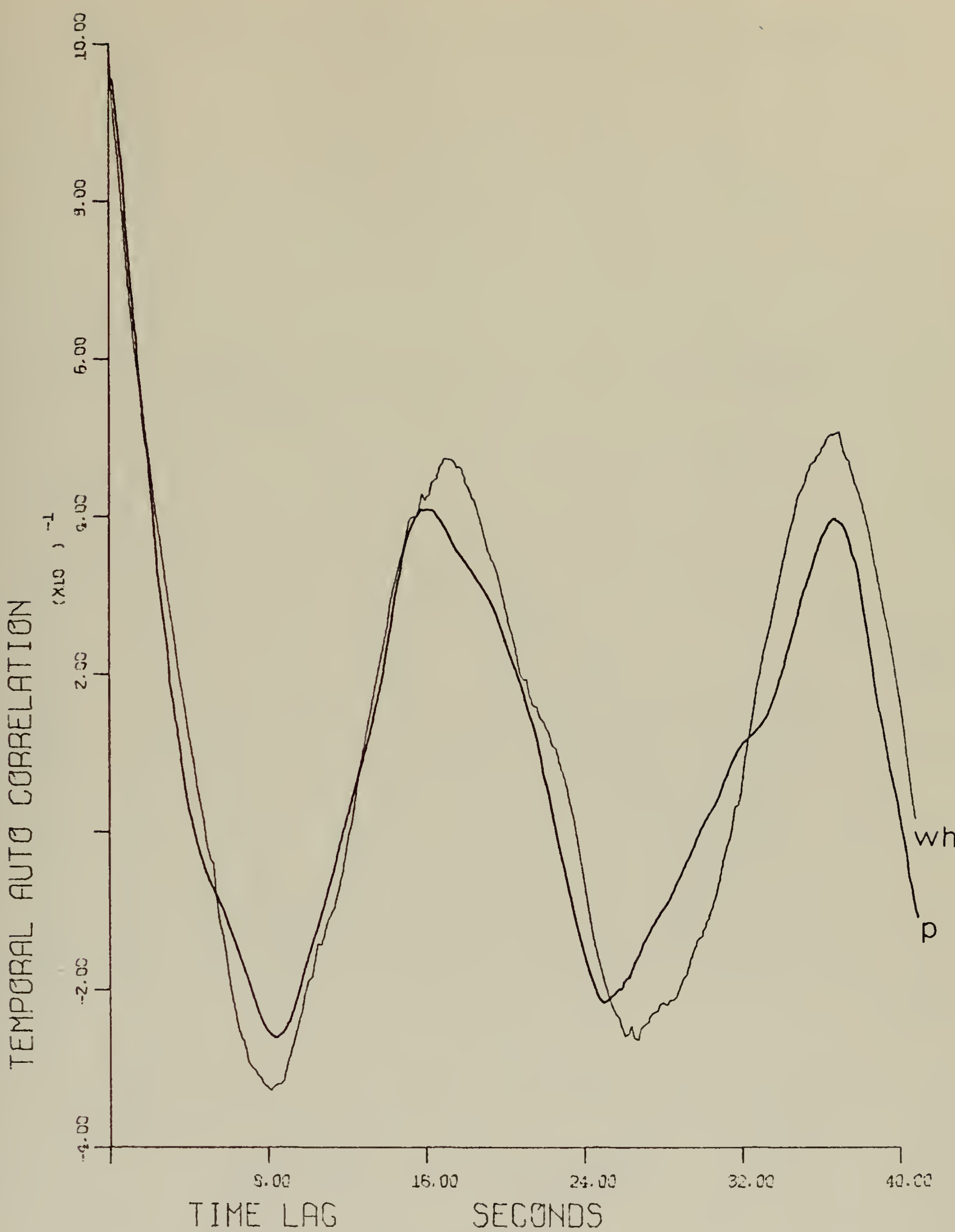

WAVE HEIGHT AND PHASE
FREQUENCY = 71130

Fig. 13

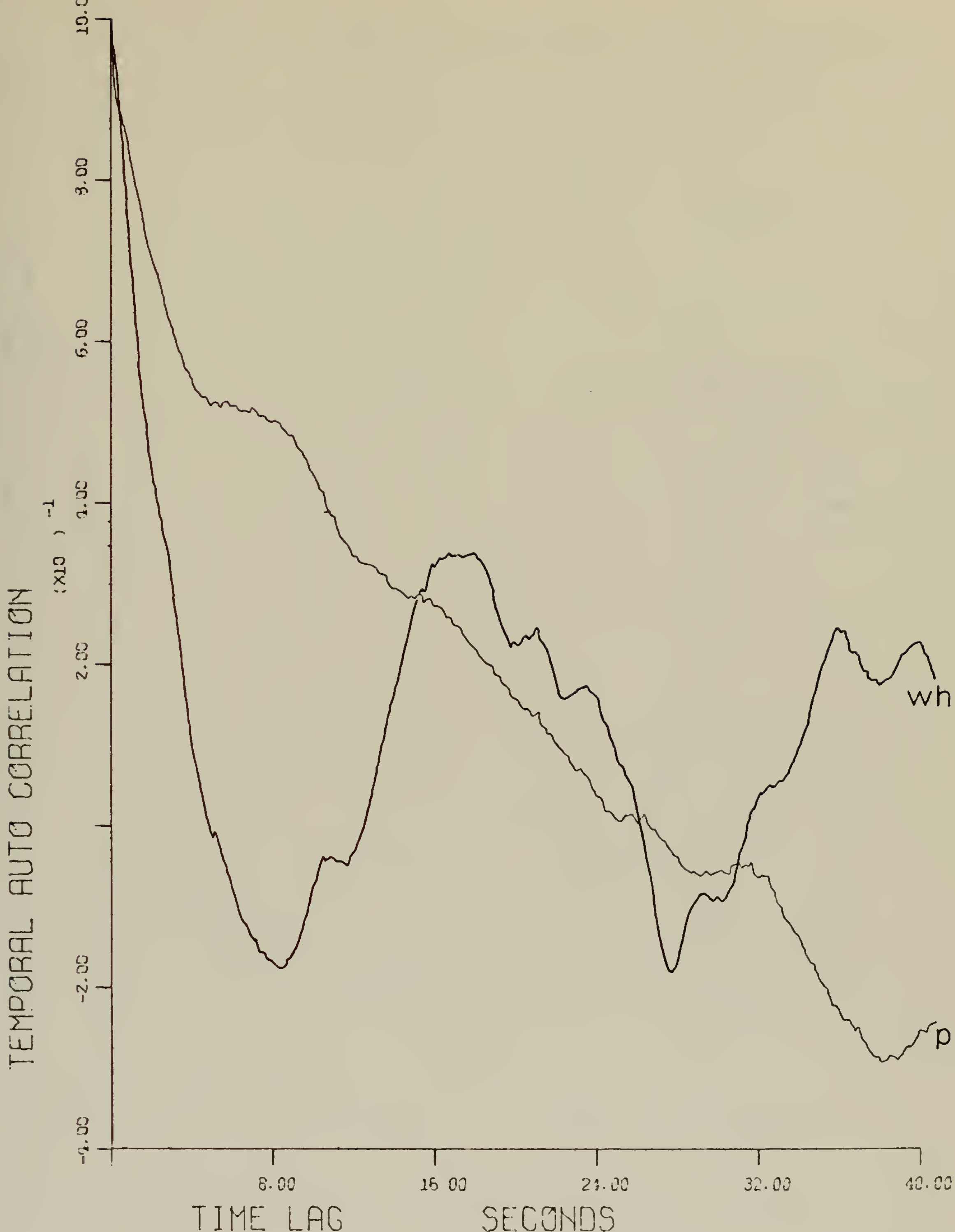

PHASE AND WAVE HEIGHT
FREQUENCY = 89900

Fig. 14

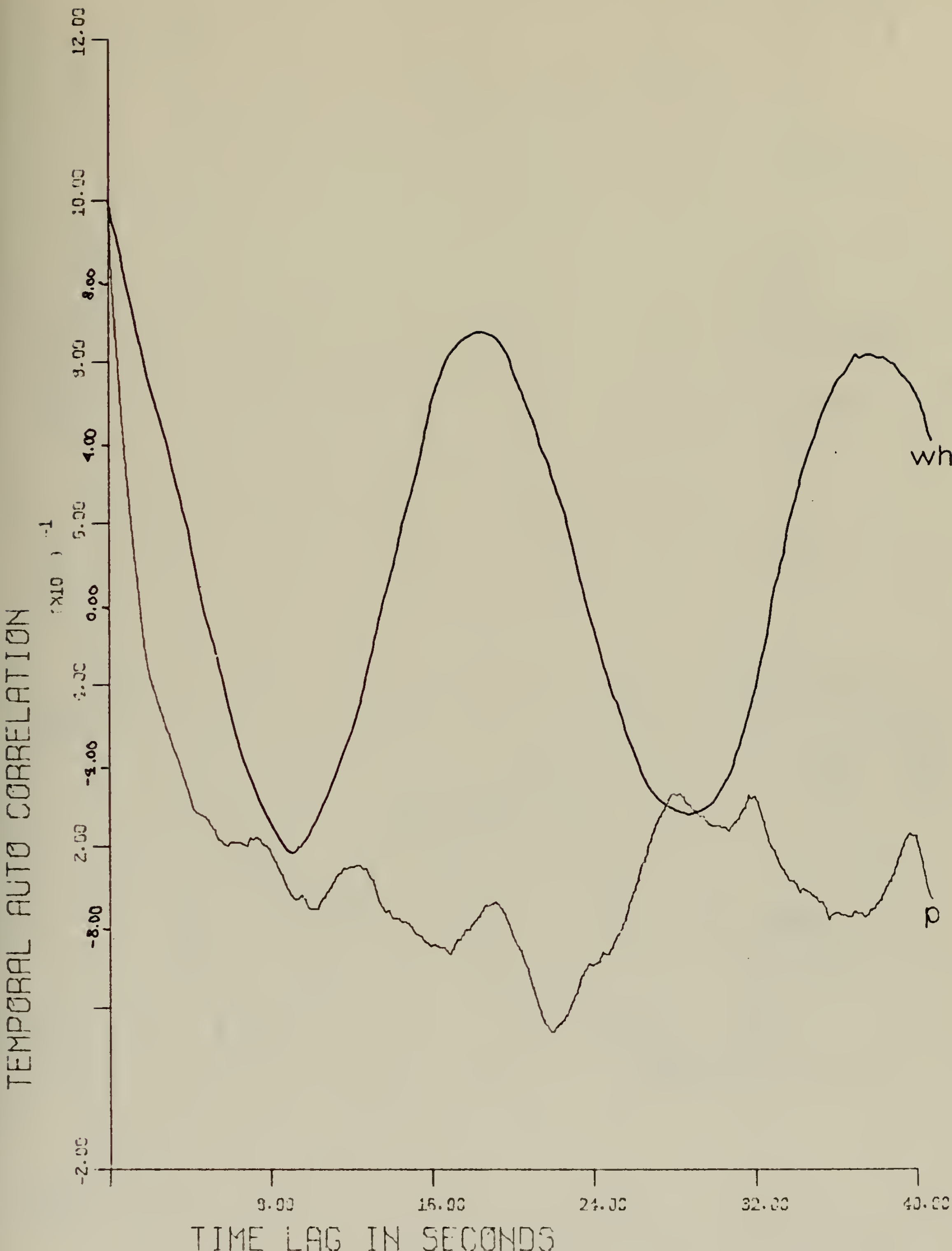

PHASE AND WAVE HEIGHT
FREQUENCY = 112519

Fig. 15

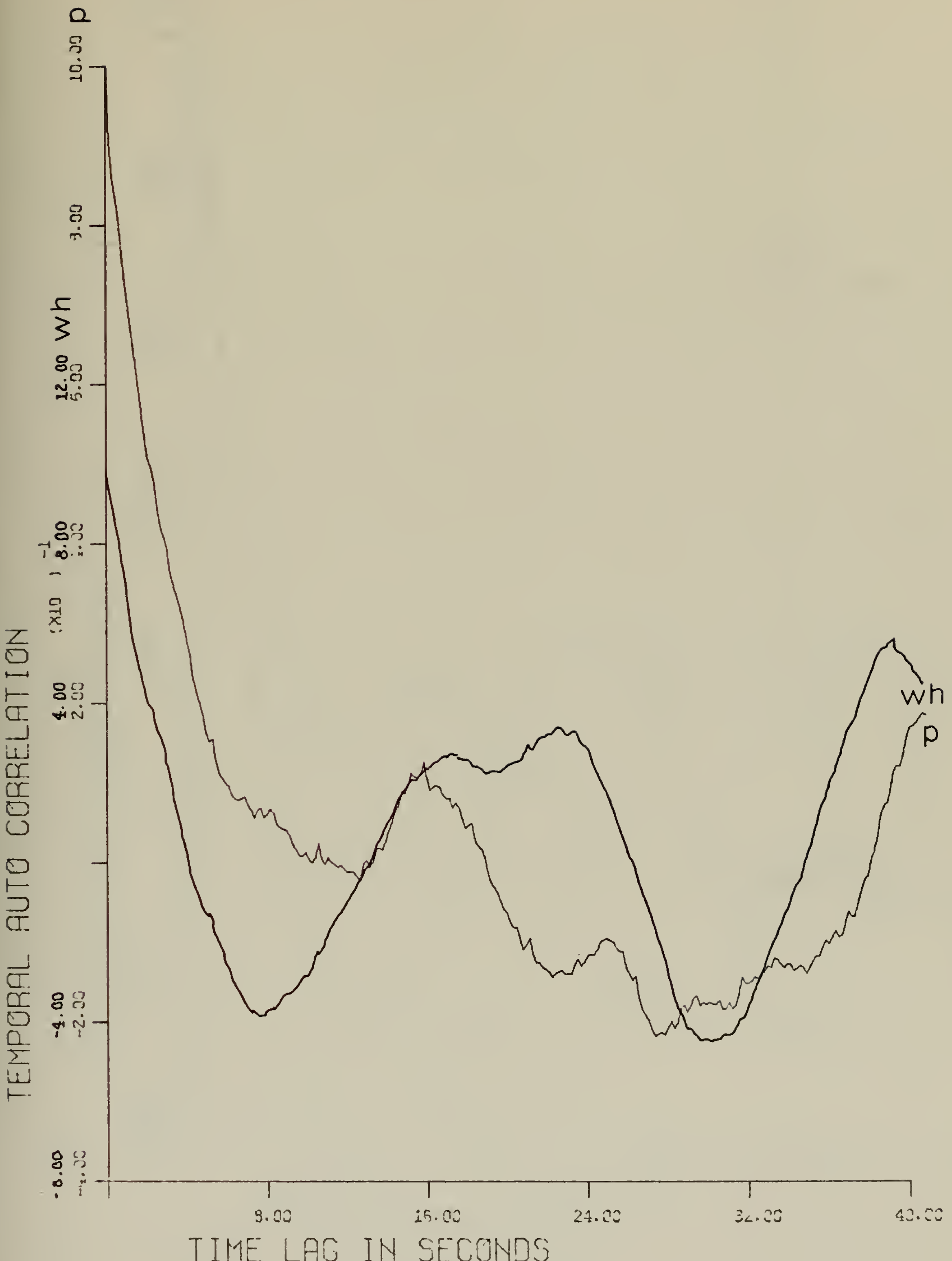

PHASE AND WAVE HEIGHT
FREQUENCY = 123720

Fig. 16

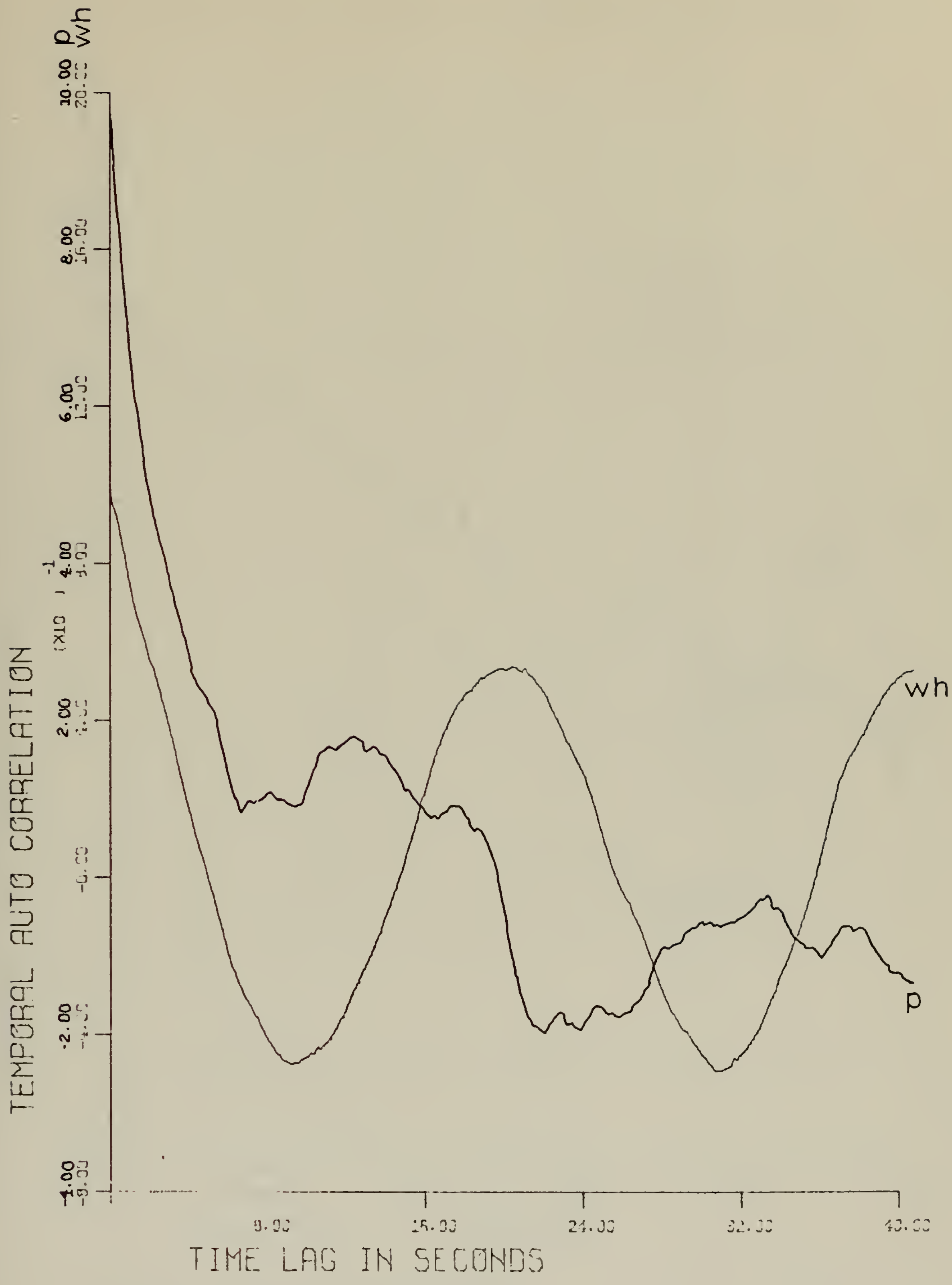

WAVE HEIGHT AND PHASE
FREQUENCY = 136800
Fig. 17

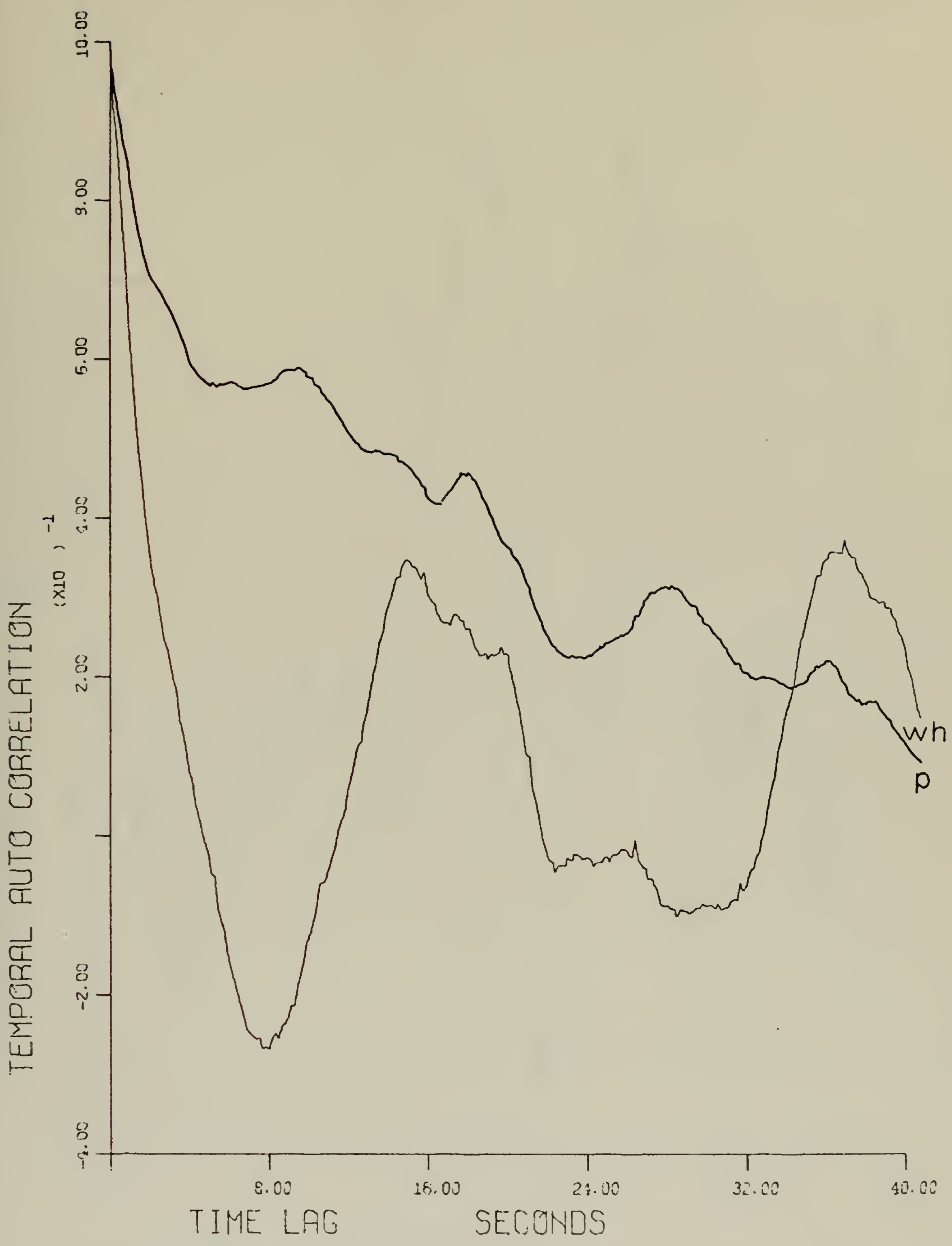

WAVE HEIGHT AND PHASE
FREQUENCY = 146100

Fig. 18

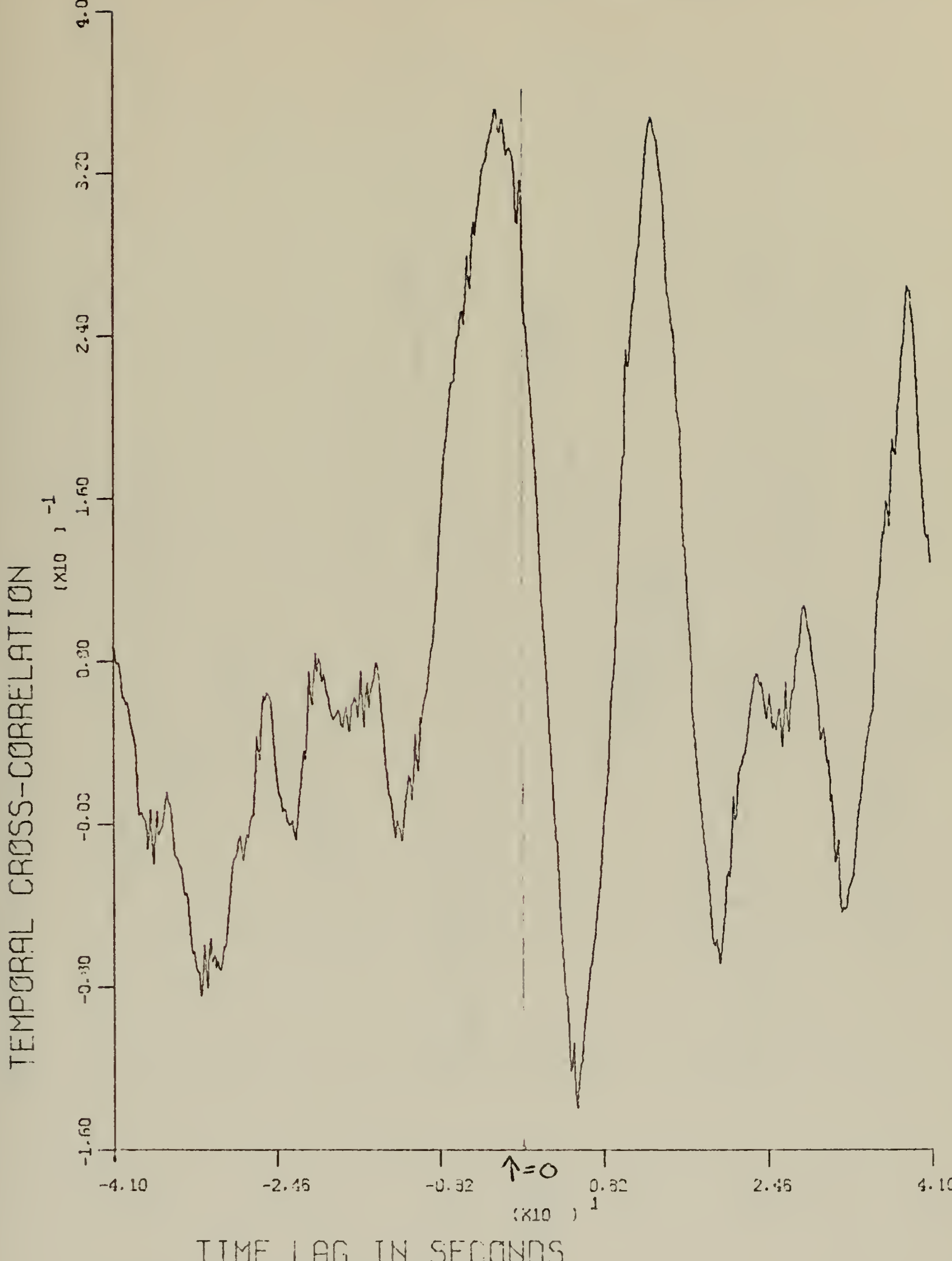

PHASE WITH WAVE HEIGHT
FREQUENCY = 14790

Fig. 19

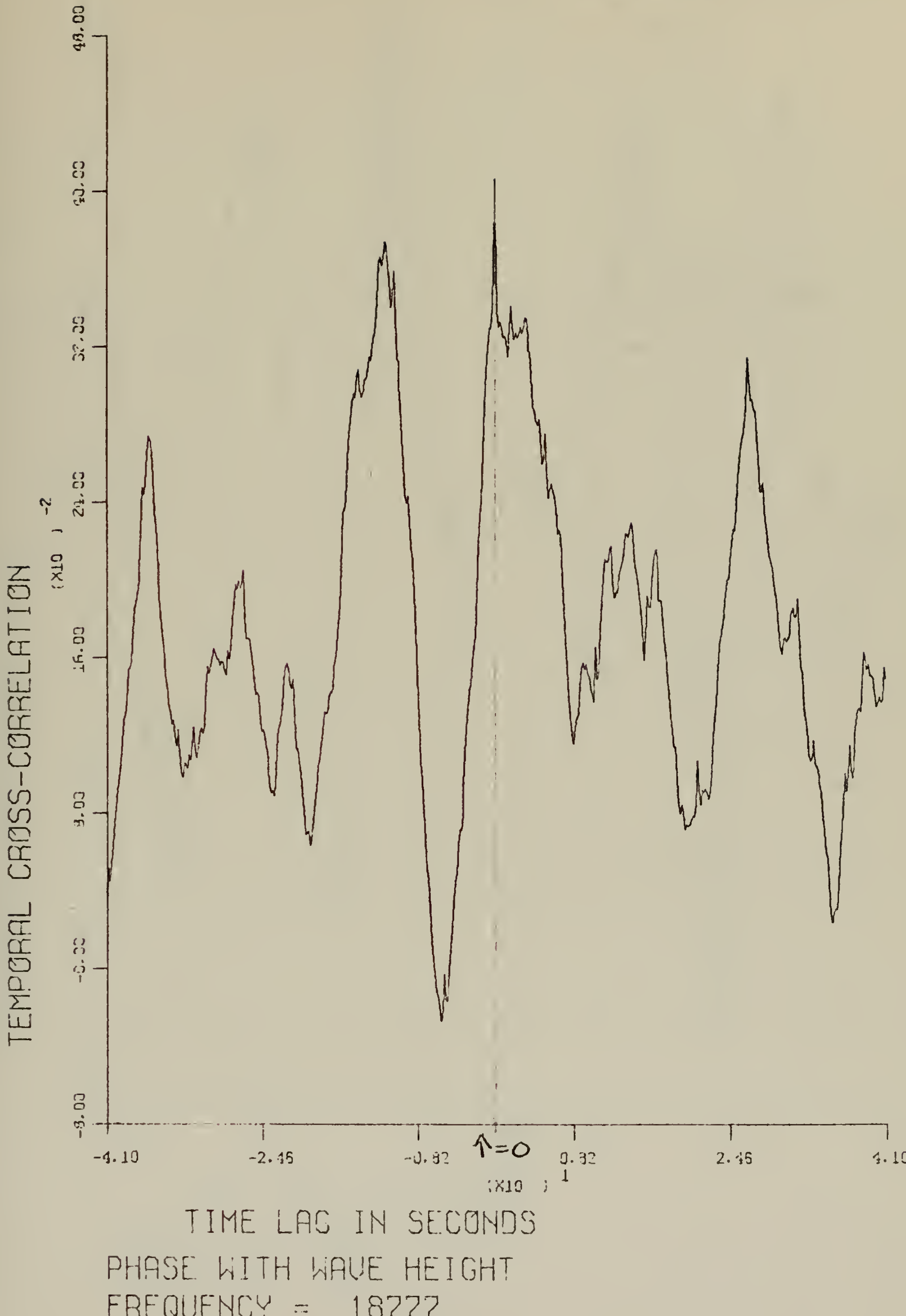
TEMPORAL CROSS-CORRELATION
(X10) -2
48.00
40.00
32.00
24.00
16.00
8.00
0.00
-8.00
-4.10
-2.46
-0.82
0.82
2.46
4.10
(X10) 1
↑=0
TIME LAG IN SECONDS
PHASE WITH WAVE HEIGHT
FREQUENCY = 18777

Fig. 20

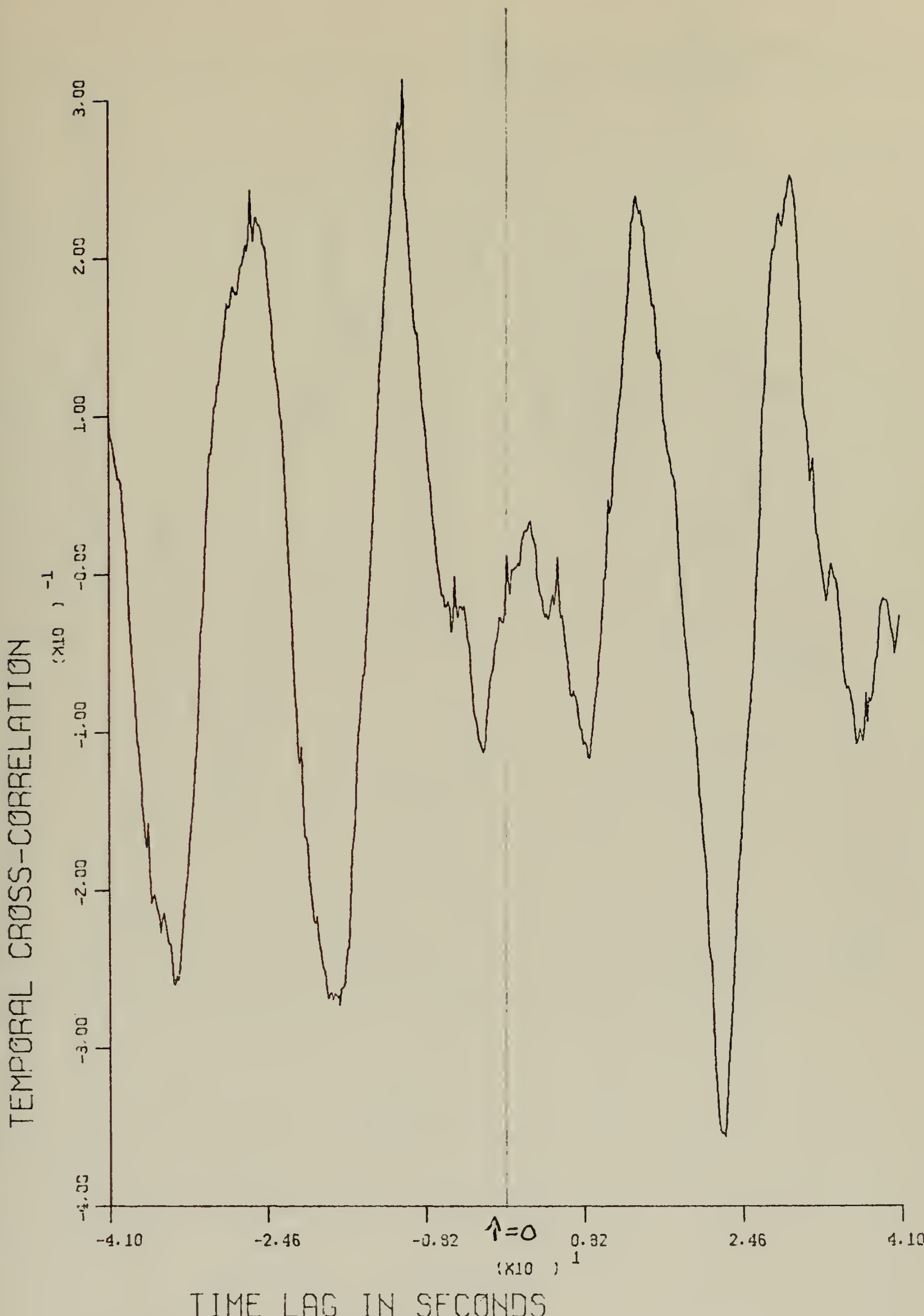

PHASE WITH WAVE HEIGHT
FREQUENCY = 26170

Fig. 21

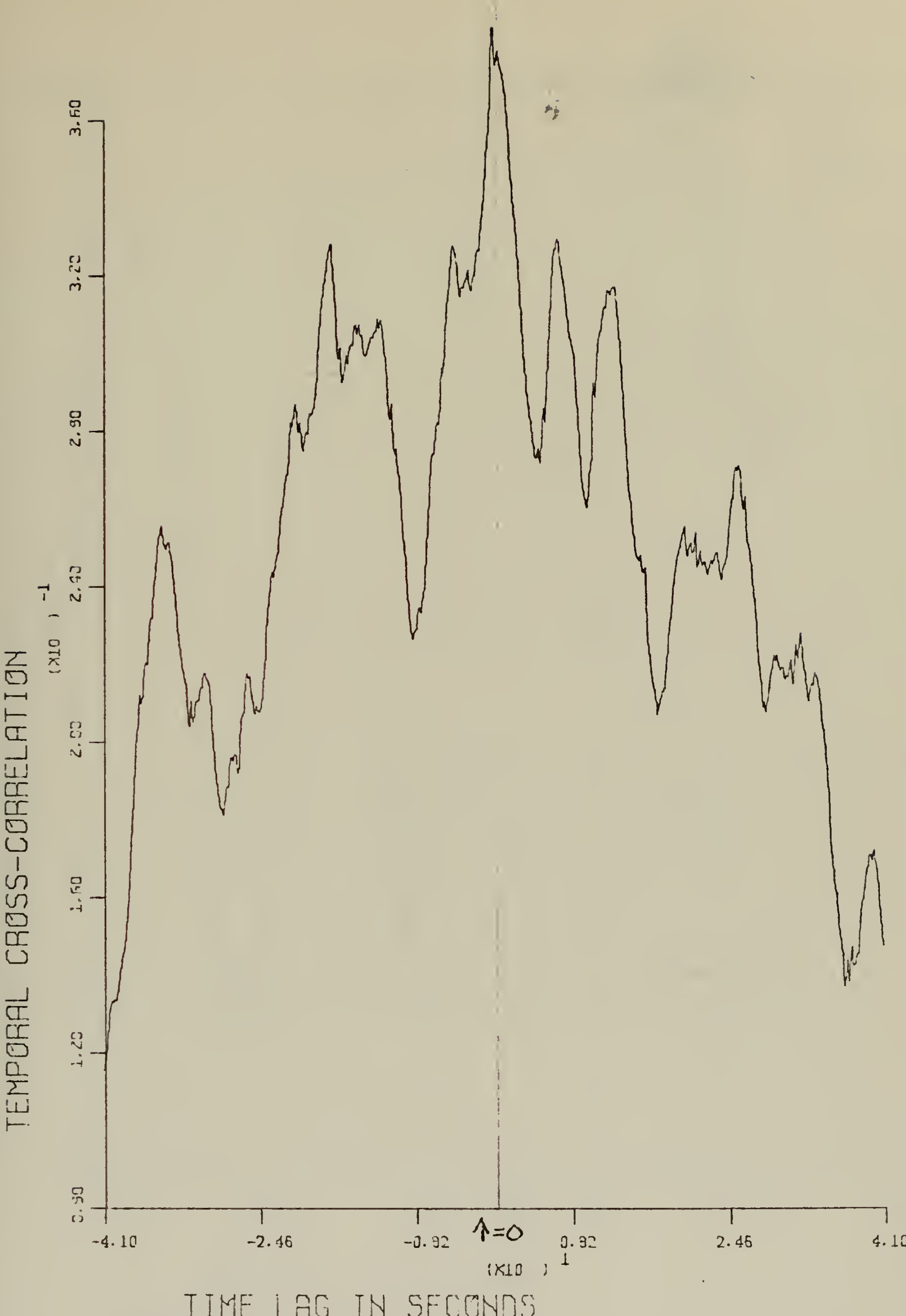

PHASE WITH WAVE HEIGHT
FREQUENCY = 41320

Fig. 22

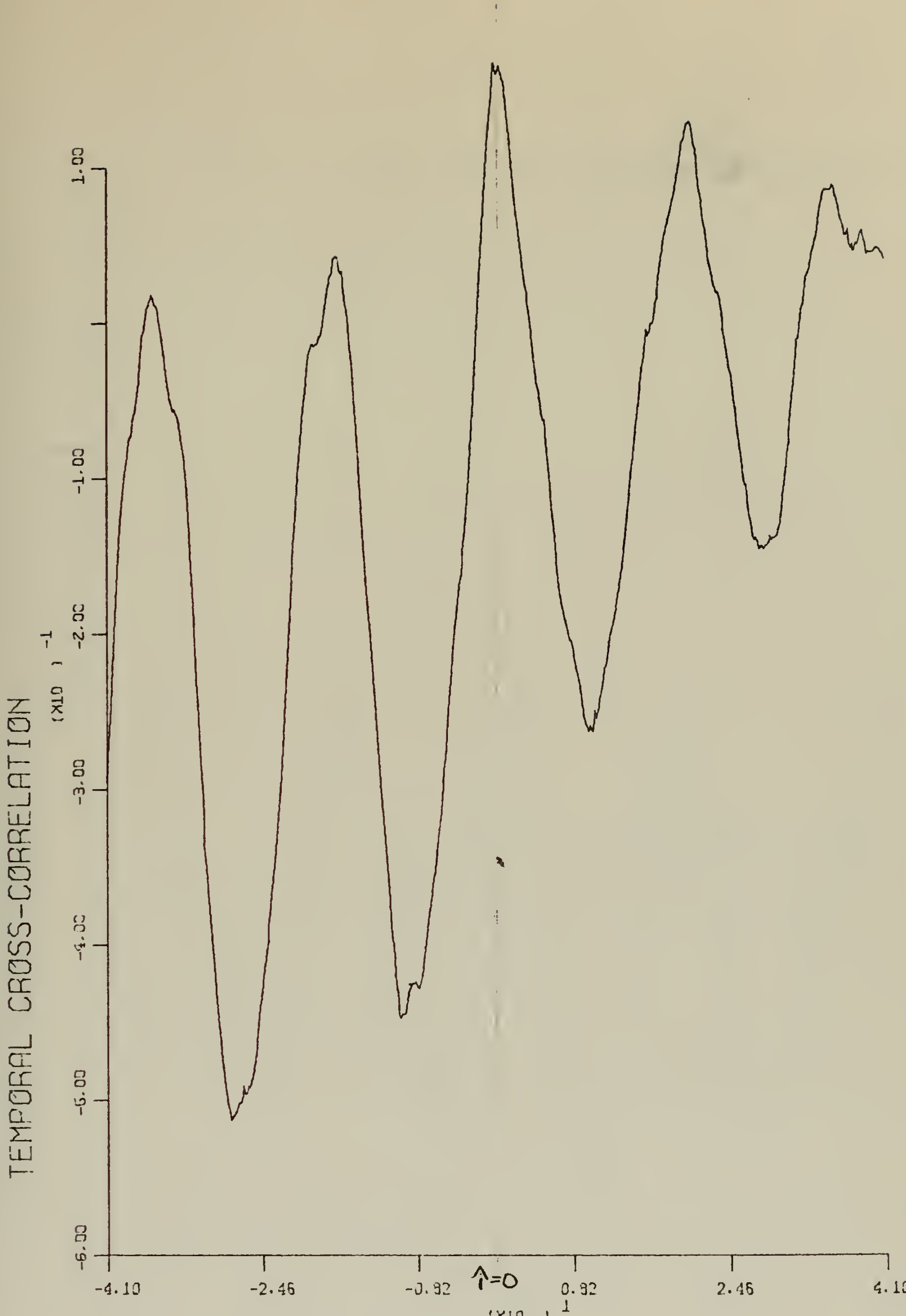

TIME LAG IN SECONDS
PHASE WITH WAVE HEIGHT
FREQUENCY = 56245

Fig. 23

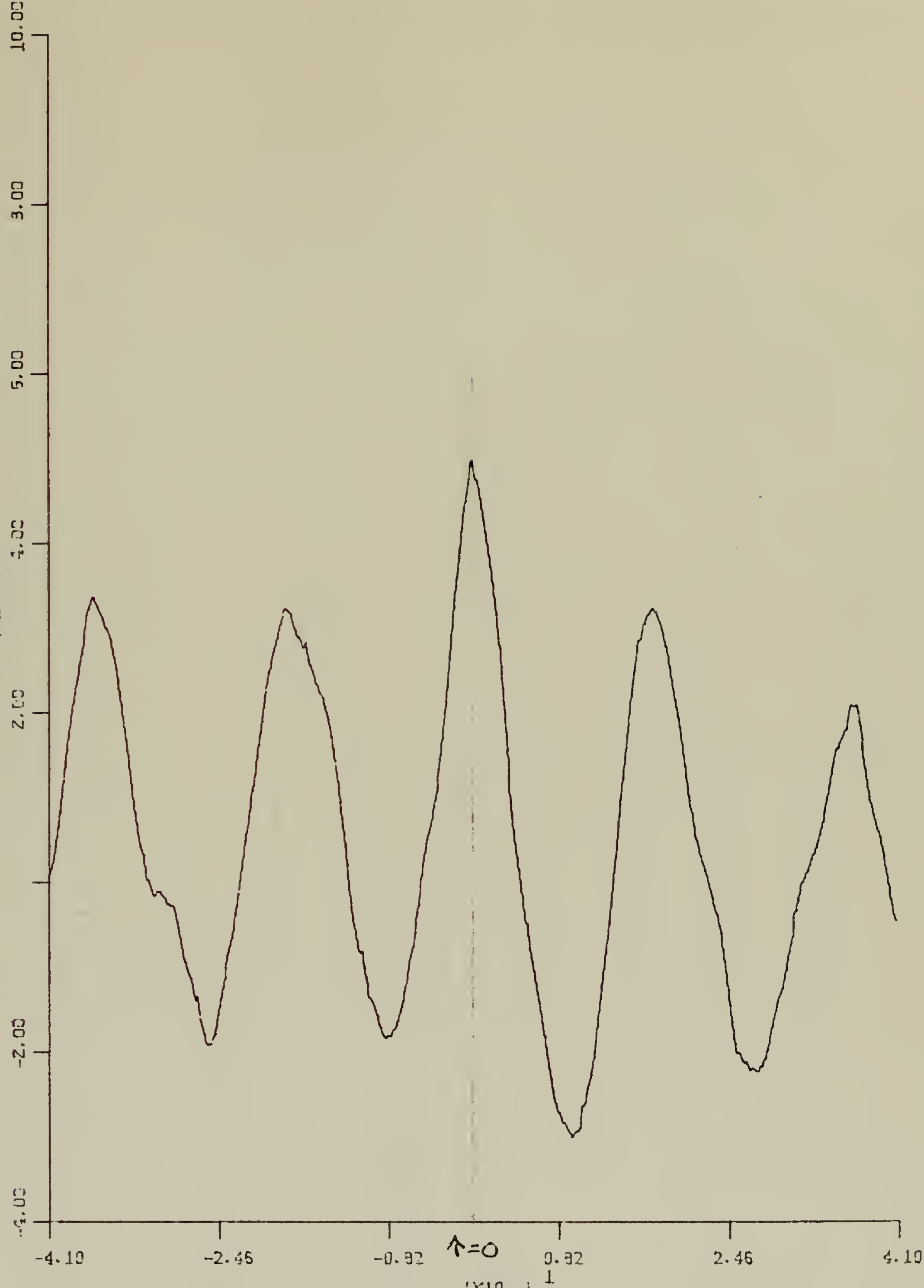

TIME LAG IN SECONDS

PHASE WITH WAVE HEIGHT

FREQUENCY = .63790

Fig. 24

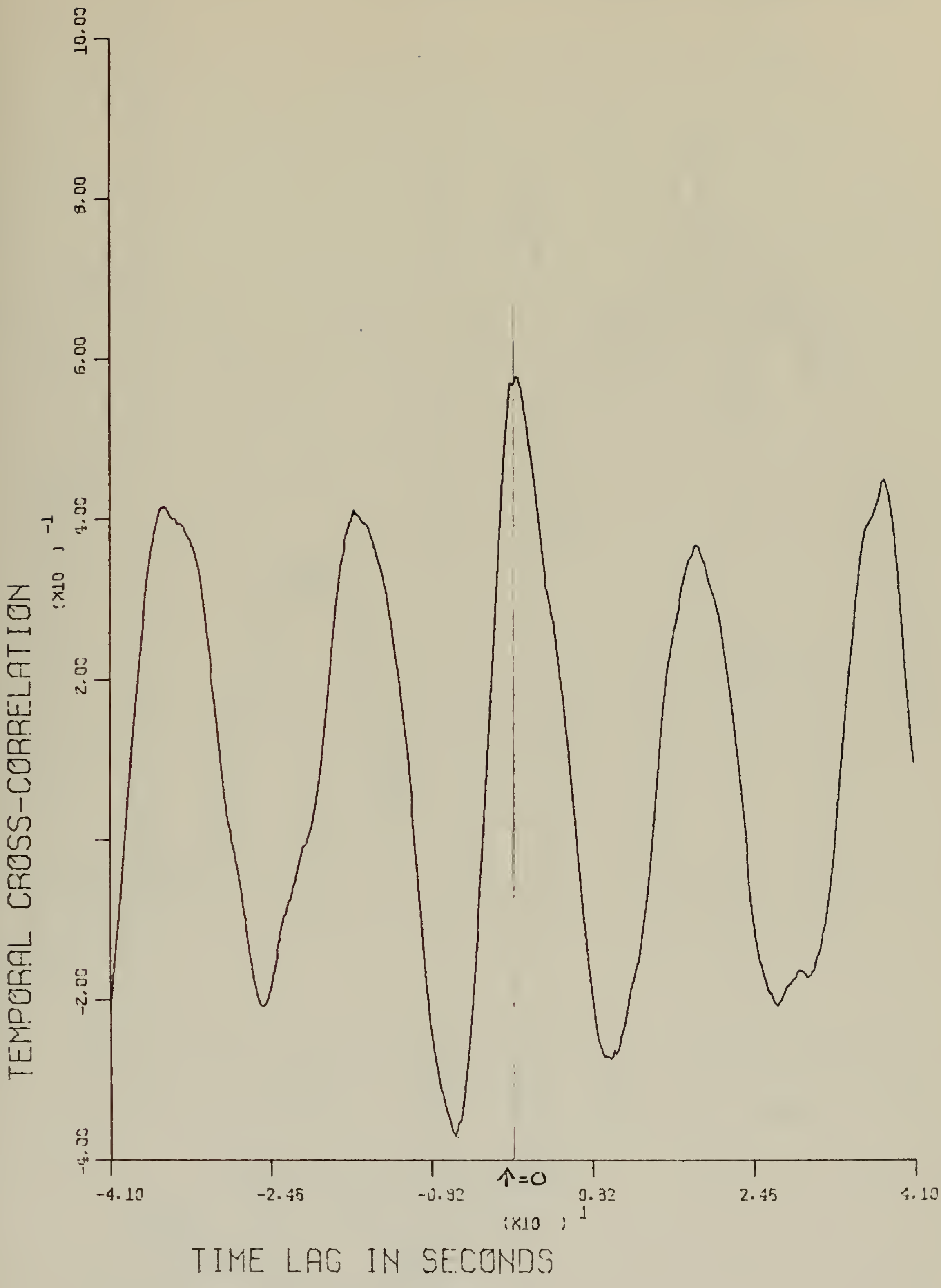

PHASE WITH WAVE HEIGHT
FREQUENCY = .71130

Fig. 25

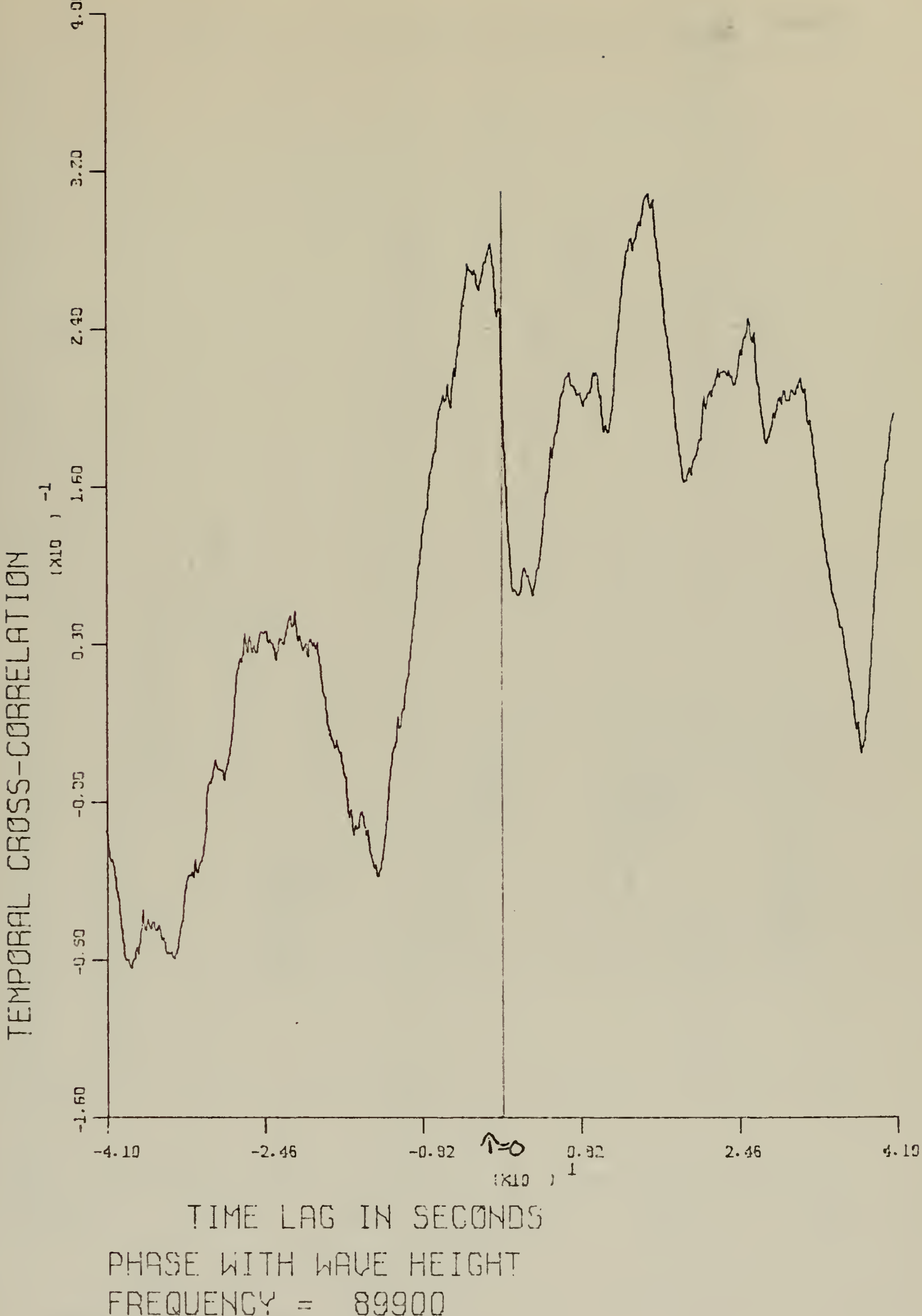
TEMPORAL CROSS-CORRELATION
(X10) -1
4.00
3.20
2.40
1.60
0.80
0.00
-0.80
-1.60
-4.10
-2.46
-0.82
τ=0
0.82
2.46
4.10
(X10) 1
TIME LAG IN SECONDS
PHASE WITH WAVE HEIGHT
FREQUENCY = 89900

Fig. 26

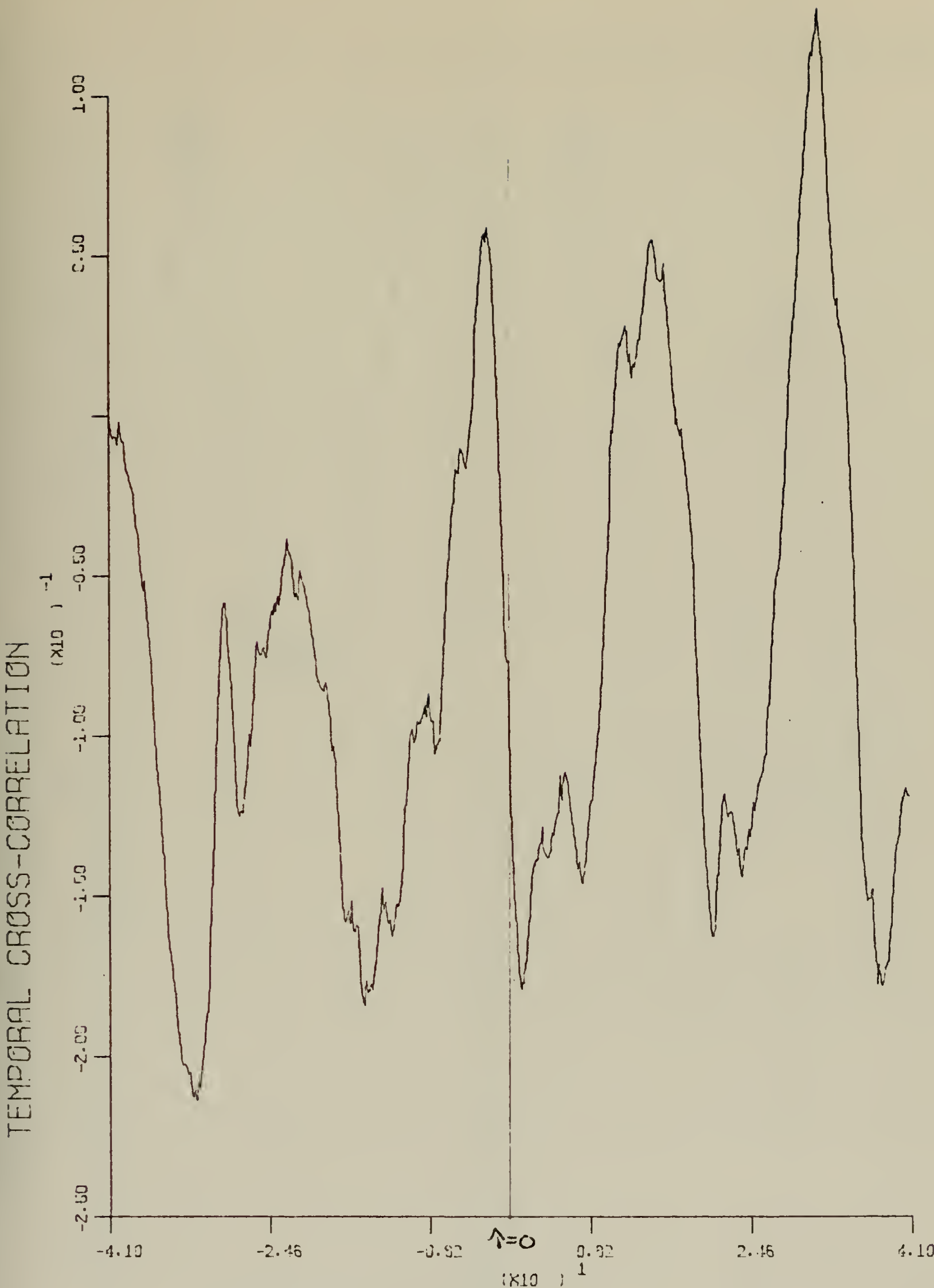

PHASE WITH WAVE HEIGHT
FREQUENCY = 112519

Fig. 27

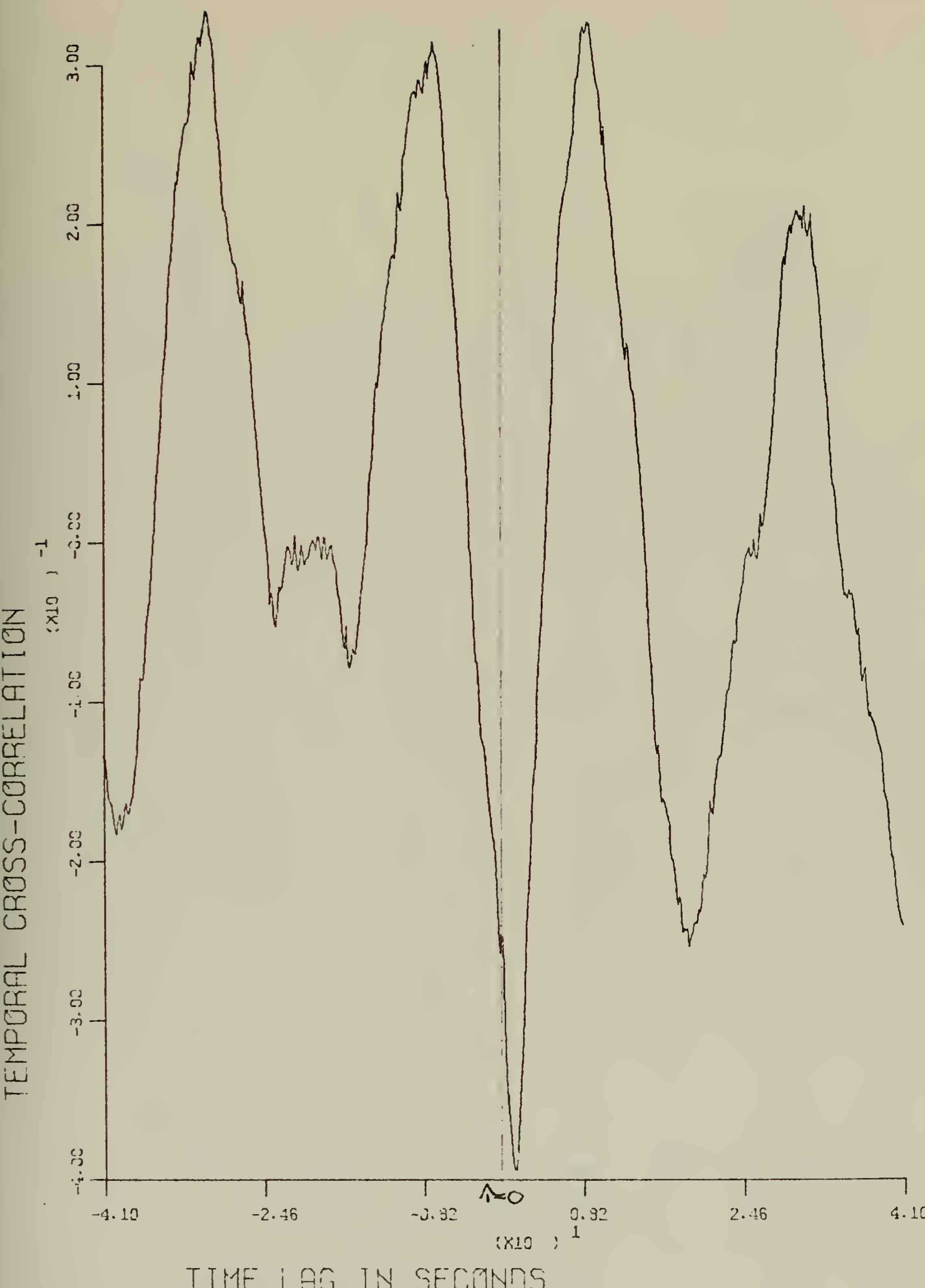

PHASE WITH WAVE HEIGHT
FREQUENCY = 123720

Fig. 28

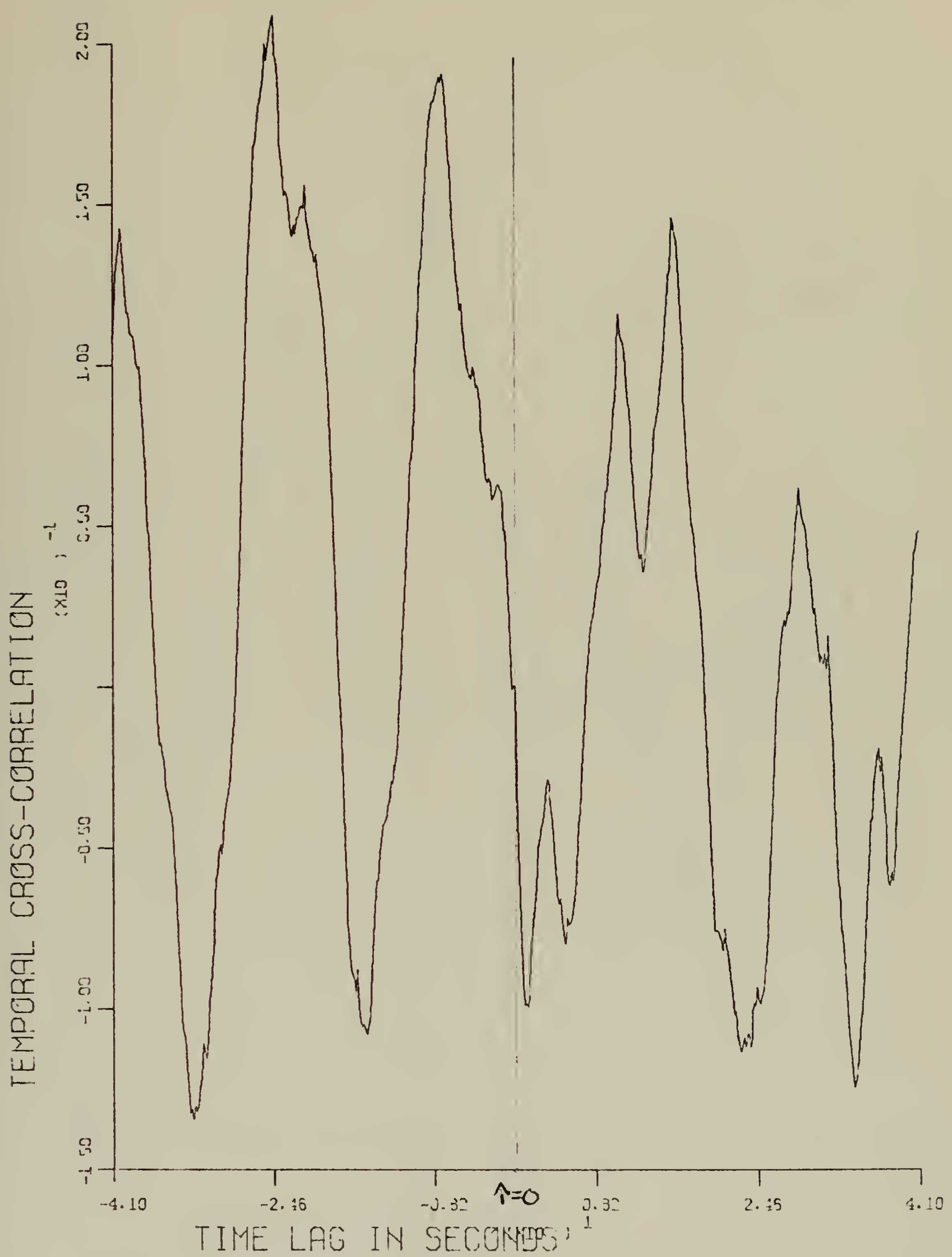

PHASE WITH WAVE HEIGHT
FREQUENCY = 136800

Fig. 29

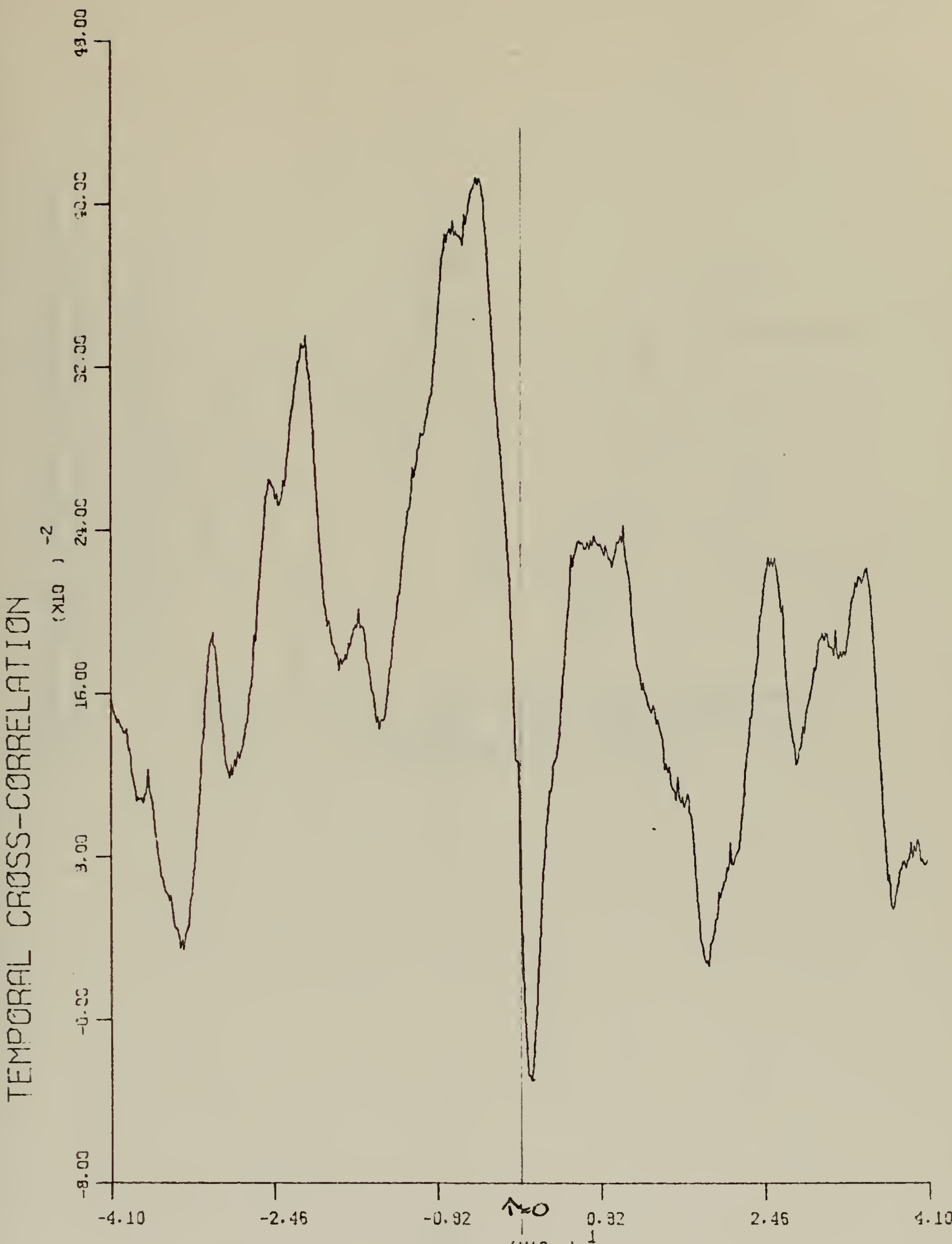

TIME LAG IN SECONDS

PHASE WITH WAVE HEIGHT

FREQUENCY = 146100

Fig. 30

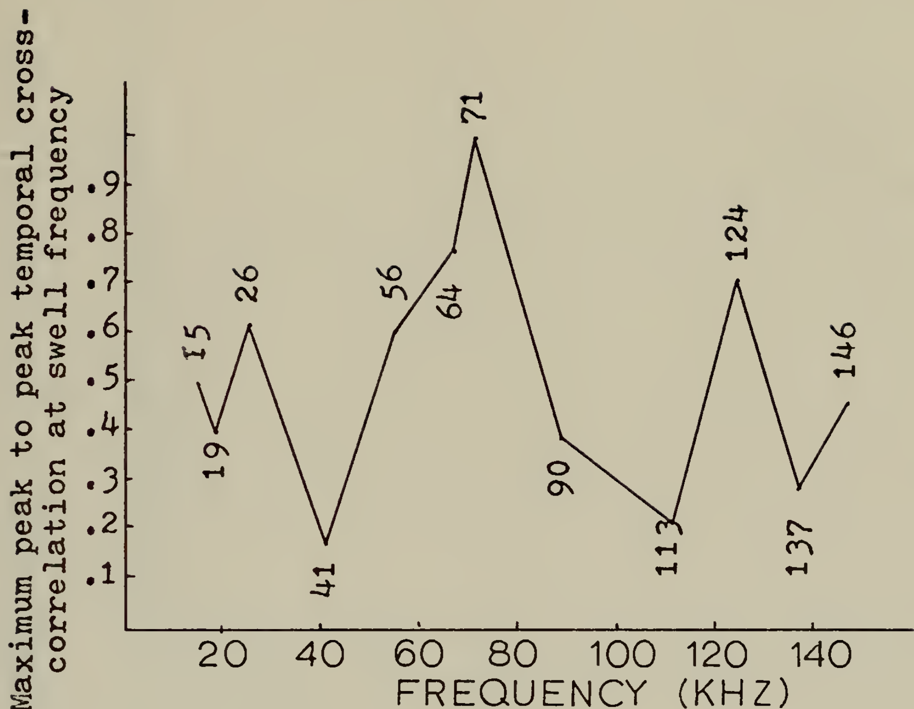
Maximum peak to peak temporal cross-correlation at swell frequency
.1
.2
.3
.4
.5
.6
.7
.8
.9
15
19
26
41
56
64
71
90
113
124
137
146
20
40
60
80
100
120
140
FREQUENCY (KHZ)

Fig. 31

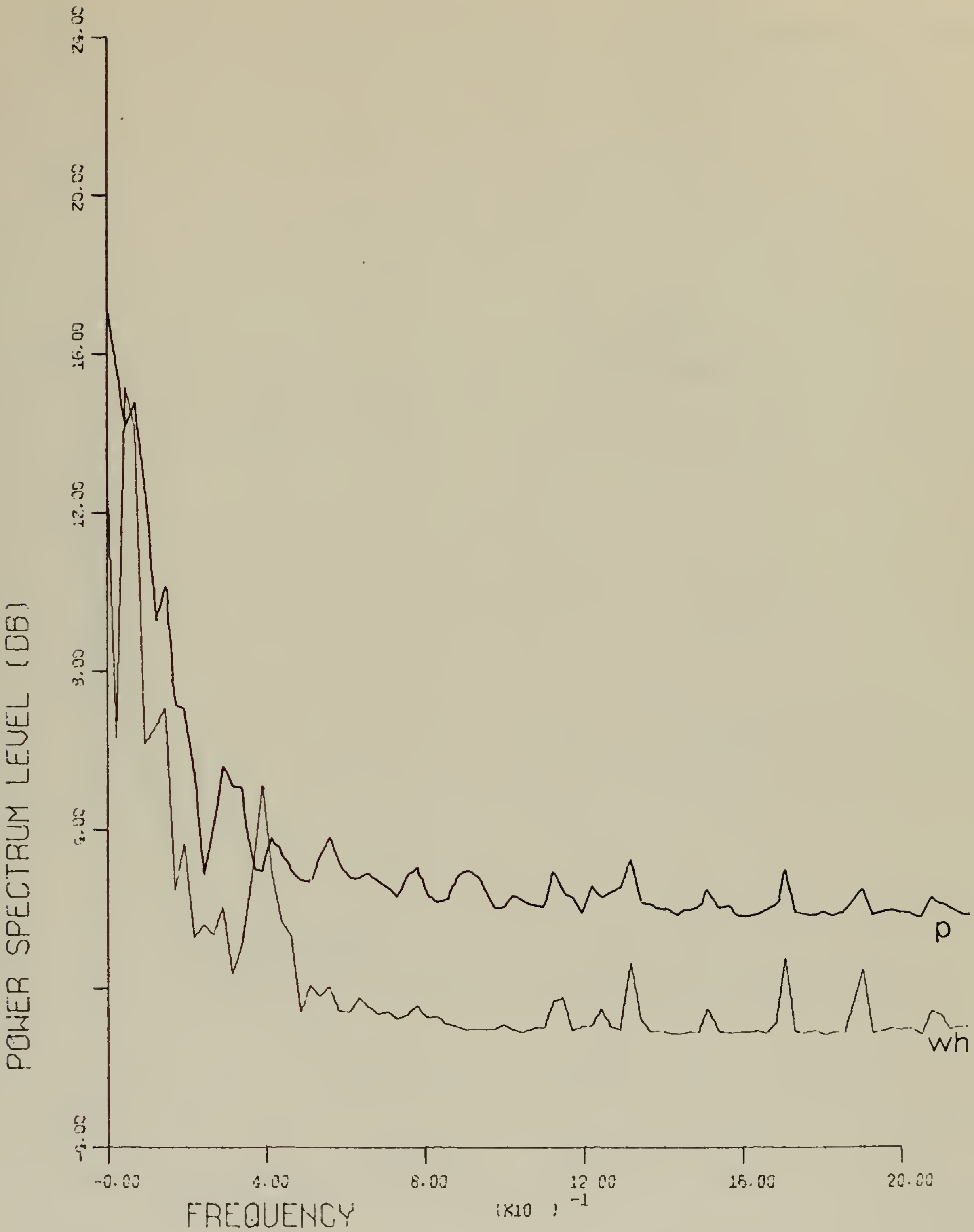

HAMMING

FREQUENCY = 14790

Fig. 32

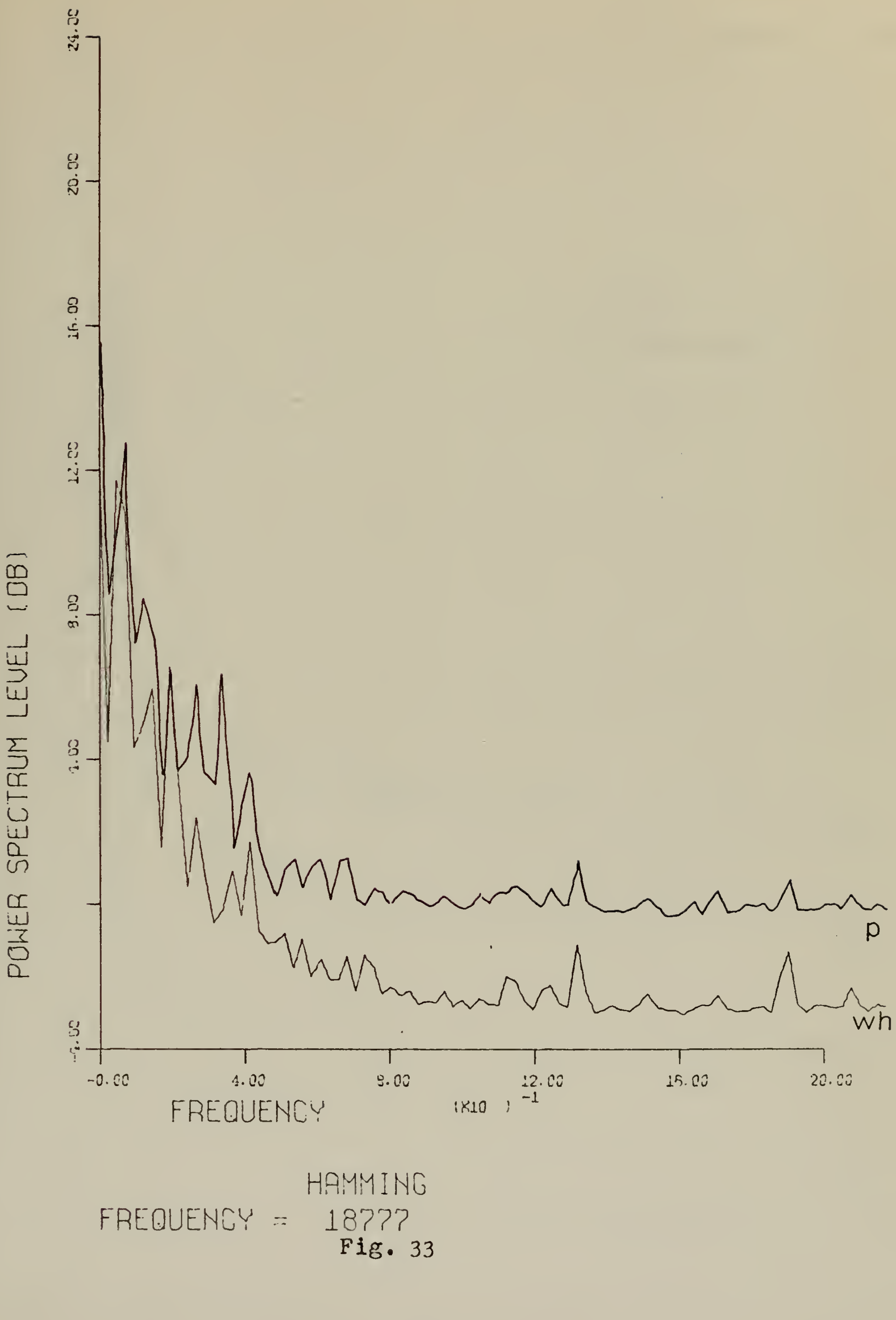
POWER SPECTRUM LEVEL (DB)
24.00
20.00
16.00
12.00
8.00
4.00
-4.00
-0.00
4.00
8.00
12.00
16.00
20.00
FREQUENCY
(X10) -1
p
wh
HAMMING
FREQUENCY = 18777

Fig. 33

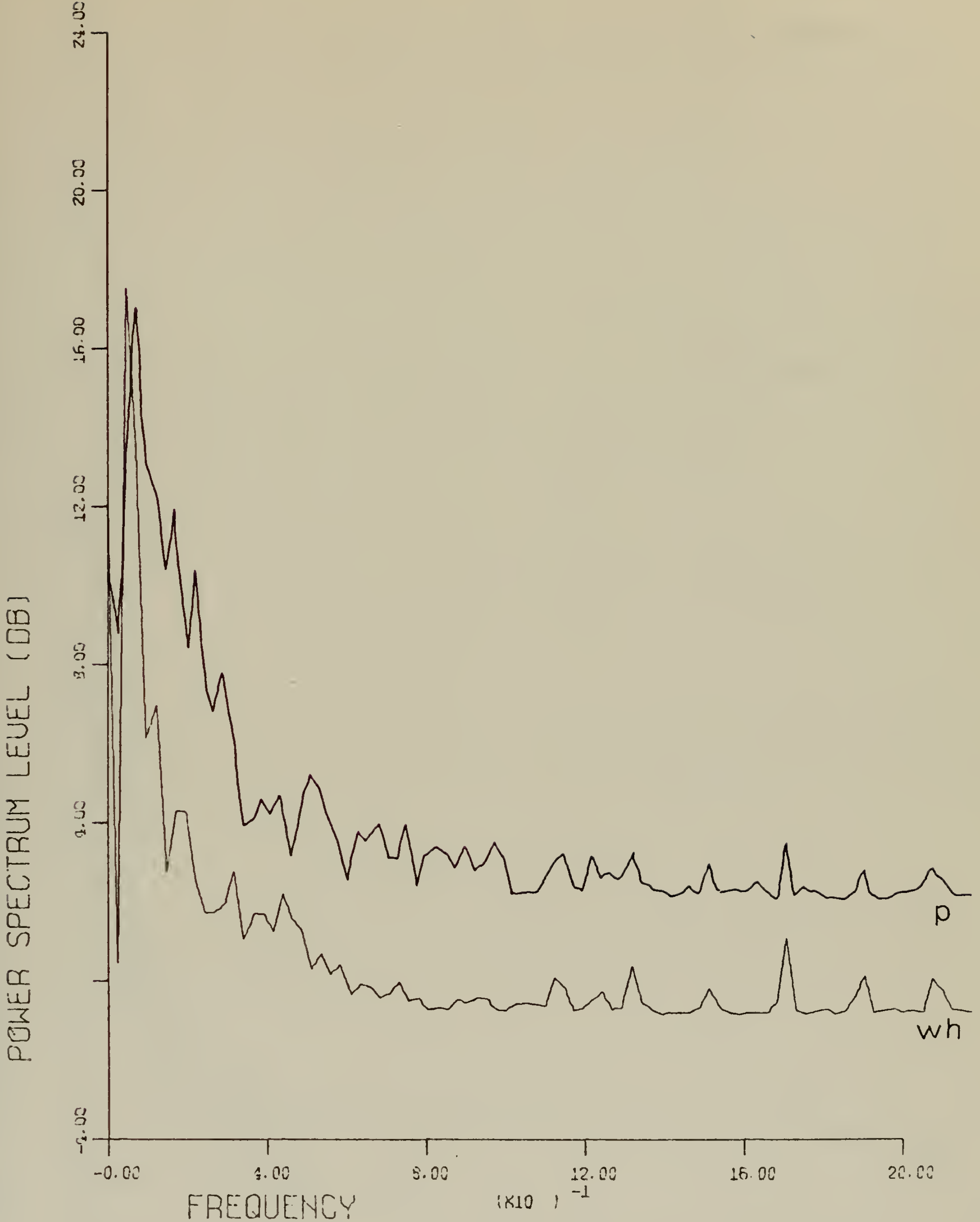

HAMMING
FREQUENCY = 26170
Fig. 34

HAMMING
FREQUENCY = 41320

Fig. 35

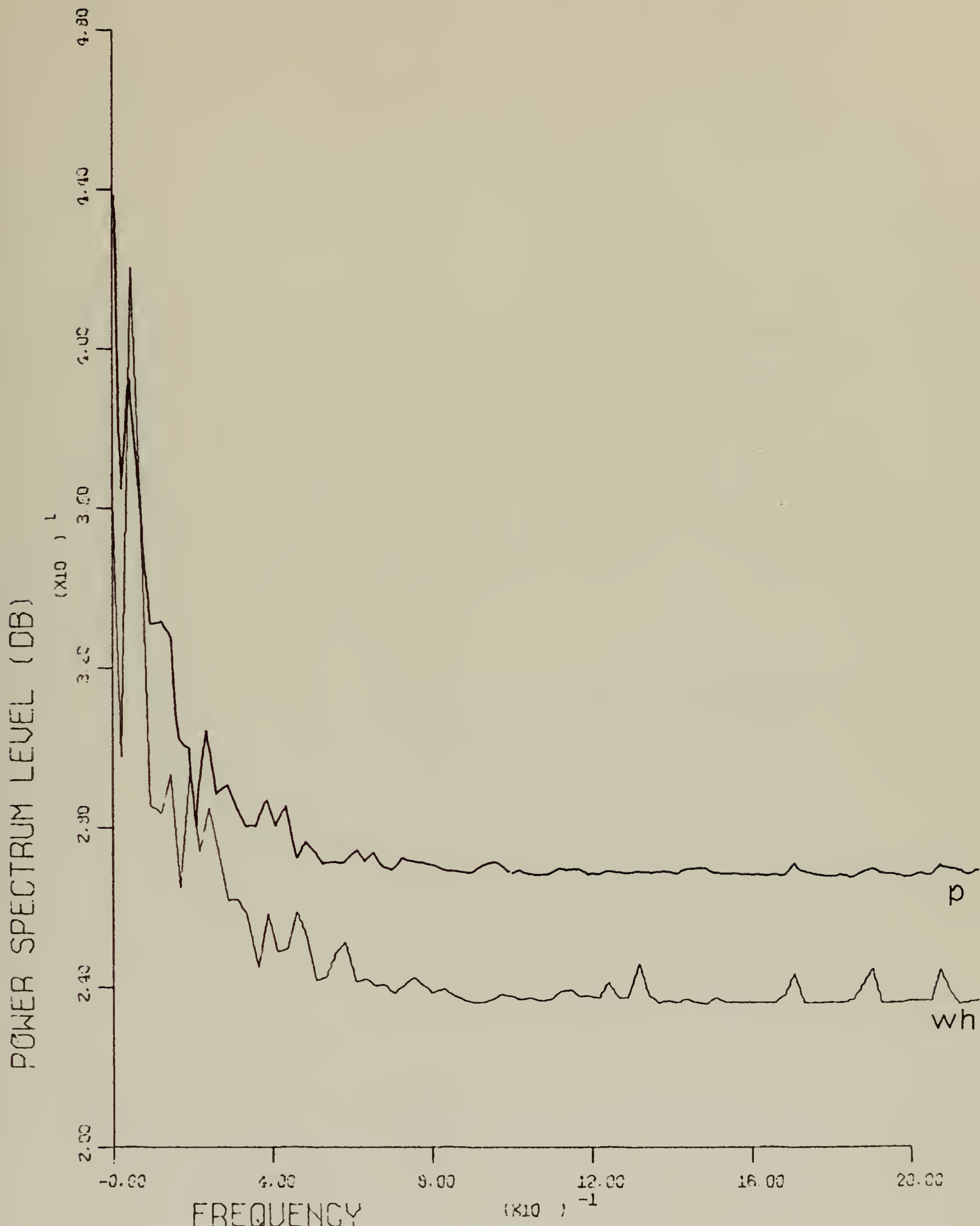

HAMMING
FREQUENCY = 56245

Fig. 36

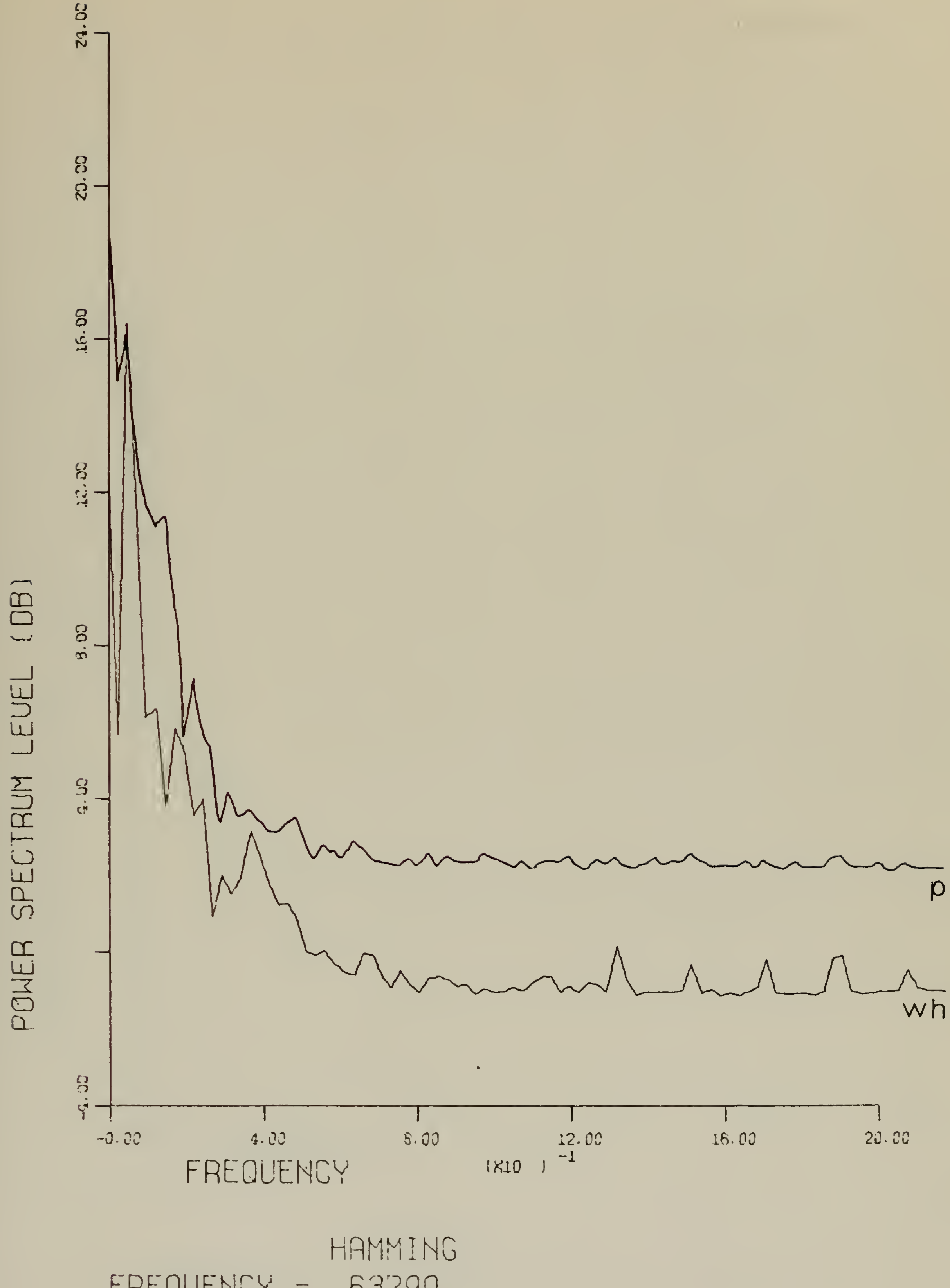
24.00
20.00
16.00
12.00
8.00
4.00
-4.00
POWER SPECTRUM LEVEL (DB)
-0.00
4.00
8.00
12.00
16.00
20.00
FREQUENCY
(X10^-1)
p
wh
HAMMING
FREQUENCY = 63790

Fig. 37

HAMMING

FREQUENCY = 71130

Fig. 38

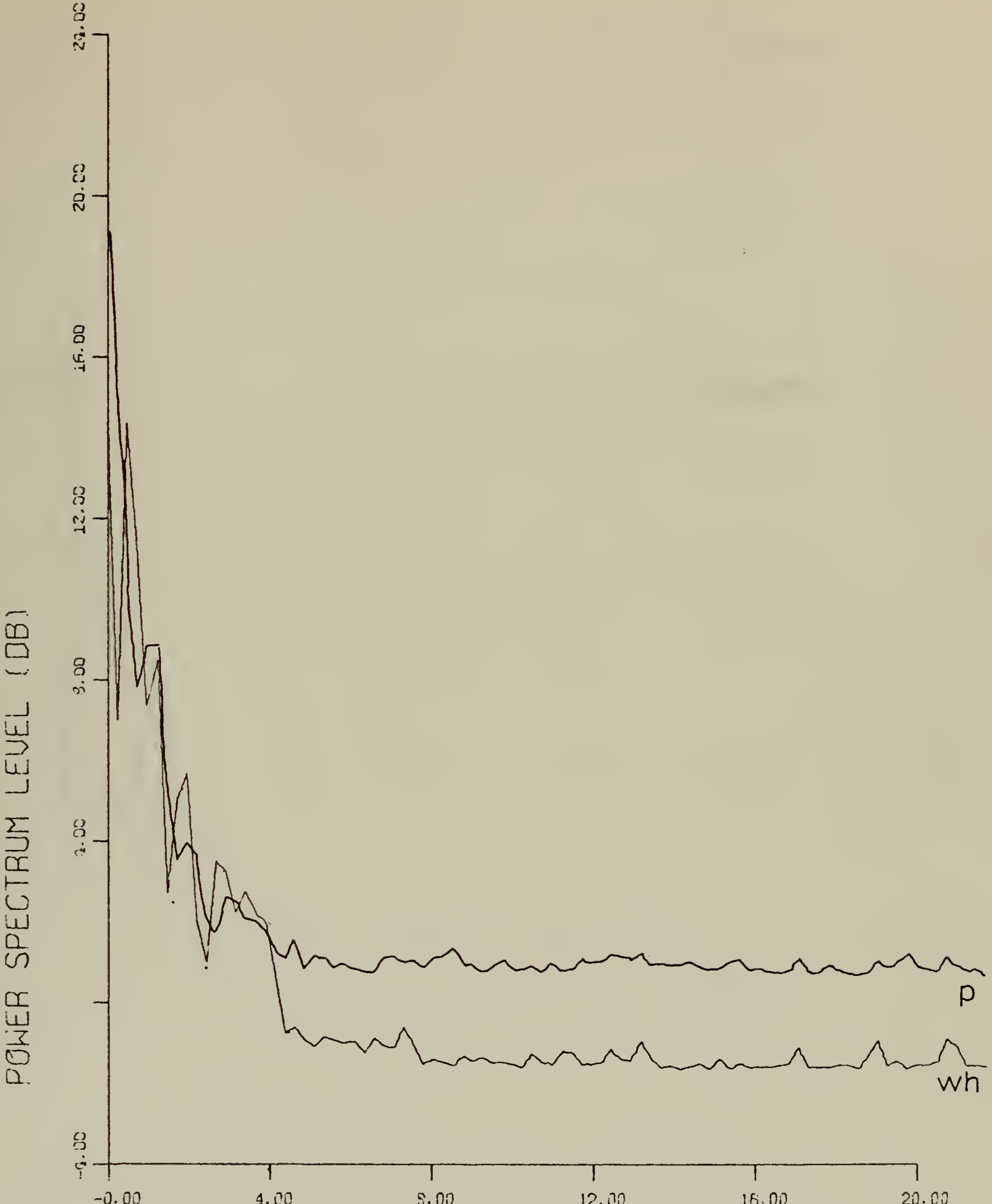

HAMMING
FREQUENCY = 89900
Fig. 39

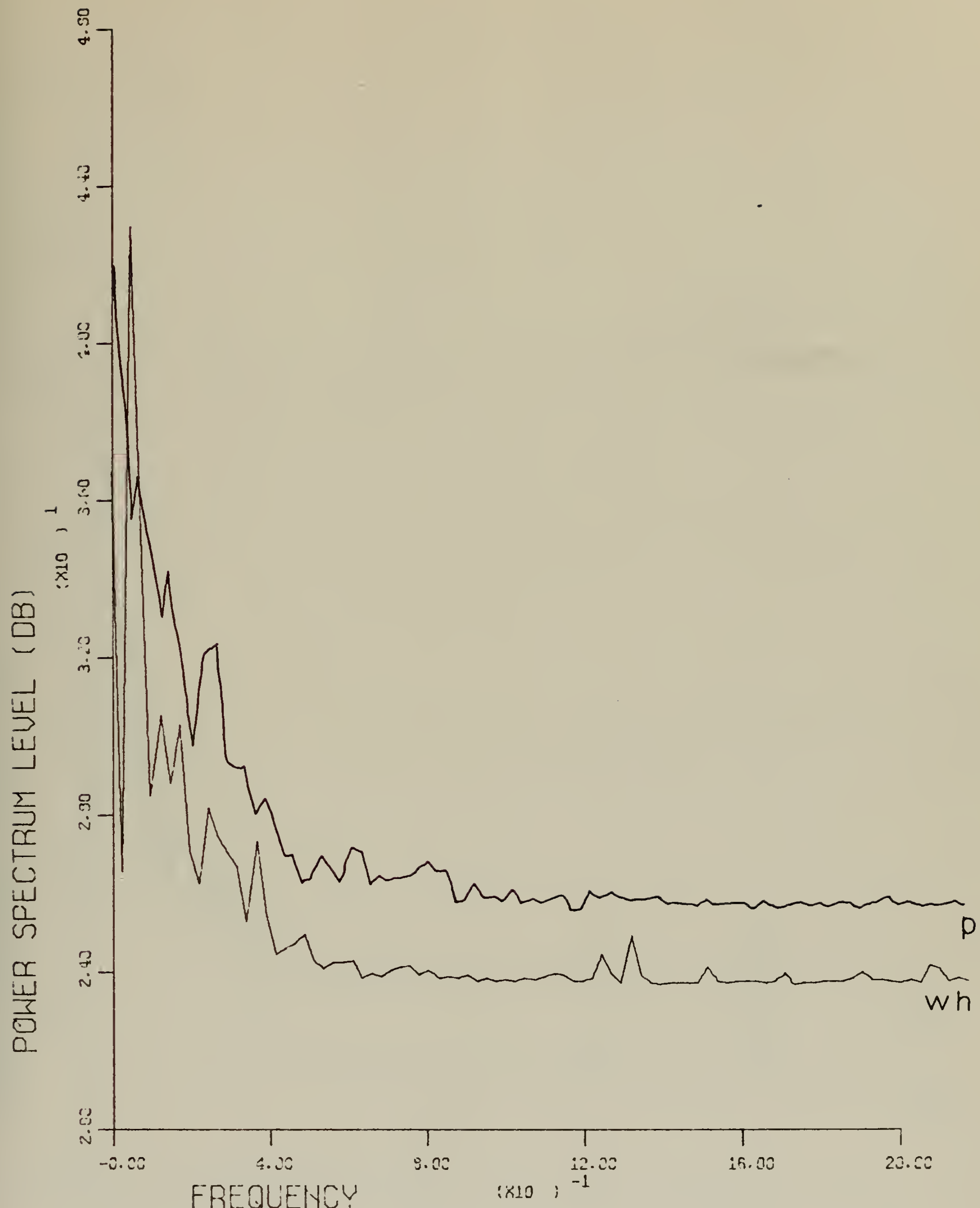

HAMMING
FREQUENCY = 112519

Fig. 40

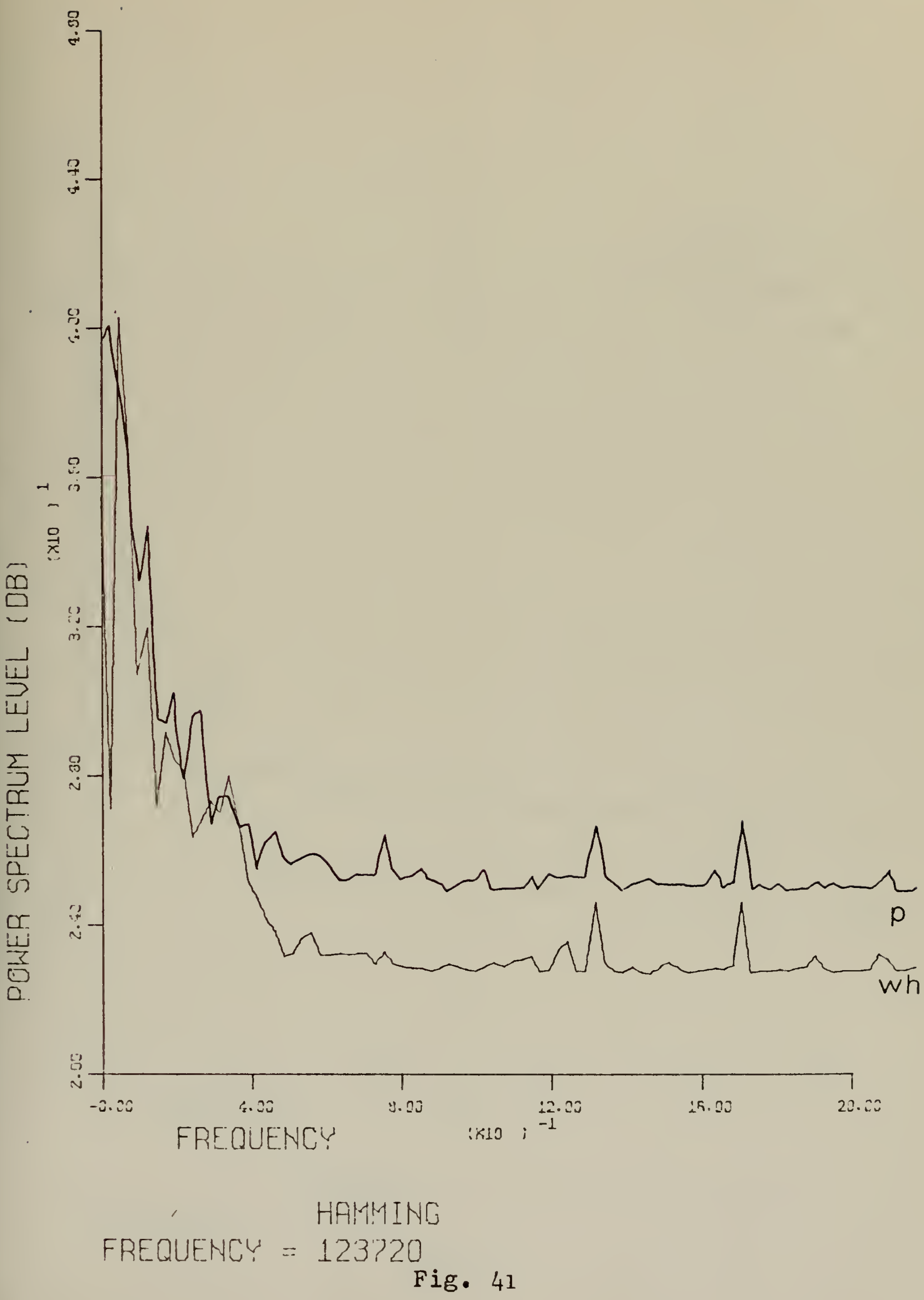

POWER SPECTRUM LEVEL (DB)
(X10) 1
FREQUENCY
(X10) -1
p
wh
HAMMING
FREQUENCY = 123720

Fig. 41

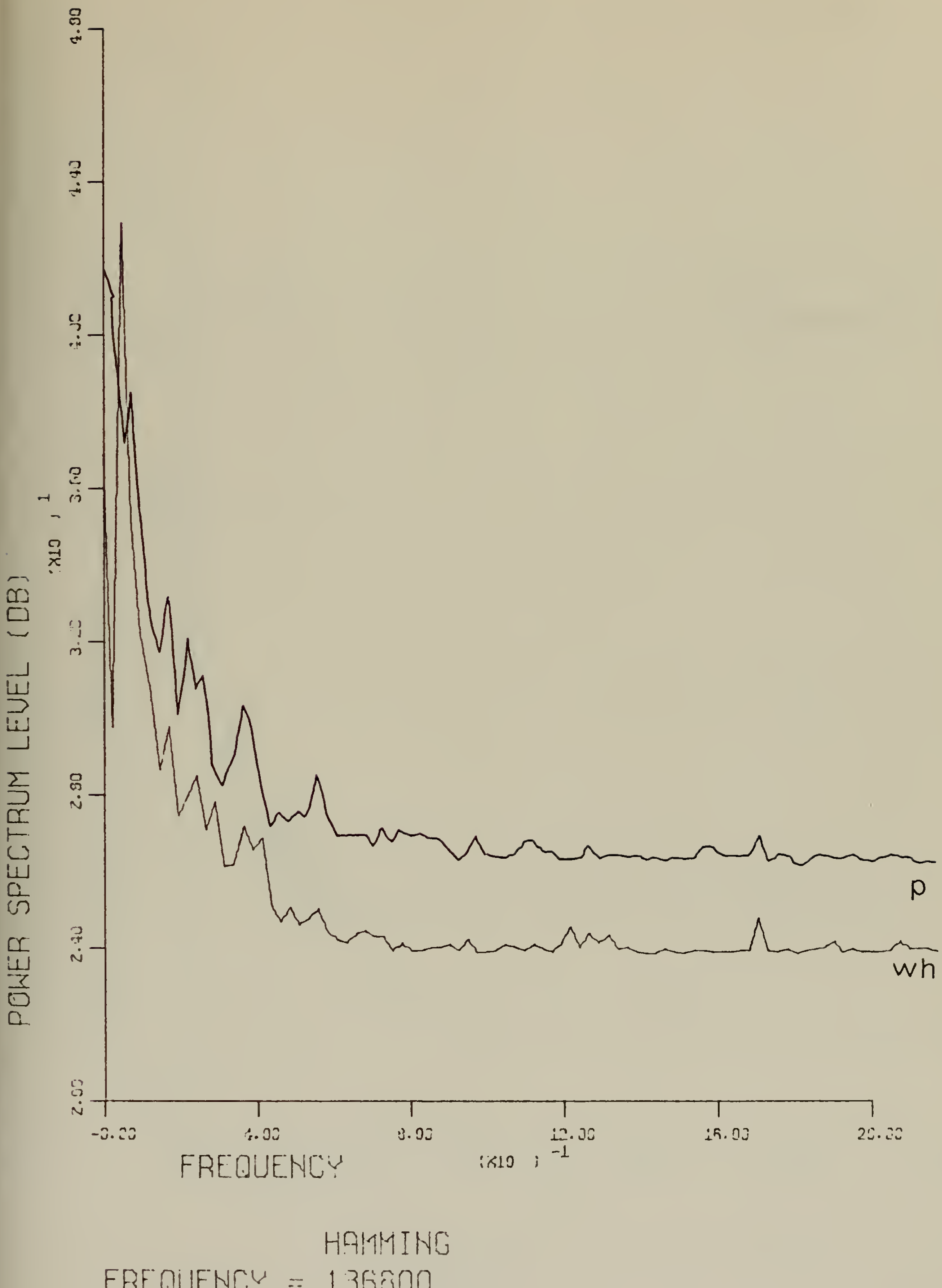
POWER SPECTRUM LEVEL (DB)
(X10) 1
FREQUENCY
(X10) -1
p
wh
HAMMING
FREQUENCY = 136800
Fig. 42

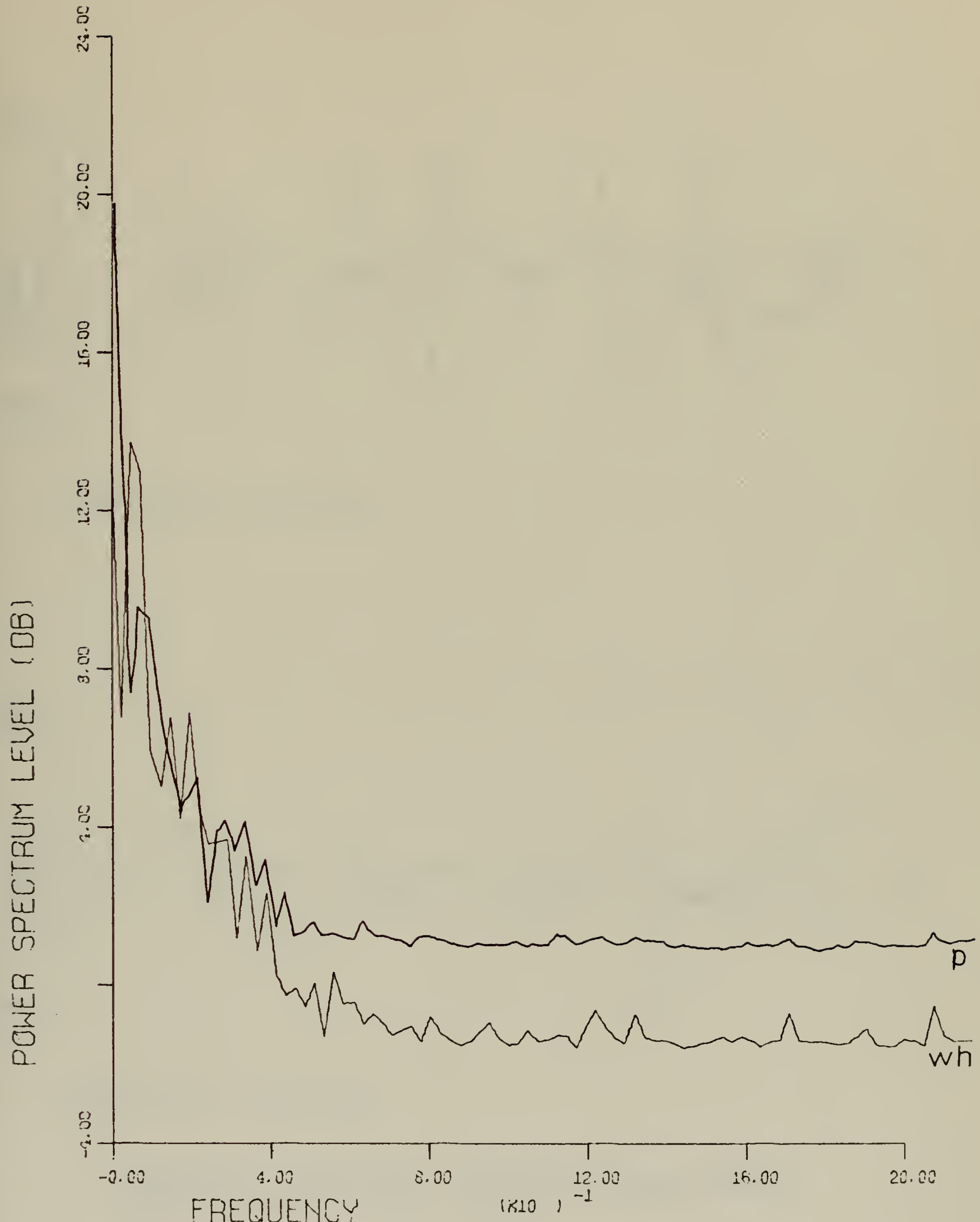

HAMMING
FREQUENCY = 146100
Fig. 43

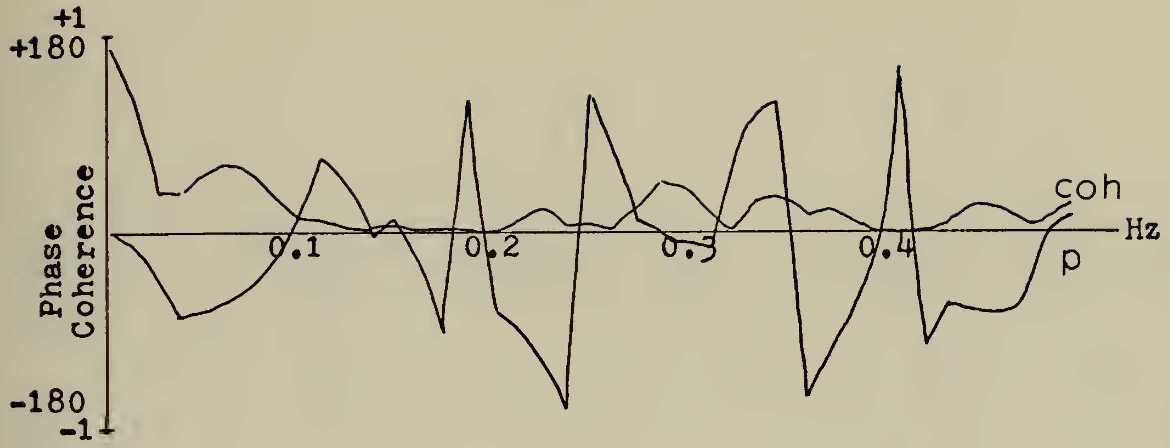

Frequency = 14790 Hz

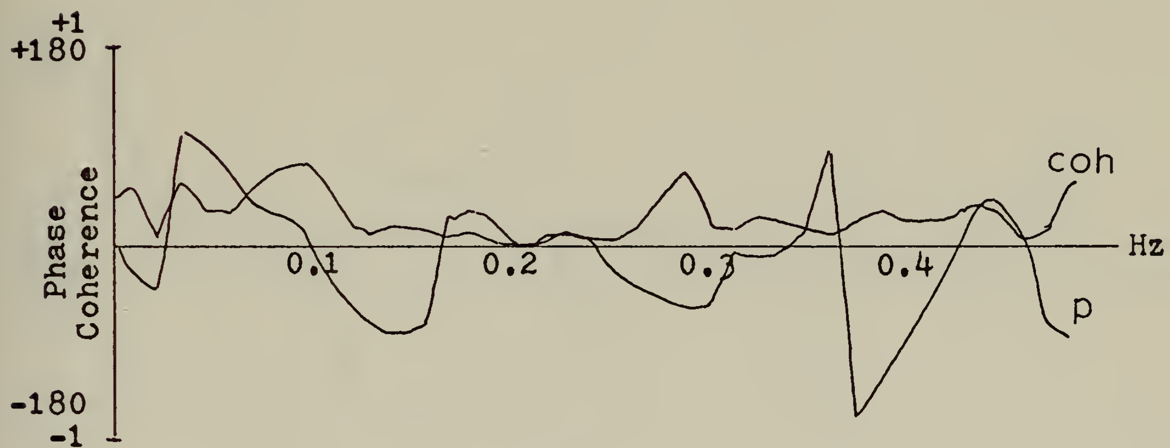

Frequency = 18777 Hz

Coherence Function: Phase and Wave Height
Cross-Spectral Phase Angle

Fig. 44

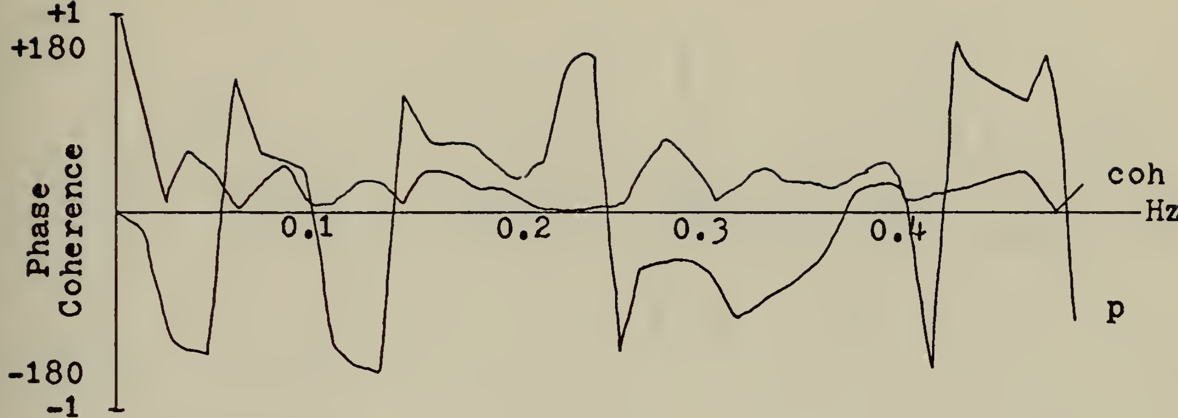

Frequency = 26170 Hz

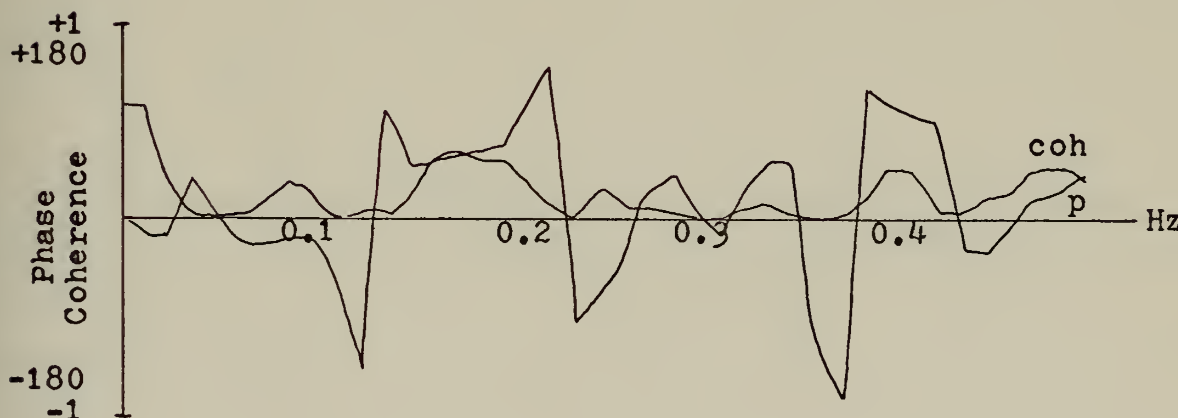

Frequency = 41320 Hz

Coherence Function: Phase and Wave Height
Cross-Spectral Phase Angle

Fig. 45

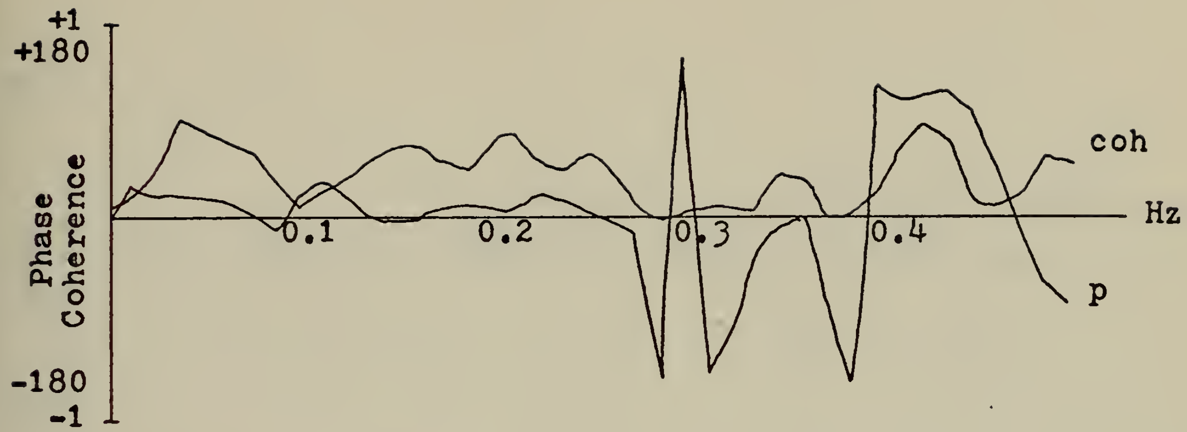

Frequency = 56245 Hz

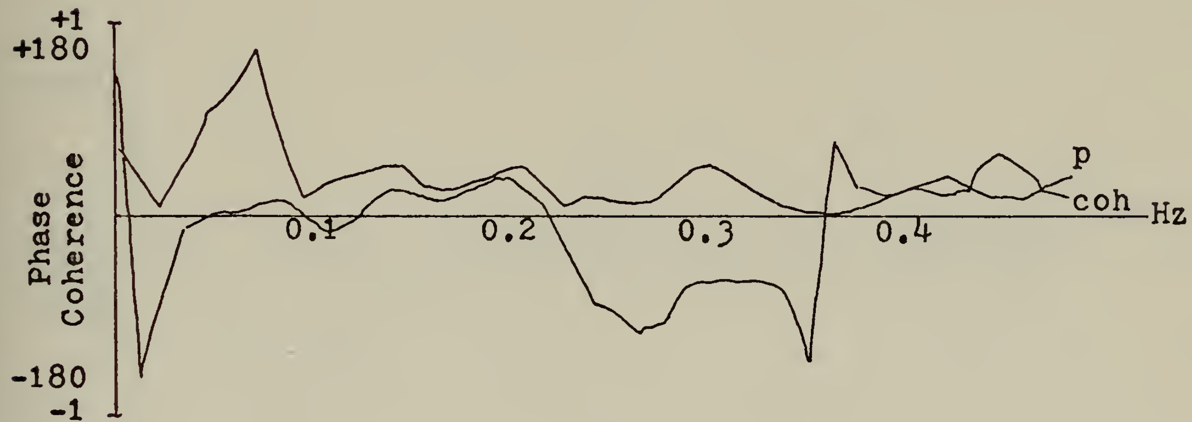

Frequency = 63790 Hz

Coherence Function: Phase and Wave Height
Cross-Spectral Phase Angle

Fig. 46

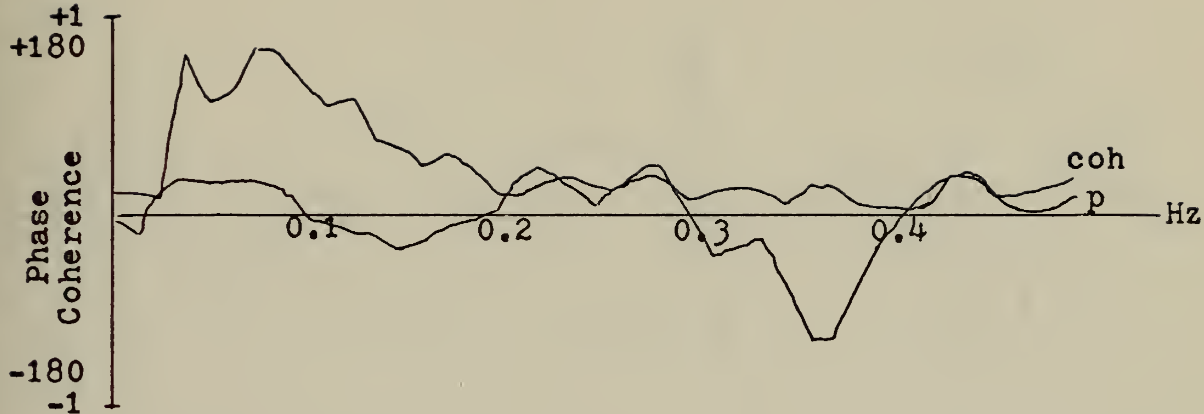

Frequency = 71130 Hz

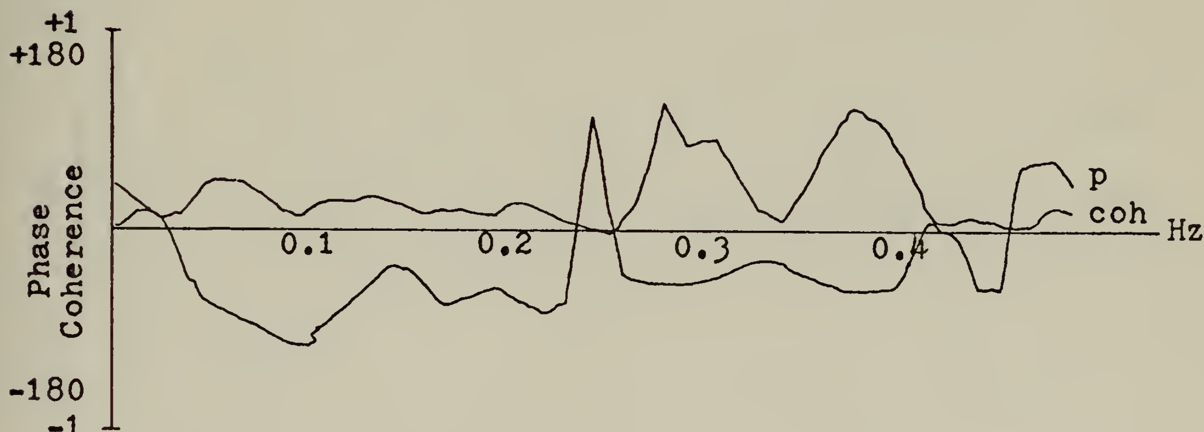

Frequency = 89900 Hz

Coherence Function: Phase and Wave Height
Cross-Spectral Phase Angle

Fig. 47

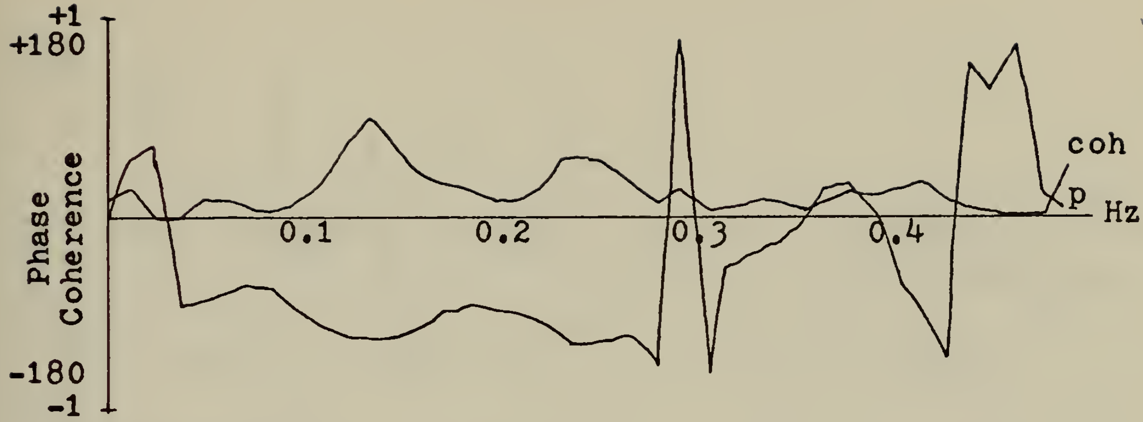

Frequency = 112519 Hz

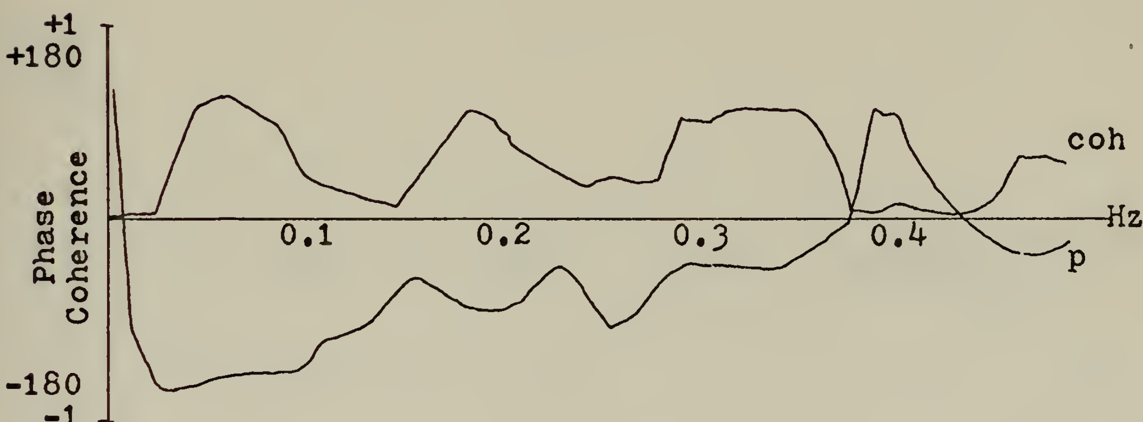

Frequency = 123720 Hz

Coherence Function: Phase and Wave Height
Cross-Spectral Phase Angle

Fig.48

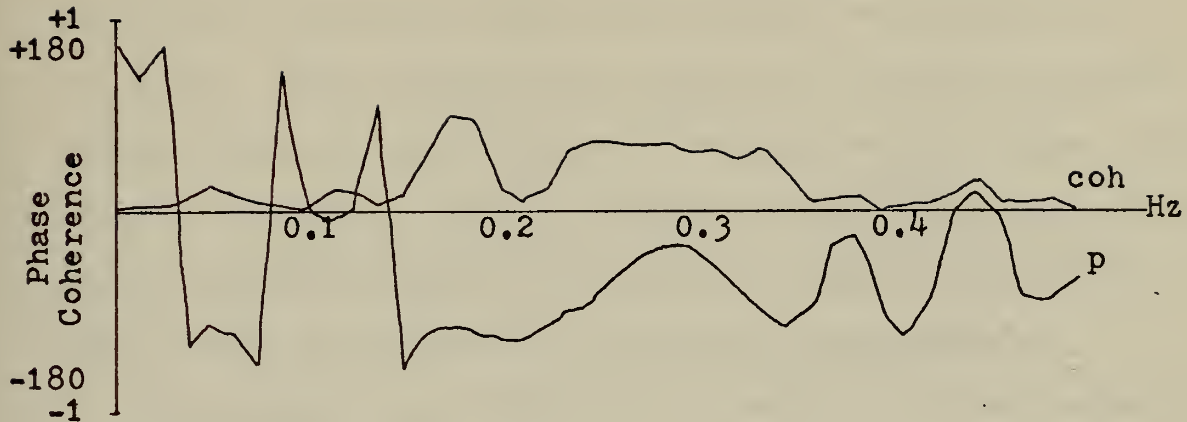

Frequency = 136800 Hz

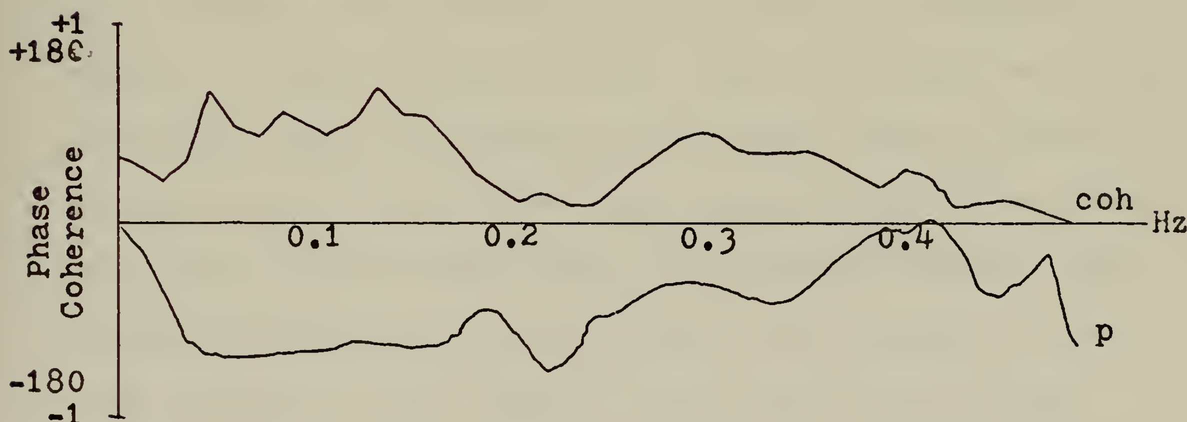

Frequency = 146100 Hz

Coherence Function: Phase and Wave Height
Cross-Spectral Phase Angle

Fig. 49

IX. SUMMARY AND CONCLUSIONS

The statistics of the instantaneous output of two hydrophones separated by one meter were studied between the frequencies of 15 to 151 kHz. The experiment was carried out from the NUC Oceanographic Research Tower off-shore at Mission Bay, San Diego. This study is of interest because bubbles and upper ocean fluctuations have significant effects on the speed of sound in addition to those caused by temperature and salinity inhomogeneities.

The experiment was conducted at a depth of 11 feet during sea state 1 conditions and a 4 ft peak to trough swell wave in the evening hours 19-2200 on 5 June 1972. The values ranged from +7.8 m/sec to -8 m/sec relative to the empirically predicted values of the Wilson and Leroy equations. The differential speed had a minimum corrected value of -2.4 m/sec at 19 kHz which suggests a batch of bubbles greater than 200 microns have been identified. Possible explanations are that these are bubbles that come from the bottom, or that they represent biological entities. There were speed of sound peaks at 41, 68 and 86 kHz. These identify a large population of bubbles, particuliarly in the range 56.3 to 71.1 kHz (bubble radii of 50 to 60 microns).

The statistical analysis shows that for frequencies below the peak bubble populations the distribution of the instantaneous sound speed can be approximated by a Gaussian probability density function. At frequencies in and above the bubble populations, the variations in the sound speed lose the smooth Gaussian envelope and become irregular, sometimes double peaked.

The correlation functions show the surface wave height and phase fluctuations are in step at frequencies where bubble populations appear. Above these frequencies the phase and wave height are relatively uncorrelated. There is evidence of long period correlation with internal waves.

The spectral densities of both the phase and wave height show strongest values at frequencies of 0.4 Hz and below. The strongest values in the phase modulation spectrum were for sound in the range 41 to 71 kHz and were identifiable with the surface wave spectrum.

APPENDIX A: PRESENTATION OF DATA

TABLE I. Speed of Sound in Meters per Second

Frequency (kHz)	Segment	Wilson	Leroy	Ramsey	Phase
14.97	1	1515.82	1515.79	1514.70	1509.76
	2	1515.73	1515.70	1514.53	1507.74
	3	1515.85	1515.82	1514.71	1507.82
	4	1515.84	1515.84	1514.75	1507.71
	5	1516.06	1516.02	1514.93	1507.51
	6	1515.97	1515.93	1514.86	1507.73
	7	1515.85	1515.82	1514.73	1507.29
18.78	1	1515.20	1515.17	1514.15	1518.70
	2	1515.29	1515.26	1514.25	1518.10
	3	1515.65	1515.61	1514.58	1517.70
	4	1516.03	1515.99	1514.95	1517.28
	5	1516.09	1516.05	1515.00	1516.39
	6	1516.00	1515.96	1515.00	1517.09
	7	1515.97	1515.03	1514.95	1516.85
22.42	1	1515.85	1515.82	1514.70	1512.15
	2	1515.59	1515.55	1514.56	1511.73
	3	1516.00	1515.96	1514.93	1511.15
	4	1516.06	1516.02	1514.76	1510.91
	5	1516.00	1515.06	1514.63	1511.61
	6	1516.12	1516.08	1515.03	1511.99
	7	1516.44	1516.40	1515.41	1512.53
26.17	1	1515.62	1515.58	1514.50	1515.16
	2	1516.00	1515.96	1514.96	1515.20
	3	1516.59	1516.54	1515.61	1514.80
	4	1515.82	1515.79	1514.66	1514.96
	5	1515.91	1515.87	1514.80	1515.31
	6	1515.59	1515.55	1514.08	1515.17
	7	1515.41	1515.38	1514.26	1515.13
33.70	1	1515.68	1515.64	1514.58	1518.71
	2	1515.65	1515.61	1514.58	1518.75
	3	1515.62	1515.58	1514.58	1518.38
	4	1515.71	1515.67	1514.73	1518.53
	5	1515.88	1515.84	1514.90	1518.78
	6	1515.85	1515.82	1514.86	1518.69
	7	1515.62	1515.58	1514.60	1518.66

TABLE I. (continued)

Frequency (kHz)	Segment	Wilson	Leroy	Ramsey	Phase
37.47	1	1515.08	1515.06	1514.15	1519.28
	2	1515.44	1515.41	1514.56	1518.73
	3	1516.29	1516.25	1515.31	1517.24
	4	1516.06	1516.02	1515.06	1516.50
	5	1515.59	1515.55	1514.63	1516.06
	6	1515.53	1515.50	1514.55	1516.41
	7	1515.94	1515.90	1514.98	1516.65
41.32	1	1514.52	1514.50	1513.56	1523.41
	2	1514.76	1514.74	1513.76	1522.88
	3	1515.68	1515.64	1514.60	1521.55
	4	1515.50	1515.47	1514.45	1520.85
	5	1515.38	1515.35	1514.38	1520.48
	6	1515.71	1515.67	1514.66	1520.79
	7	1515.38	1515.35	1514.38	1521.02
45.04	1	1515.56	1515.53	1514.51	1521.24
	2	1515.68	1515.64	1514.55	1520.48
	3	1515.47	1515.44	1514.41	1520.38
	4	1515.50	1515.47	1514.48	1520.27
	5	1515.85	1515.82	1514.81	1519.79
	6	1516.09	1516.05	1515.08	1519.37
	7	1516.09	1516.05	1515.06	1519.16
48.73	1	1515.20	1515.17	Invalid	1519.81
	2	1515.35	1515.32	1514.40	1519.10
	3	1515.35	1515.32	1514.31	1519.02
	4	1515.35	1515.32	1514.33	1518.91
	5	1515.29	1515.26	1514.30	1518.47
	6	1515.29	1515.26	1514.30	1518.09
	7	1515.59	1515.55	1514.60	1517.89
52.46	1	1515.44	1515.41	1514.45	1519.09
	2	1515.71	1515.67	1514.73	1518.46
	3	1515.79	1515.76	1514.78	1518.08
	4	1515.71	1515.67	1514.75	1517.64
	5	1515.79	1515.76	1514.88	1517.97
	6	1515.73	1515.70	1514.70	1517.57
	7	1515.32	1515.29	1514.36	1517.51

TABLE I. (continued)

Frequency (kHz)	Segment	Wilson	Leroy	Ramsey	Phase
56.25	1	1515.82	1515.79	1514.55	1520.98
	2	1515.59	1515.55	1514.53	1520.53
	3	1515.56	1515.53	1514.41	1520.75
	4	1515.17	1515.15	1514.16	1521.86
	5	1515.50	1515.44	1514.43	1522.07
	6	1515.08	1515.06	1514.05	1522.16
	7	1515.79	1514.76	1513.73	1521.99
63.79	1	1515.76	1515.73	1514.61	1523.16
	2	1515.08	1515.06	1513.88	1522.95
	3	1514.67	1514.65	1513.40	1523.41
	4	1515.05	1515.03	1513.86	1523.26
	5	1515.03	1515.00	1513.86	1523.30
	6	1515.44	1515.41	1514.23	1522.65
	7	1515.56	1515.53	1514.33	1522.27
67.50	1	1516.06	1516.00	1514.73	1522.46
	2	1515.65	1515.61	1514.36	1522.74
	3	1515.65	1515.61	1514.51	1522.44
	4	1515.62	1515.58	1514.31	1522.48
	5	1515.32	1515.29	1514.20	1521.93
	6	1515.44	1515.41	1514.13	1522.41
	7	1515.44	1515.41	1514.23	1522.18
71.13	1	1515.47	1515.44	1514.26	1519.81
	2	1515.76	1515.73	1514.53	1519.95
	3	1516.15	1516.11	1514.88	1519.38
	4	1515.65	1515.61	1514.25	1518.98
	5	1515.68	1515.64	1514.30	1519.51
	6	1515.91	1515.87	1514.58	1519.58
	7	1516.09	1516.05	1514.68	1519.08
74.97	1	1517.66	1517.60	1517.03	1521.76
	2	1517.69	1517.63	1517.18	1521.59
	3	1517.58	1517.51	1516.80	1521.50
	4	1517.40	1517.34	1516.90	1521.47
	5	1517.72	1517.66	1517.13	1521.58
	6	1518.01	1517.94	1517.63	1521.65
	7	1518.18	1518.11	1517.60	1521.55

TABLE I. (continued)

Frequency (kHz)	Segment	Wilson	Leroy	Ramsey	Phase
82.55	1	1518.13	1518.05	1517.48	1523.69
	2	1517.87	1517.80	1517.38	1523.49
	3	1517.90	1517.83	1517.42	1523.44
	4	1517.98	1517.91	1517.50	1523.37
	5	1518.33	1518.25	1517.62	1523.67
	6	Invalid	Invalid	1517.62	1523.50
	7	Invalid	Invalid	1517.72	1523.27
86.21	1	1518.27	1518.20	1517.42	1521.76
	2	1517.98	1517.91	1517.20	1521.87
	3	1517.87	1517.80	1517.10	1521.93
	4	1517.66	1517.60	1516.88	1621.93
	5	1516.88	1516.83	1516.97	1521.91
	6	1517.90	1517.83	1517.12	1522.10
	7	1517.98	1517.91	1517.20	1522.20
89.90	1	Invalid	Invalid	1517.53	1521.05
	2	Invalid	Invalid	1517.40	1520.70
	3	1517.87	1517.80	1517.00	1520.62
	4	1518.16	1518.08	1517.27	1520.74
	5	1518.36	1518.28	1517.58	1520.48
	6	1518.41	1518.33	1517.65	1520.54
	7	1518.44	1518.37	1517.62	1520.82
93.67	1	1518.50	1518.42	1517.77	1521.21
	2	1518.50	1518.42	1517.78	1521.17
	3	1518.53	1518.45	1517.83	1521.10
	4	1518.47	1518.39	1517.75	1520.89
	5	1518.39	1518.30	1517.78	1521.14
	6	1518.50	1518.42	1517.85	1521.19
	7	Invalid	Invalid	1517.87	1521.22
97.44	1	1518.44	1518.37	1517.73	1521.86
	2	1518.27	1518.20	1517.63	1521.87
	3	1518.39	1518.31	1517.77	1521.88
	4	1518.39	1518.31	1517.73	1521.83
	5	1518.36	1518.28	1517.68	1521.82
	6	1518.41	1518.34	1517.57	1522.09
	7	1518.27	1518.20	1517.62	1521.89

TABLE I. (continued)

Frequency (kHz)	Segment	Wilson	Leroy	Ramsey	Phase
101.18	1	1518.44	1518.37	1517.78	1521.82
	2	1518.44	1518.37	1517.78	1521.71
	3	1518.53	1518.45	1517.67	1521.76
	4	1518.59	1518.51	1517.93	1521.87
	5	1518.50	1518.42	1517.83	1521.78
	6	1518.47	1518.39	1517.85	1521.81
	7	1518.59	1518.51	1517.67	1521.71
104.94	1	1518.24	1518.17	1517.43	1522.19
	2	1518.36	1518.28	1517.57	1522.16
	3	1518.47	1518.39	1517.65	1522.18
	4	1518.41	1518.34	1517.60	1522.28
	5	1518.07	1518.00	1517.35	1522.21
	6	1518.47	1518.39	1517.22	1522.08
	7	1518.64	1518.56	1517.84	1522.39
108.72	1	1518.24	1518.17	1517.50	1522.66
	2	1518.24	1518.17	1517.50	1522.79
	3	1518.30	1518.22	1517.48	1522.71
	4	1518.50	1518.42	1517.77	1522.72
	5	1518.59	1518.51	1517.77	1523.02
	6	1518.62	1518.53	1517.80	1522.97
	7	1518.30	1518.22	1517.72	1522.85
112.52	1	1518.44	1518.37	1517.68	1523.69
	2	1518.39	1518.31	1517.62	1523.57
	3	1518.18	1518.11	1517.68	1523.62
	4	1518.07	1519.00	1517.48	1523.67
	5	1518.50	1518.42	1517.83	1523.89
	6	1518.53	1518.45	1517.77	1524.01
	7	1518.33	1518.25	1517.55	1523.79
116.26	1	1518.21	1518.14	1517.55	1523.84
	2	1518.41	1518.34	1517.63	1523.83
	3	1518.56	1518.48	1517.78	1523.75
	4	1518.59	1518.51	1517.76	1523.77
	5	1518.47	1518.39	1517.70	1523.50
	6	1518.56	1518.48	1517.72	1523.52
	7	1518.50	1518.42	1517.75	1523.52

TABLE I. (continued)

Frequency (kHz)	Segment	Wilson	Leroy	Ramsey	Phase
120.00	1	1518.50	1518.42	1517.76	1523.41
	2	1518.53	1518.45	1517.85	1523.34
	3	1518.56	1518.48	1517.80	1523.26
	4	1518.59	1518.51	1517.62	1523.74
	5	1518.21	1518.14	1517.62	1523.33
	6	1518.30	1518.22	1517.45	1523.23
	7	1518.21	1518.14	1517.45	1523.22
123.72	1	1518.41	1518.34	1517.55	1522.86
	2	1518.41	1518.34	1517.55	1523.01
	3	1518.47	1518.39	1517.58	1522.90
	4	1518.44	1518.37	1517.61	1522.81
	5	1518.47	1518.39	1517.65	1522.93
	6	1518.50	1518.42	1517.68	1522.80
	7	1518.50	1518.42	1517.65	1522.87
127.46	1	1518.44	1518.37	1517.45	1522.97
	2	1518.44	1518.37	1517.55	1522.82
	3	1518.44	1518.37	1517.57	1522.77
	4	1518.44	1518.37	1517.25	1522.80
	5	1518.44	1518.37	1517.58	1522.75
	6	1518.44	1518.37	1517.53	1522.78
	7	1518.39	1518.31	1517.50	1522.87
131.19	1	1518.36	1518.28	1517.22	1522.75
	2	1518.36	1518.28	1517.25	1522.70
	3	1518.39	1518.31	1517.27	1522.75
	4	1518.36	1518.28	1517.28	1522.67
	5	1518.44	1518.37	1517.38	1522.68
	6	1518.41	1518.34	1517.40	1522.38
	7	1518.39	1518.31	1517.40	1522.27
136.80	1	1518.13	1518.05	1516.83	1522.78
	2	1518.01	1517.94	1516.75	1522.71
	3	1518.07	1518.00	1516.87	1522.66
	4	1518.30	1518.22	1516.95	1522.65
	5	1518.27	1518.20	1517.17	1522.78
	6	1518.27	1518.20	1517.10	1522.79
	7	1518.27	1518.20	1517.15	1522.39

TABLE I. (continued)

Frequency (kHz)	Segment	Wilson	Leroy	Ramsey	Phase
142.39	1	1518.04	1517.97	1516.90	1522.46
	2	1517.72	1517.66	1516.98	1522.40
	3	1518.10	1518.03	1517.08	1522.78
	4	1518.07	1518.00	1517.17	1522.48
	5	1518.04	1517.97	1517.13	1522.28
	6	1517.98	1517.91	1517.10	1522.34
	7	1517.95	1517.88	1517.10	1522.36
146.10	1	1518.04	1518.00	1518.85	1523.08
	2	1518.13	1518.05	1519.38	1521.92
	3	1517.98	1517.91	1519.15	1521.76
	4	1518.10	1518.03	1519.22	1521.61
	5	1518.10	1518.03	1518.67	1521.63
	6	1517.90	1517.83	1518.75	1521.82
	7	1517.98	1517.91	1519.62	1521.66
151.63	1	1518.24	1518.17	1517.71	1519.80
	2	1518.27	1518.20	1517.42	1520.96
	3	1518.27	1518.20	1517.23	1520.83
	4	1518.21	1518.14	1517.13	1520.76
	5	1518.07	1518.00	Invalid	1520.76
	6	1518.30	1518.22	1517.63	1520.88
	7	1518.39	1518.31	1517.60	1520.72

COMPUTER PROGRAM 1: 7 TO 9 TRACK CONVERT,FILTER AND SCALE

```
      DIMENSION IDAT(1024),DAT(1024),DAT1(512),DAT2(512),
     1DAT1C(512),DAT2C(512),XPLOT(5120),Y1PLOT(5120),Y2PLOT(5120),
     2Y3PLOT(5120),Y4PLOT(5120)
      DIMENSION DAT1CB(512)
      REAL*4 Y1/'PHNC'/
      REAL*4 Y2/'PHCL'/
      REAL*4 Y3/'WHNC'/
      REAL*4 Y4/'WHCL'/
      FACTOR=100.0/( 2**23)
      SCALE1=1.000000
      SCALE2=6.096000
      REWIND 2
      REWIND 4
      N=1
      LRECL=1024
      DIF=4.00000
      CLIMB=.2000000
      K=0
      KEEP=0
   11 J=0
   10 READ(2,15,END=50,ERR=60) IDAT
   15 FORMAT(8(128A4))
      J=J+1
      WRITE(6,70)J
   70 FORMAT('0',10X,'RECORD NO.=',I4)
      CALL FORM(IDAT,LRECL)
      DO 22 I=1,LRECL
   22 DAT(I)=IDAT(I)*FACTOR
   23 DO 199 I=2,LRECL,2
      M=I/2
      DAT1(M)=DAT(I-1)*SCALE1
  199 DAT2(M)=DAT(I)*SCALE2
      WRITE(8,16) DAT1
      WRITE(9,16) DAT2
   16 FORMAT(4(128A4))
      DO 400 LL=1,512
  400 DAT2C(LL)=DAT2(LL)
      WRITE(11,16) DAT2C
      DO 293 JJ=1,512
      IF(JJ.EQ.1) GO TO 209
      DEL1=ABS(DAT1(JJ-1)-DAT1(JJ))
      IF(DEL1.GT.DIF) GO TO 200
      IF(K.GT.0) GO TO 202
      GO TO 212
  200 IF(K.EQ.0) GO TO 201
```

```
      GO TO 202
  201 JSAVE=JJ
      SAVE1=DAT1(JSAVE-1)
  202 DELTA1=(SAVE1-DAT1(JJ))
      ADELTA=ABS(DELTA1)
      ACLIMB=CLIMB*(K+1)
  206 IF(ADELTA.LT.ACLIMB) GO TO 203
      GO TO 217
  203 IF(KEEP.GT.0) GO TO 214
      DO 207 KK=1,K
  207 DAT1CB(JSAVE-1+KK)=SAVE1-KK*DELTA1/(K+1)
      K=0
      GO TO 212
  209 IF(J.EQ.1) GO TO 212
      IF(K.EQ.0) GO TO 213
      GO TO 214
  213 DELS1=ABS(SAVE2-DAT1(1))
      IF(DELS1.GT.DIF) GO TO 401
      GO TO 212
  401 JSAVE=1
      DELTA1=DELS1
      GO TO 217
  214 DELTA1=(SAVE1-DAT1(JJ))
      ADELTA=ABS(DELTA1)
      IF(ADELTA.LT.ACLIMB) GO TO 223
      GO TO 217
  223 DO 237 KKK=1,KEEP
  237 DAT1C(JSAVE-1+KKK)=SAVE1-KKK*DELTA1/(K+1)
      WRITE(10,16) DAT1C
      WRITE(6,3000) K,JJ
 3000 FORMAT(1H ,'K= 'I4,5X,'JJ= ',I4)
      IF(JJ.EQ.1) GO TO 248
      KT=JJ-1
      WRITE(6,1000)
 1000 FORMAT(1H ,'CHECK')
  245 DO 247 KIK=1,KT
      DAT1CB(KIK)=SAVE1-(KIK+KEEP)*DELTA1/(K+1)
  247 WRITE(6,2000) DAT1CB(KIK)
 2000 FORMAT(F9.4)
      KEEP=0
      WRITE(6,2001)
 2001 FORMAT(1H ,'CHECK2')
  248 K=0
      GO TO 292
  217 K=K+1
  212 ICK=1
  292 DAT1CB(JJ)=DAT1(JJ)
  293 CONTINUE
```

```
      IF(K.GT.0) GO TO 218
      SAVE2=DAT1(512)
      WRITE(10,16) DAT1CB
      GO TO 10
  218 SAVE1=DAT1(JSAVE-1)
      KEEP=K
      WRITE(6,3001) KEEP,SAVE1
 3001 FORMAT(1H ,'KEEP= ',I4,5X,'SAVE1= ',F9.4)
      DO 219 L1=1,512
  219 DAT1C(L1)=DAT1CB(L1)
      GO TO 10
   60 WRITE(6,61) J
   61 FORMAT('0',5X,'READ ERROR,RECORD NO.=',I3)
      GO TO 10
   50 WRITE(6,51) N,J
   51 FORMAT('0',5X,'END OF FILE ',I2,'RECORD NO.=',I3)
      IF(K.GT.0) WRITE(10,16) DATICB
      REWIND 8
      REWIND 9
  101 READ(8,16,END=102) DAT1
      WRITE(4,16) DAT1
      GO TO 101
  102 READ(9,16,END=104) DAT2
      WRITE(4,16) DAT2
      GO TO 102
  104 END FILE 4
      REWIND 10
      REWIND 11
  301 READ(10,16,END=302) DAT1C
      WRITE(4,16) DAT1C
      GO TO 301
  302 READ(11,16,END=304) DAT2C
      WRITE(4,16) DAT2C
      GO TO 302
  304 END FILE 4
      DO 220 I=1,5120
  220 XPLOT(I)=.02*I
      REWIND 8
      REWIND 9
      REWIND 10
      REWIND 11
      READ(8,18) (Y1PLOT(J),J=1,5120)
   18 FORMAT(4(128A4))
      READ(10,18) (Y2PLOT(J),J=1,5120)
      READ(9,18) (Y3PLOT(J),J=1,5120)
      READ(11,18) (Y4PLOT(J),J=1,5120)
      WRITE(6,20)
   20 FORMAT(1H1,4X,'TIME',5X,'PHASE NC',5X,'PHASE CL',5X,'WAVEH NC',5X,
```

```
     1'WAVEH CL')
      WRITE(6,19)(XPLOT(I),Y1PLOT(I),Y2PLOT(I),Y3PLOT(I),Y4PLOT(I),I=1,
     15120)
   19 FORMAT(5(F9.4,5X))
      DO 500 J1=1,2560
      TEMP=Y1PLOT(5121-J1)
      Y1PLOT(5121-J1)=Y1PLOT(J1)
      Y1PLOT(J1)=TEMP
      TEMP=Y2PLOT(5121-J1)
      Y2PLOT(5121-J1)=Y2PLOT(J1)
      Y2PLOT(J1)=TEMP
      TEMP=Y3PLOT(5121-J1)
      Y3PLOT(5121-J1)=Y3PLOT(J1)
      Y3PLOT(J1)=TEMP
      TEMP=Y4PLOT(5121-J1)
      Y4PLOT(5121-J1)=Y4PLOT(J1)
  500 Y4PLOT(J1)=TEMP
      CALL SCALE(XPLOT,5120,1,20.0,0.50,XMIN,DX)
      CALL SCALE(Y1PLOT,5120,1,2.0,0.5,Y1MIN,DY1)
      CALL SCALE(Y2PLOT,5120,1,2.0,0.5,Y2MIN,DY2)
      CALL SCALE(Y3PLOT,5120,1,2.0,0.5,Y3MIN,DY3)
      CALL SCALE(Y4PLOT,5120,1,2.0,0.5,Y4MIN,DY4)
      CALL PLOTS
      CALL PLOT(0.0,0.0,-3)
      CALL AXIS(0.0,20.5,Y1,+4,2.0,0.0,Y1MIN,DY1)
      CALL AXIS(2.25,20.5,Y2,+4,2.0,0.0,Y2MIN,DY2)
      CALL AXIS(4.50,20.5,Y3,+4,2.0,0.0,Y3MIN,DY3)
      CALL AXIS(6.75,20.5,Y4,+4,2.0,0.0,Y4MIN,DY4)
      CALL PLOT(0.0,0.0,-3)
      CALL LINE(Y1PLOT,XPLOT,5120,1,1)
      CALL PLOT(2.25,0.0,-3)
      CALL LINE(Y2PLOT,XPLOT,5120,1,1)
      CALL PLOT(2.25,0.0,-3)
      CALL LINE(Y3PLOT,XPLOT,5120,1,1)
      CALL PLOT(2.25,0.0,-3)
      CALL LINE(Y4PLOT,XPLOT,5120,1,1)
      CALL SYMBOL(-7.75,22.0,0.49,'FITZGERALD J.R.',0.0,15)
      CALL PLOT(-7.75,25.0,-3)
      CALL PLOTE
      REWIND 8
      REWIND 9
      REWIND 10
      REWIND 11
      N=N+1
      IF (N.LT.11) GO TO 11
      RETURN
      END
//GO.FT06F001  DD  SYSOUT=A,SPACE=(CYL,(50,1))
```

```
//GO.SYSPLOT   DD   SYSOUT=C,SPACE=(CYL,(25,2))
//GO.FT02F001   DD   UNIT=2400-1,VOL=SER=CON7,LABEL=(48,NL,,IN),
//     DISP=OLD,DCB=(DEN=1,RECFM=F,BLKSIZE=4096)
//GO.FT04F001  DD   UNIT=2400,VOL=SER=PHASE1,DSNAME=RUFSR2,LABEL=(83,SL),
//     DISP=(OLD,KEEP),DCB=(DEN=2,RECFM=FB,LRECL=2048,BLKSIZE=2048)
//GO.FT04F002  DD   UNIT=2400,VOL=SER=PHASE1,DSNAME=RUFSR2,LABEL=(84,SL),
//     DISP=(OLD,KEEP),DCB=(DEN=2,RECFM=FB,LRECL=2048,BLKSIZE=2048)
//GO.FT08F001   DD   UNIT=SYSDA,DSNAME=F2614.CHAN1A,
//   DCB=(RECFM=FB,LRECL=2048,BLKSIZE=2048),DISP=(NEW,DELETE),
//   SPACE=(CYL,(4,1))
//GO.FT09F001   DD   UNIT=SYSDA,DSNAME=F2614.CHAN2A,
//   DCB=(RECFM=FB,LRECL=2048,BLKSIZE=2048),DISP=(NEW,DELETE),
//   SPACE=(CYL,(4,1))
//GO.FT10F001   DD   UNIT=SYSDA,DSNAME=F2614.CHAN3A,
//   DCB=(RECFM=FB,LRECL=2048,BLKSIZE=2048),DISP=(NEW,DELETE),
//   SPACE=(CYL,(4,1))
//GO.FT11F001   DD   UNIT=SYSDA,DSNAME=F2614.CHAN4A,
//   DCB=(RECFM=FB,LRECL=2048,BLKSIZE=2048),DISP=(NEW,DELETE),
//   SPACE=(CYL,(4,1))
```

COMPUTER PROGRAM 2: COMPUTE STATISTICS FOR SEVEN SEGMENTS OF RECORD

```
      DIMENSION PHI(1536),CJJ(1536)
      REAL*8 DELC,CO
      NN=1
   77 READ (5,17) FREQ,N,X,DELTA
   17 FORMAT (F9.1,I3,2F7.4)
      EN=N
      DO 30 L=1,7
      READ (4,16) (PHI(K),K=1,1536)
   16 FORMAT (4(128A4))
      DO 40 J=1,1536
   40 PHI(J)=PHI(J)-DELTA
      CO=0.0
      PHIAV=0.0
      DELC=0.0
      PHISQ=0.0
      DO 20 J=1,1536
      PHISQ=PHISQ+(PHI(J)*PHI(J))/1536.0
      PHIAV=PHIAV+(PHI(J))/1536.0
      CJ=((FREQ*X)/(EN+PHI(J)/360.0))/1536.0
      CJJ(J)=CJ*1536.0
   20 CO=CO+CJ
      DO 199 I=1,1536
  199 DELC=DELC+((CJJ(I)-CO)**2)/1536.0
      CALL HIST(CJJ,1536,'SPEED OF SOUND',14,'OCCURRANCES',11)
      CSTAR=(FREQ*X)/(EN+PHIAV/360.0)
      RATIO=CSTAR/CO
      DELPHI=SQRT(PHISQ-PHIAV**2)
      DELC=DSQRT(DELC)
      W=(CO**2-CO*CSTAR)/(2*DELC)
      DELCN=DELC/CO**2
      WRITE (6,19)
   19 FORMAT (1H0,5X,'CO',10X,'CSTAR',12X,'STDEV',10X,'DELCN',10X,'PHIAV
     1',10X,'W',10X,'FREQ',12X,'N',4X,'CSTAR/CO',3X,'SEGMENT')
      WRITE (6,18) CO,CSTAR,DELC,DELCN,PHIAV,W,FREQ,N,RATIO,L
   18 FORMAT (7(E15.7),I3,2X,E15.7,I3)
      WRITE(6,99) PHISQ,DELPHI
   99 FORMAT(1H0,'PHI MEAN SQUARE = ',E15.7,5X,'STAN DEV = ',E15.7)
   30 CONTINUE
      STOP
      END
```

```
      SUBROUTINE HIST (/X/,/N/,/XTITLE/,/NX/,/YTITLE/,/NY/)
      REAL*8 XMEAN,SUMSQ,STDEV
      REAL*4 XRANGE,XQ1,XQ2,XQ3,R
      REAL*4 XSUM,X(1),DIV,YMAX,DY,DY2,XLABEL(15)
      INTEGER J,K,L,M,N,Q1,Q2,Q3,M2M,M1,M12,FMAX,LINE,F(14)
      LOGICAL*1 SORTED,YT,POINTS (49, 125), YTITLE (49), XTITLE (131)
      LOGICAL*1 BLANK/' '/,EM/'M'/,CROSS/'+'/,VERT/'|'/,DASH/'-'/,
     *     MEAN/.TRUE./,Q/.TRUE./,DOT/'.'/,STAR/'*'/,PLUS/'+'/,CARRGE
       EQUIVALENCE (SORTED,YT),(Q1,K),(Q2,L,FMAX),(M2M,J)
      EQUIVALENCE (Q3,TEMP,DIV,YMAX)
C-----SORT BY BUBBLE-UP METHOD
      SORTED=.TRUE.
      DO 20 J=2,N
      L=N-J+2
      DO 10 K= 2,L
      IF (X(K).GE.X(K-1)) GO TO 10
      SORTED=.FALSE.
      TEMP=X(K-1)
      X(K-1)=X(K)
      X(K)=TEMP
   10 CONTINUE
      IF (SORTED) GO TO 30
   20 CONTINUE
C-----DETERMINE 14 FREQUENCIES
   30 XRANGE = X(N) - X(1)
      R = 126./XRANGE
      DELTA X = XRANGE/14.
      K=1
      DO 50 J=1,14
      F(J)=0
      DIV=X(1)+J*DELTAX
   40 IF(X(K).GT.DIV) GOTO50
      F(J)=F(J)+1
      K=K+1
      IF (K.GT.N) GO TO 55
      GO TO  40
   50 CONTINUE
   55 IF (K.GT.N+1 .OR. K.LT.N) WRITE(6,9000) K,N
 9000 FORMAT(' ERROR:- K = ',I5,10X,'N =',I5)
      IF (K.LE.N) F(14)=F(14)+N-K+1
C-----THE FREQUENCIES ARE NOW LISTED IN ARRAY F.
C-----SET SCALING
      FMAX=F(1)
      DO 60 J=2,14
      IF (F(J).GT.FMAX) FMAX=F(J)
   60 CONTINUE
      YMAX=1.1*FMAX
C-----BLANK OUT ARRAY
```

```
      DO 70 J=1,49                                          HIST 460
      DO 70 K=1,125                                         HIST 470
   70 POINTS(J,K)=BLANK                                     HIST 480
C-----DRAW THE BARS                                         HIST 490
      DO 80 J=1,14                                          HIST 500
      LINE = 50.5 - 50.*F(J)/YMAX                           HIST 510
      IF(LINE.GT.49) GO TO 80                               HIST 520
      J9M8=J*9-8                                            HIST 530
      DO 80 K=LINE,49                                       HIST 540
      DO 80 L=1,6                                           HIST 550
      POINTS(K,J9M8+L)=EM                                   HIST 560
   80 CONTINUE                                              HIST 570
C-----COMPUTE QUARTILE VALUES                               HIST 580
      IF (.NOT.Q) GO TO 82                                  HIST 590
      Q1 = N/4                                              HIST 600
      Q2 = N/2                                              HIST 610
      Q3 = N - Q1                                           HIST 620
      M2M = 1 - MOD(N,2)                                    HIST 630
      M1 = 1 - MOD(N,4)/2                                   HIST 640
      M12 = 1 + M1                                          HIST 650
      XQ1 = (M1*X(Q1) + X(Q1+1)) / M12                      HIST 660
      XQ2 = (M2M*X(Q2) + X(Q2+1)) / (1 + M2M)               HIST 670
      XQ3 = (M1*X(Q3 + 1) + X(Q3)) / M12                    HIST 680
C-----DRAW QUARTILE LINES                                   HIST 690
      Q1 = R*(XQ1 - X(1)) + 0.5                             HIST 700
      Q2 = R*(XQ2 - X(1)) + 0.5                             HIST 710
      Q3 = R*(XQ3 - X(1)) + 0.5                             HIST 720
      IF (Q1.LE.0) Q1=1                                     HIST 730
      IF (Q3.GE.126) Q3 = 125                               HIST 740
      DO 240 J=1,49                                         HIST 750
      POINTS(J,Q1) = DOT                                    HIST 760
      POINTS(J,Q2) = DOT                                    HIST 770
      POINTS(J,Q3) = DOT                                    HIST 780
  240 CONTINUE                                              HIST 790
C-----COMPUTE MEAN AND DRAW IT IN                           HIST 800
   82 IF (.NOT.MEAN) GO TO 85                               HIST 810
      SUMSQ=0                                               HIST 820
      XMEAN = 0                                             HIST 830
      DO 25 J = 1,N                                         HIST 840
      SUMSQ=SUMSQ+(X(J)**2)/1536.0                          HIST 850
   25 XMEAN = XMEAN + X(J)/1536.0                           HIST 860
      STDEV=DSQRT(DABS(SUMSQ-XMEAN**2))
      M = R*(XMEAN - X(1)) + 0.5                            HIST 890
      DO 81 J=1,49                                          HIST 900
   81 POINTS(J,M) = STAR                                    HIST 910
C-----PRINT THE FREQUENCIES                                 HIST 920
   85 WRITE(6,90)F                                          HIST 930
   90 FORMAT ('1',3X,'FREQUENCIES'/2X,14I9)                 HIST 940
```

```
C-----PRINT THE PICTURE
C      L=NARGS(L)
       L=6
       NZ=0
       IF (L.EQ.6) NZ = NY
       WRITE (6,100) BLANK,BLANK,BLANK,CROSS,(DASH,K=1,125),CROSS
  100  FORMAT(132A1)
       DO 110 J=1,49
       YT=BLANK
       IF (J.LE.NZ) YT=YTITLE(J)
       WRITE(6,100)BLANK,YT,BLANK,VERT,(POINTS(J,K),K=1,125),VERT
  110  CONTINUE
  115  WRITE(6,100) BLANK,YT,BLANK,(CROSS,(DASH,K=1,8),J=1,14),CROSS
C-----COMPUTE AND PRINT VALUES ALONG X AXIS
       DO 120 J=1,15
  120  XLABEL(J)=X(1)+(J-1)*DELTA X
  901  DO 130 J=2,10
  902  IF (XLABEL(J-1).EQ.0) GO TO 130
  903  IF (ABS(XLABEL(J)/XLABEL(J-1)).LT.0.1) XLABEL(J)=0.0
  130  CONTINUE
  904  XSUM=AMAX1(ABS(X(1)),ABS(X(N)))
  905  IF (XSUM.LT.1.) GO TO 150
  906  IF (XSUM.LT.10.) GO TO 170
  907  IF (XSUM.LT.100.) GO TO 190
  908  IF(XSUM.GE.1000) GO TO 220
  909  WRITE (6,140) XLABEL
  140  FORMAT(1X,14(F5.0,4X),F5.0)
  910  GO TO 210
  150  WRITE (6,160) XLABEL
  160  FORMAT (1X,14(F5.2,4X),F5.2)
  911  GO TO 210
  170  WRITE (6,180) XLABEL
  180  FORMAT (1X,14(F5.1,4X),F5.1)
  912  GO TO 210
  190  WRITE (6,200) XLABEL
  200  FORMAT (1X,14(F5.0,4X),F5.0)
  913  GO TO 210
  220  WRITE (6,230)  X(1),X(N)
  230  FORMAT(' X OUT OF RANGE -999 TO +999',10X,'X(1) = ',E13.6,10X,'X(N
      *) = ',E13.6)
C-----PRINT XTITLE
  210  IF (L.LT.4) GO TO 270
  914  K=121-NX
  915  IF (K.LT.1) K=(133-NX)/2
  916  WRITE (6,100) (BLANK,J=1,K),(XTITLE(J),J=1,NX)
  270  IF (Q) WRITE (6,250) XQ1,XQ2,XQ3
  250  FORMAT (' QUARTILE BOUNDARIES AT ',2(E13.6,','),E13.6)
  917  CARRGE=BLANK
```

```
918 IF (Q) CARRGE=PLUS
919 IF (MEAN) WRITE (6,260) CARRGE,XMEAN,STDEV
260 FORMAT (A1 ,T75,'MEAN = ',E13.6,10X,'ST DEV = ',E13.6)
920 MEAN=.TRUE.
921 Q=.TRUE.
930 RETURN
    ENTRY NOMEAN
    MEAN=.FALSE.
    RETURN
    ENTRY NOQUAR
    Q=.FALSE.
    RETURN
    END
```

COMPUTER PROGRAM 3: COMPUTE AUTO AND CROSS CORRELATION FNS AND SPECTRA

```
      CALL AUTO(ANORM,BNORM)
      CALL CROSS(ANORM,BNORM)
      CALL SPECTR(ANORM,BNORM)
      CALL PLOTER
      STOP
      END


      SUBROUTINE AUTO(ANORM,BNORM)
      DIMENSION A(512),B(512),SUMA(40),SUMB(40),ATCOR(256),BTCOR(256),
     1GAR(512),AX(2048),BX(2048)
      REAL*8 AVERTA,AVERTB,SUMA,SUMB
      REAL*4 MSQVLA,MSQVLB,MVSQA,MVSQB
      CALL SETIME
      READ(5,15) NDEC,NLAG,NSAMP,N,NREC
   15 FORMAT(5I6)
      REWIND 4
      KD=NLAG/NSAMP
      NREAD=5
   17 FORMAT(4(128A4))
      DO 3000 IN=1,NREAD
      READ(4,17) (AX(K),K=1,2048)
      J=0
      DO 100 I=1,2048,8
      J=J+1
      A(J)=AX(I)
  100 CONTINUE
      WRITE(8,16) (A(K),K=1,256)
 3000 CONTINUE
      DO 4321 IM=1,3
 4321 READ(4,17) (GAR(K),K=1,512)
      DO 3001 JN=1,NREAD
      READ(4,17) (BX(K),K=1,2048)
      J=0
      DO 101 I=1,2048,8
      J=J+1
      B(J)=BX(I)
  101 CONTINUE
      WRITE(9,16) (B(L),L=1,256)
 3001 CONTINUE
      REWIND 8
      REWIND 9
      NLES=NDEC-1
      FN=N*NDEC
      DO 133 J=1,NLAG
```

```
      ATCOR(J)=0.0
      BTCOR(J)=0.0
  133 CONTINUE
   16 FORMAT(128A4)
      AVERTA=0.0
      AVERTB=0.0
      DO 331 II=1,NDEC
      READ(8,16) (A(K),K=1,NLAG)
      READ(9,16) (B(L),L=1,NLAG)
      DO 110 I=1,N
      AVERTA=AVERTA+A(I)
  110 AVERTB=AVERTB+B(I)
  331 CONTINUE
      AVERTA=AVERTA/FN
      AVERTB=AVERTB/FN
      REWIND 8
      REWIND 9
      DO 131 II=1,NLES
      ILAG=2*NLAG
      READ(8,16) (A(K),K=1,ILAG)
      READ(9,16) (B(L),L=1,ILAG)
      DO 130 J=1,NLAG
      FNJ=FN-J+1
      SUMA(II)=0.0
      SUMB(II)=0.0
      DO 120 I=1,N
      IJ=I+J-1
      SUMA(II)=SUMA(II)+(A(I)-AVERTA)*(A(IJ)-AVERTA)
  120 SUMB(II)=SUMB(II)+(B(I)-AVERTB)*(B(IJ)-AVERTB)
      ATCOR(J)=ATCOR(J)+SUMA(II)/FNJ
  130 BTCOR(J)=BTCOR(J)+SUMB(II)/FNJ
      DO 79 IJ=1,KD
      BACKSPACE 8
      BACKSPACE 9
   79 CONTINUE
  131 CONTINUE
      READ(8,16) (A(K),K=1,NLAG)
      READ(9,16) (B(L),L=1,NLAG)
      DO 132 J=1,NLAG
      NJ=N-J+1
      FNJ=FN-J+1
      SUMA(NDEC)=0.0
      SUMB(NDEC)=0.0
      DO 121 I=1,NJ
      IJ=I+J-1
      SUMA(NDEC)=SUMA(NDEC)+(A(I)-AVERTA)*(A(IJ)-AVERTA)
  121 SUMB(NDEC)=SUMB(NDEC)+(B(I)-AVERTB)*(B(IJ)-AVERTB)
      ATCOR(J)=ATCOR(J)+SUMA(NDEC)/FNJ
```

```
132 BTCOR(J)=BTCOR(J)+SUMB(NDEC)/FNJ
    WRITE(11,16) ATCOR
    WRITE(12,16) BTCOR
    ANORM=ATCOR(1)
    BNORM=BTCOR(1)
    DO 38 MN=1,NLAG
    ATCOR(MN)=ATCOR(MN)/ANORM
    BTCOR(MN)=BTCOR(MN)/BNORM
 38 CONTINUE
    MVSQA=AVERTA*AVERTA
    MVSQB=AVERTB*AVERTB
    VARA=ANORM
    STDA=SQRT(ANORM)
    MSQVLA=ANORM+AVERTA**2
    VARB=BNORM
    STDB=SQRT(BNORM)
    MSQVLB=BNORM+AVERTB**2
    WRITE(6,22)
 22 FORMAT(1H1,20X,'CORRELATION FUNCTION')
    WRITE(6,26)
 26 FORMAT(1H0,'FIRST CHANNEL',8X,'SECOND CHANNEL')
    DO 5 I=1,NLAG
  5 WRITE(6,23) ATCOR(I),BTCOR(I)
 23 FORMAT(1H ,2(E11.4,10X))
    WRITE(6,26)
    WRITE(6,24)
 24 FORMAT(1H0, 40X,'MEAN')
    WRITE(6,23) AVERTA,AVERTB
 33 FORMAT(1H0,40X,'MEAN VALUE SQUARED')
    WRITE(6,33)
    WRITE(6,23) MVSQA,MVSQB
    WRITE(6,27)
 27 FORMAT(1H0,40X,'VARIANCE')
    WRITE(6,23) ANORM,BNORM
    WRITE(6,29)
 29 FORMAT(1H0,40X,'STANDARD DEVIATION')
    WRITE(6,23) STDA,STDB
    WRITE(6,28)
 28 FORMAT(1H0,40X,'MEAN SQUARE VALUE')
    WRITE(6,23) MSQVLA,MSQVLB
    WRITE(11,16) ATCOR
    WRITE(12,16) BTCOR
3003 CONTINUE
    CALL GETIME(IET)
    X=IET*.000026
    WRITE(6,99) X
 99 FORMAT(1H0,'REAL TIME CLOCK READS',2X,E16.6,3X,'SECONDS')
    RETURN
```

```
      END

      SUBROUTINE CROSS(ANORM,BNORM)
      DIMENSION SUMAB(40),SUMBA(40),ABTCOR(256),BATCOR(256),A(512),B(512
     1)
      REAL*8 AVERTA,AVERTB,SUMAB,SUMBA
      ABNORM=ANORM*BNORM
      READ(5,15) NDEC,NLAG,NSAMP,N,NREC
      CALL SETIME
   15 FORMAT(5I6)
   16 FORMAT(128A4)
      KD=NLAG/NSAMP
      FN=N*NDEC
      NLES=NDEC-1
      DO 500 J=1,NLAG
      ABTCOR(J)=0.0
  500 BATCOR(J)=0.0
      IF(N0) 2001,2000,2001
 2001 WRITE(6,29)
   29 FORMAT(1H1,20X,'CROSS CORRELATION FUNCTIONS')
      WRITE(6,1001)
 1001 FORMAT(1H0,'FIRST CHANNEL WITH SECOND CHANNEL', 5X,'SECOND CHANNEL
     1 WITH FIRST CHANNEL')
      REWIND 8
      REWIND 9
      AVERTA=0.0
      AVERTB=0.0
      DO 331 II=1,NDEC
      READ(8,16) (A(K),K=1,NLAG)
      READ(9,16) (B(K),K=1,NLAG)
      DO 110 I=1,N
      AVERTA=AVERTA+A(I)
  110 AVERTB=AVERTB+B(I)
  331 CONTINUE
      AVERTA=AVERTA/FN
      AVERTB=AVERTB/FN
      REWIND 8
      REWIND 9
      ILAG=NLAG*2
      DO 231 II=1,NLES
      READ(8,16) (A(K),K=1,ILAG)
      READ(9,16) (B(L),L=1,ILAG)
      DO 230 J=1,NLAG
      FNJ=FN-J+1
      SUMBA(II)=0.0
      SUMAB(II)=0.0
      DO 220 I=1,N
```

```
      IJ=I+J-1
      SUMAB(II)=SUMAB(II)+(A(I)-AVERTA)*(B(IJ)-AVERTB)
  220 SUMBA(II)=SUMBA(II)+(B(I)-AVERTB)*(A(IJ)-AVERTA)
      ABTCOR(J)=ABTCOR(J)+SUMAB(II)/FNJ
  230 BATCOR(J)=BATCOR(J)+SUMBA(II)/FNJ
      DO 79 IJ=1,KD
      BACKSPACE 8
      BACKSPACE 9
   79 CONTINUE
  231 CONTINUE
      READ(8,16)  (A(K),K=1,NLAG)
      READ(9,16)  (B(L),L=1,NLAG)
      DO 232  J=1,NLAG
      NJ=N-J+1
      FNJ=FN-J+1
      SUMAB(NDEC)=0.0
      SUMBA(NDEC)=0.0
      DO 221  I=1,NJ
      IJ=I+J-1
      SUMAB(NDEC)=SUMAB(NDEC)+(A(I)-AVERTA)*(B(IJ)-AVERTB)
  221 SUMBA(NDEC)=SUMBA(NDEC)+(B(I)-AVERTB)*(A(IJ)-AVERTA)
      ABTCOR(J)=ABTCOR(J)+SUMAB(NDEC)/FNJ
  232 BATCOR(J)=BATCOR(J)+SUMBA(NDEC)/FNJ
      DO 234  J=1,NLAG
      WRITE(6,1002)  ABTCOR(J),BATCOR(J)
  234 CONTINUE
      WRITE(14,16) ABTCOR
      WRITE(14,16) BATCOR
 1002 FORMAT(1H ,2(E11.4,27X))
 2000 CONTINUE
      CALL GETIME(IET)
      X=IET*.000026
      WRITE(6,99) X
   99 FORMAT(1H0,'REAL TIME CLOCK READS',2X,E16.6,3X,'SECONDS')
      RETURN
      END


      SUBROUTINE SPECTR(ANORM,BNORM)
      DIMENSION SPECA(256),SPECB(256),HAMMA(256),HAMMB(256),PARZAB(512),
     1RHAMMA(256),RHAMMB(256),M(3),INV(256),S(256),PARZR(1025),PARZI(102
     25),PHASE(256),COH(256),ATCOR(256),BTCOR(256),
     3SRECA(256),SRECB(256),ABTCOR(256),BATCOR(256),COR1(512),COR(512),
     4TAU(512),FREQ(1025),SCOR(256),DCOR(256)
      READ(5,15) NDEC,NLAG,NSAMP,N,NREC
   15 FORMAT(5I6)
      COMPLEX*8 SPECA,SPECB,HAMMA,HAMMB,PARZAB
      IF(NO.EQ.-1) GO TO 29
```

```
      REWIND 11
      REWIND 12
      READ(11,16) ATCOR
      READ(12,16) BTCOR
   16 FORMAT(128A4)
      DO 1 I=1,NLAG
      SPECA(I)=CMPLX(ATCOR(I),0.0)
    1 SPECB(I)=CMPLX(BTCOR(I),0.0)
      M(1)=8
      M(2)=0
      M(3)=0
      WRITE(6,24)
   24 FORMAT(1H1,50X,'SPECTRA - AUTO')
      WRITE(6,25)
   25 FORMAT(1H0,10X,'FIRST CHANNEL',10X,'SECOND CHANNEL')
      CALL SETIME
      CALL HARM(SPECA,M,INV,S,+1,IFERR)
      CALL GETIME(IET)
      X=IET*.000026
      WRITE(6,99) X
   99 FORMAT(1H0,'REAL TIME CLOCK READS',2X,E16.6,3X,'SECONDS')
      CALL SETIME
      CALL HARM(SPECB,M,INV,S,+1,IFERR)
      DO 700 I=1,NLAG
      SRECA(I)=REAL(SPECA(I))
      SRECB(I)=REAL(SPECB(I))
   26 FORMAT(1H ,2(11X,E11.4))
  700 WRITE(6,26) SRECA(I),SRECB(I)
      WRITE(6,24)
      WRITE(6,51)
   51 FORMAT(1H0,5X,'HAMMING')
      WRITE(6,25)
      DO 2 I=1,NLAG
      HAMMA(I)=(+.540000+.460000*COS(3.1416*(FLOAT(I-1))/(FLOAT(NLAG-1))
     1))*CMPLX(ATCOR(I),0.0)
    2 HAMMB(I)=(+.540000+.460000*COS(3.1416*(FLOAT(I-1))/(FLOAT(NLAG-1))
     1))*CMPLX(BTCOR(I),0.0)
      CALL HARM(HAMMA,M,INV,S,+1,IFERR)
      CALL HARM(HAMMB,M,INV,S,+1,IFERR)
      DO 710 I=1,NLAG
      RHAMMA(I)=REAL(HAMMA(I))
      RHAMMB(I)=REAL(HAMMB(I))
  710 WRITE(6,26) RHAMMA(I),RHAMMB(I)
      READ(11,16) ATCOR
      READ(12,16) BTCOR
      WRITE(11,16) RHAMMA
      WRITE(12,16) RHAMMB
   29 WRITE(6,27)
```

```
   27 FORMAT(1H1,50X,'SPECTRA - CROSS')
      WRITE(6,28)
   28 FORMAT(1H0,'FIRST CHANNEL WITH SECOND CHANNEL')
      WRITE(6,31)
   31 FORMAT(1H0,5X,'CO-SPECTRA',5X,'QUAD-SPECTRA',5X,'PHASE',10X,
     1'COHERENCE')
      REWIND 14
      REWIND 15
      READ(14,16) ABTCOR
      READ(14,16) BATCOR
      DO 900 J=1,256
      COR1(J)=BATCOR(257-J)
  900 COR(J)=BATCOR(257-J)
      DO 901 I=257,512
      COR1(I)=ABTCOR(I-256)
  901 COR(I)=ABTCOR(I-256)
      MLAG=NLAG/2
      MLAG1=MLAG+1
      DO 87 K=1,MLAG
      MM=K-1
      R=MM
      RM=R/NLAG
      MA=NLAG+MM
      MB=NLAG-MM
      UM=1.0-6.0*RM*RM*(1.0-RM)
      COR(MA)=COR(MA)*UM
      COR(MB)=COR(MB)*UM
   87 CONTINUE
      DO 88 KK=MLAG1,NLAG
      MM=KK-1
      R=MM
      RM=R/NLAG
      RM1=(1.0-RM)
      MA=NLAG+MM
      MB=NLAG-MM
      UM=2.0*RM1*RM1*RM1
      COR(MA)=COR(MA)*UM
      COR(MB)=COR(MB)*UM
   88 CONTINUE
      FHZ=3.125
      DFHZ=1.00/(DT*NLAG*2.00)
      NFREQ=FHZ/DFHZ+0.1
      DF=DFHZ*6.28318
      DT=0.1600
      MT=2*NLAG-1
      DO 46 JJ=1,MT
      TAU(JJ)=JJ-NLAG
   46 TAU(JJ)=TAU(JJ)*DT
```

```
      DO 47 MM=1,NFREQ
      XN=MM
   47 FREQ(MM)=(XN-1.0)*DF
      DO 30 JK=1,NLAG
      MM=JK-1
      MA=NLAG+MM
      MB=NLAG-MM
      SCOR(JK)=COR(MA)+COR(MB)
   30 DCOR(JK)=COR(MA)-COR(MB)
      DO 40 N=1,NFREQ
      SUM1=0.5*(SCOR(1)+SCOR(NLAG)*COS(FREQ(N)*TAU(NLAG)))
      SUM2=0.5*(DCOR(1)+DCOR(NLAG)*SIN(FREQ(N)*TAU(NLAG)))
      C1=COS(FREQ(N)*DT)
      S1=SIN(FREQ(N)*DT)
      CC=1.0
      SC=0.0
      NLAG1=NLAG-1
      DO 36 KJ=2,NLAG1
      CT=CC*C1-SC*S1
      ST=SC*C1+CC*S1
      CC=CT
      SC=ST
      SUM1=SUM1+SCOR(KJ)*CC
   36 SUM2=SUM2+DCOR(KJ)*SC
      PARZR(N)=SUM1/NLAG
   40 PARZI(N)=SUM2/NLAG
      DO 703 II=1,NLAG
      IF(PARZR(II).EQ.0.0) GO TO 999
      GO TO 6000
  999 IF (PARZI(II)) 1000,2000,3000
 1000 PHASE(II)=-90.0
      GO TO 4000
 2000 PHASE(II)=0.0
      GO TO 4000
 3000 PHASE(II)=+90.0
      GO TO 4000
 6000 PHASE(II)=ATAN(PARZI(II)/PARZR(II))*180.000/3.1416
 4000 COH(I)=((PARZR(I))**2+(PARZI(I))**2)/((RHAMMA(II))*(RHAMMB(II)))
      II=II+1
   32 FORMAT(1H ,4(5X,E11.4))
  703 WRITE(6,32) PARZR(II),PARZI(II),PHASE(II),COH(II)
   38 FORMAT(1H ,11X,E11.4)
      ABNORM=ANORM*BNORM
      DO 438 JK=1,512
      COR1(JK)=COR1(JK)/SQRT(ABNORM)
  438 WRITE(6,38) COR1(JK)
      WRITE(15,16) COR1
      WRITE(14,16) COH
```

```
      WRITE(14,16) PHASE
 8000 CONTINUE
      CALL GETIME(IET)
      X=IET*.000026
      WRITE(6,99) X
      RETURN
      END


      SUBROUTINE PLOTER
      DIMENSION X1PLOT(256),X2PLOT(256),X3PLOT(256),Y1PLOT(256),Y2PLOT(5
     112),X4PLOT(512)
      READ(5,15) NDEC,NLAG,NSAMP,N,NREC
   15 FORMAT(5I6)
      CALL SETIME
      REAL*4 XX/'    '/
      M=4
      MLAG=90
      SMRT=6.2500
      DELS=SMRT/NLAG
      X3PLOT(1)=-2.0
      JLAG=NLAG/2
      DO 4001 J=1,512
      X4PLOT(J)=(J-1)/102.4
 4001 CONTINUE
      DO 4000 I=1,NLAG
      X1PLOT(I)=(I-1)/SMRT
      X2PLOT(I)=(I-1)*DELS
      IF(I.EQ.1) GO TO 4000
      X3PLOT(I)=ALOG10(X2PLOT(I))
 4000 CONTINUE
      CALL SCALE(X1PLOT,NLAG,1,5.0,0.5,X1MIN,DX1)
      CALL SCALE(X2PLOT,MLAG,1,5.0,0.5,X2MIN,DX2)
      CALL SCALE(X3PLOT,JLAG,1,5.0,0.5,X3MIN,DX3)
      IF(NO.EQ.-1) GO TO 29
    2 REWIND 11
      REWIND 12
      READ(11,16) (Y1PLOT(J),J=1,NLAG)
      READ(11,16) (Y1PLOT(J),J=1,NLAG)
   16 FORMAT(128A4)
      CALL SCALE (Y1PLOT,NLAG,1,7.00,0.5,Y1MIN,DY)
      CALL PLOTS
      CALL PLOT(-10.0,12.0,-3)
      CALL PLOTE
      CALL PLOTS
      CALL PLOT(.75,0.0,-3)
      CALL PLOTE
      CALL PLOTS
```

```
      CALL PLOT(0.0,0.0,-3)
      CALL AXIS (0.78,2.0,XX,M,7.0,90.0,Y1MIN,DY)
      CALL AXIS(0.78,2.0,XX,-4,5.0,0.0,X1MIN,DX1)
      CALL PLOT(0.78,2.0,-3)
      CALL LINE(X1PLOT,Y1PLOT,NLAG,1,1)
      CALL SYMBOL(0.5,-0.5,0.14,'TIME LAG IN SECONDS',0.0,19)
      CALL SYMBOL(0.0,-1.0,0.14,'PHASE',0.0,5)
      CALL SYMBOL(-0.5,0.5,0.14,'TEMPORAL AUTO CORRELATION',90.0,25)
      CALL PLOT(-0.78,16.0,-3)
      CALL PLOTE
      CALL PLOTS
      CALL PLOT(-10.0,12.0,-3)
      CALL PLOTE
      CALL PLOTS
      CALL PLOT(.75,0.0,-3)
      CALL PLOTE
      READ(12,16) (Y1PLOT(J),J=1,NLAG)
      READ(12,16) (Y1PLOT(J),J=1,NLAG)
      CALL SCALE (Y1PLOT,NLAG,1,7.00,0.5,Y1MIN,DY)
      CALL PLOTS
      CALL PLOT(0.0,0.0,-3)
      CALL AXIS(0.78,2.0,XX,-4,5.0,0.0,X1MIN,DX1)
      CALL AXIS (0.78,2.0,XX,M,7.0,90.0,Y1MIN,DY)
      CALL PLOT(0.78,2.0,-3)
      CALL LINE(X1PLOT,Y1PLOT,NLAG,1,1)
      CALL SYMBOL(0.5,-0.5,0.14,'TIME LAG IN SECONDS',0.0,19)
      CALL SYMBOL(0.0,-1.0,0.14,'WAVE HEIGHT',0.0,11)
      CALL SYMBOL(-0.5,0.5,0.14,'TEMPORAL AUTO CORRELATION',90.0,25)
      CALL PLOT(-0.78,16.0,-3)
      CALL PLOTE
      READ(11,16) (Y1PLOT(J),J=1,NLAG)
      DO 3840 KK=1,NLAG
 3840 Y1PLOT(KK)=10.0*ALOG10(Y1PLOT(KK))
      CALL SCALE (Y1PLOT,MLAG,1,7.00,0.5,Y1MIN,DY)
      CALL PLOTS
      CALL PLOT(0.0,0.0,-3)
      CALL AXIS(0.78,2.0,XX,-4,5.0,0.0,X2MIN,DX2)
      CALL AXIS (0.78,2.0,XX,M,7.0,90.0,Y1MIN,DY)
      CALL PLOT(0.78,2.0,-3)
      CALL LINE(X2PLOT,Y1PLOT,MLAG,1,1)
      CALL SYMBOL(0.5,-0.5,0.14,'FREQUENCY',0.0,9)
      CALL SYMBOL(0.0,-1.0,0.14,'PHASE HAMMING',0.0,13)
      CALL SYMBOL(-0.5,0.5,0.14,'POWER SPECTRUM LEVEL (DB)',90.0,25)
      CALL PLOT(-0.78,16.0,-3)
      CALL PLOTE
      READ(12,16) (Y1PLOT(J),J=1,NLAG)
      DO 3841 KK=1,NLAG
 3841 Y1PLOT(KK)=10.0*ALOG10(Y1PLOT(KK))
```

```
      CALL SCALE (Y1PLOT,MLAG,1,7.00,0.5,Y1MIN,DY)
      CALL PLOTS
      CALL PLOT(0.0,0.0,-3)
      CALL AXIS(0.78,2.0,XX,-4,5.0,0.0,X2MIN,DX2)
      CALL AXIS (0.78,2.0,XX,M,7.0,90.0,Y1MIN,DY)
      CALL PLOT(0.78,2.0,-3)
      CALL LINE(X2PLOT,Y1PLOT,MLAG,1,1)
      CALL SYMBOL(0.5,-0.5,0.14,'FREQUENCY',0.0,9)
      CALL SYMBOL(0.0,-1.0,0.14,'WAVE HEIGHT HAMMING',0.0,19)
      CALL SYMBOL(-0.5,0.5,0.14,'POWER SPECTRUM LEVEL (DB)',90.0,25)
      CALL PLOT(-0.78,16.0,-3)
      CALL PLOTE
   29 REWIND 14
      REWIND 15
      READ(15,16) (Y2PLOT(J),J=1,512)
      CALL SCALE (Y2PLOT,512,1,7.0,0.5,Y2MIN,DY)
      CALL PLOTS
      CALL PLOT(0.0,0.0,-3)
      CALL AXIS(0.78,2.0,XX,-4,5.0,0.0,-40.96,16.385)
      CALL AXIS (0.78,2.0,XX,M,7.0,90.0,Y2MIN,DY)
      CALL PLOT(0.78,2.0,-3)
      CALL LINE(X4PLOT,Y2PLOT,512,1,1)
      CALL SYMBOL(0.5,-0.7,0.14,'TIME LAG IN SECONDS',0.0,19)
      CALL SYMBOL(0.0,-1.0,0.14,'PHASE WITH WAVE HEIGHT',0.0,22)
      CALL SYMBOL(-0.5,0.5,0.14,'TEMPORAL CROSS-CORRELATION',90.0,26)
      CALL PLOT(-0.78,16.0,-3)
      CALL PLOTE
      GO TO 8000
    4 READ(14,16) (Y1PLOT(J),J=1,NLAG)
      READ(14,16) (Y1PLOT(J),J=1,NLAG)
      READ(14,16) (Y1PLOT(J),J=1,NLAG)
      CALL SCALE (Y1PLOT,MLAG,1,7.00,0.5,Y1MIN,DY)
      CALL PLOTS
      CALL PLOT(0.0,0.0,-3)
      CALL AXIS(0.78,2.0,XX,-4,5.0,0.0,X2MIN,DX2)
      CALL AXIS (0.78,2.0,XX,M,7.0,90.0,Y1MIN,DY)
      CALL PLOT(0.78,2.0,-3)
      CALL LINE(X2PLOT,Y1PLOT,MLAG,1,1)
      CALL SYMBOL(0.5,-0.5,0.14,'FREQUENCY',0.0,9)
      CALL SYMBOL(0.0,-1.0,0.14,'PHASE WITH WAVE HEIGHT',0.0,22)
      CALL SYMBOL(-0.5,0.5,0.14,'COHERENCE VALUE',90.0,15)
      CALL PLOT(-0.78,16.0,-3)
      CALL PLOTE
      READ(14,16) (Y1PLOT(J),J=1,NLAG)
      CALL SCALE (Y1PLOT,MLAG,1,7.00,0.5,Y1MIN,DY)
      CALL PLOTS
      CALL PLOT(0.0,0.0,-3)
      CALL AXIS(0.78,2.0,XX,-4,5.0,0.0,X2MIN,DX2)
```

```
      CALL AXIS (0.78,2.0,XX,M,7.0,90.0,Y1MIN,DY)
      CALL PLOT(0.78,2.0,-3)
      CALL LINE(X2PLOT,Y1PLOT,MLAG,1,1)
      CALL SYMBOL(0.5,-0.5,0.14,'FREQUENCY',0.0,9)
      CALL SYMBOL(0.0,-1.0,0.14,'PHASE WITH WAVE HEIGHT',0.0,22)
      CALL SYMBOL(-0.5,0.5,0.14,'CROSS SPECTRAL PHASE ANGLE',90.0,26)
      CALL PLOT(-0.78,16.0,-3)
      CALL PLOTE
 8000 CONTINUE
      CALL GETIME(IET)
      X=IET*.000026
      WRITE(6,99) X
   99 FORMAT(1H0,'REAL TIME CLOCK READS',2X,E16.6,3X,'SECONDS')
      RETURN
      END
//LINK.SYSIN  DD  *
      ENTRY MAIN
      INSERT MAIN
      OVERLAY ONE
      INSERT AUTO
      OVERLAY ONE
      INSERT CROSS
      OVERLAY ONE
      INSERT SPECTR,HARM
      OVERLAY ONE
      INSERT PLOTER,PLOTS,PLOT,PLOTE,SCALE,AXIS,LINE,SYMBOL
      INSERT EBCDO,PTBITS,EBCDOP,FTCHR,NUMBER,ENCODE,PLTSYM
//GO.FT06F001 DD  SPACE=(CYL,(3,1))
//GO.SYSPLOT DD SYSOUT=B
//GO.FT04F001 DD DISP=(OLD,KEEP),UNIT=2311,DSNAME=RUFSR2.FILE38,
//              VOLUME=SER=SYS005
//GO.FT08F001  DD  UNIT=SYSDA,DSNAME=F2614.CHAN1A,
//  DCB=(RECFM=FB,LRECL=1024,BLKSIZE=2048),DISP=(NEW,PASS),
//  SPACE=(CYL,(4,1))
//GO.FT09F001  DD  UNIT=SYSDA,DSNAME=F2614.CHAN2A,
//  DCB=(RECFM=FB,LRECL=1024,BLKSIZE=2048),DISP=(NEW,PASS),
//  SPACE=(CYL,(4,1))
//GO.FT11F001  DD  UNIT=SYSDA,DSNAME=F2614.CHAN1B,
//  DCB=(RECFM=FB,LRECL=1024,BLKSIZE=2048),DISP=(NEW,PASS),
//  SPACE=(CYL,(4,1))
//GO.FT12F001  DD  UNIT=SYSDA,DSNAME=F2614.CHAN1C,
//  DCB=(RECFM=FB,LRECL=1024,BLKSIZE=2048),DISP=(NEW,PASS),
//  SPACE=(CYL,(4,1))
//GO.FT14F001  DD  UNIT=SYSDA,DSNAME=F2614.CHAN1E,
//  DCB=(RECFM=FB,LRECL=1024,BLKSIZE=2048),DISP=(NEW,PASS),
//  SPACE=(CYL,(4,1))
//GO.FT15F001  DD  UNIT=SYSDA,DSNAME=F2614.CHAN1F,
//  DCB=(RECFM=FB,LRECL=1024,BLKSIZE=2048),DISP=(NEW,PASS),
```

```
//   SPACE=(CYL,(4,1))
//GO.SYSIN  DD  *
```

COMPUTER PROGRAM 4: COMPUTE COHERENCE AND CROSS SPECTRAL PHASE ANGLE

```
C      DATA MUST BE SAMPLED AT EQUAL INTERVALS OF DT
C      IF NFLAG1=0 , AUTOSPECTRA.........IF NFLAG1=1    COSPECTRA
C  NTS= NUMBER OF TIME SAMPLES
C  MLAG = NUMBER OF TIME LAGS
C  DT = TIME INCREMENT
C  DHZ = FREQUECY SPACING
C  DHZ = 1/(2*TM)
C  TM =DT*MLAG
C  FBHZ = LOWEST FREQUENCY (HZ)
C  FBHZ = 1/(2*TM) 1/(2*MLAG*DT)
C  FEHZ = HIGHEST FREQUENCY OF INTEREST (HZ)
C  FEHZ = NIQUEST FREQUENCY = 1/(2*DT)
C  CALX1 = CALIBRATION FACTOR FOR TIME SERIES F1
C  CALX2 = CALIBRATION FACTOR FOR TIME SERIES F2
C  H = WATER DEPTH (METERS)
C  X2 = DEPTH OF WAVE PRESSURE TRANSDUCER BELOW SURFACE
C
       DIMENSION F1(1300),F2(1300)
       DIMENSION PHI(511),TAU(511),AX(2048),A(256),SPHI(256),APHI(256),
      1PHN(256),BX(2048),PHN2(511),PHN1(256),B(256),CSPEC(513),QSPEC(513)
      2,RESPF(513),PER(513),PHASE(513),COHER(513),FREQ(513),CYCL(513),SPE
      3C(513),SPE2(513),GAR(512),DFREQ(512)
       REAL*8 ITITLE(12),ITITEL(12),ITITIL(12),ITITLI(12),ITITLA(12),
      1ITITAL(12),ITITLC(12)
       REAL*4 LABEL/4H  PM/,LABEL2/4H  PM/,LABLE2/4HWVHT/,LABEL3/4HEND
      1 /
       REAL*4 LABEL1/4H XX /,LABEL4/4HWVHT/,LABEL5/5HPHASE/
       REAL*4 LABEL6/4HCCOR/
    96 FORMAT(2I6)
    98 FORMAT(7H NTS = ,I6//,8H MLAG = ,I6//,6H DT = ,F9.5//,6H DHZ= ,F10
      1.8//,' FBHZ = ',F10.8//,' FEHZ = ',F12.8//,' CALX1 = ',F10.8//,
      2' CALX2 = ',F10.8//,' H = ',F10.3//,' X2 = ',F10.3//)
    99 FORMAT(2I6,3F10.8)
   101 FORMAT(4X,10H FREQUENCY,4X,15H AUTO-SPECTRUM1,3X,15H AUTO-SPECTRUM
      12,3X,12H CO-SPECTRUM,2X,14H QUAD-SPECTRUM,3X15H  WAVE PERIOD  ,
      2'   PHASE   ','  COHERENCE',//)
   102 FORMAT(4X,F8.5,7X,E13.7,5X,E13.7,5X,E13.6,5X,E13.6,3X,F10.5,3X,
      1F10.5,3X,F10.5)
   103 FORMAT    (9X,49H SMOOTHED(PARZEN  WINDOW) ENERGY SPECTRAL DENSITY
      1///)
   104 FORMAT(3X,10H (CYC/SEC), 6X,7H  M2/HZ)
   105 FORMAT (10X,24H ENERGY SPECTRAL DENSITY///,5X,10H FREQUENCY,5X,13H
      1     SPECTRUM)
   106 FORMAT (5X,F10.5,6X,E12.6)
   107 FORMAT(5X,F10.6,6X,F10.6,6X,F10.6)
```

```
  108 FORMAT(2F10.8)
  109 FORMAT (I6)
  110 FORMAT(1X,'LAG TIME CROSS CORRELATION FN',//)
  111 FORMAT(5X,F10.6,6X,F10.6)
  112 FORMAT('0',7X,'LAGTIME',8X,'AUTO 1',11X,'AUTO 2',//)
  200 FORMAT(6A8)
  201 FORMAT(I3,2(1X, F3.1),6(1X,I1))
  651 FORMAT (25H       VARIANCE OF SPECTRUM//,3X,16H      VARIANCE = ,F12.
     13,10H   M2       //)
  798 FORMAT('          PHI(0) = ',F12.3//)
  801 FORMAT(4F10.5)
  803 FORMAT(40H UPPER OCEAN TURBULENCE STUDY              ,5X,7H DATE   ,2A
     14,10H   HOUR    ,2A4//,5X,10A4///)
  806 FORMAT('0',18H WAVE RECORD NO. 2//)
  811 FORMAT(1H1)
  900 FORMAT(14F5.2)
  901 FORMAT(14F9.3)
C
C  READING IN TITLE CARDS FOR PLOTS
C   READ ARGUMENTS FOR SCIENTIFIC SUBROUTINE-- DRAW -- SEE WRITE UP FOR
C     DESCRIPTION OF VARIABLES READ IN CORRESPONDING TO THE FOLLOWING...
C     READ(5,200) ITIT--
C     USING FORMAT(6A8)   WHICH REQUIRES TWO CARDS
C      READ(5,201) NPTS,EXSC,YSCL,IXUP,IYRJ,MDXAX,MDYAX,IWIDE,IHIGH,IGRID)
C      USING A FORMAT(I3,2(X1,2F3.1),6(X1,I1))
C
C
C  TITLE FOR PRINT OUT TO DESCRIBE EXPERIMENT- DATE,HOUR,SITE, INSTRUMENT, ETC.
C            (TWO CARDS)
      READ(5,200) (ITITEL(I),I=1,12)
C  TITLE FOR AUTO-COVARIANCE FUNCTION PLOT(TWO CARDS)
      READ(5,200) (ITITLA(I),I=1,12)
C  TITLE FOR ENERGY DENSITY SPECTRA (TWO CARDS)
      READ(5,200) (ITITLE(I),I=1,12)
C  TITLE FOR PHASE SPECTRUM PLOT (TWO CARDS)
      READ(5,200) (ITITIL(I),I=1,12)
C  TITLE FOR COHERENCE SPECTRUM PLOT (TWO CARDS)
      READ(5,200) (ITITLI(I),I=1,12)
C  TITLE FOR CROSS-CORRELATION FN PLOT (TWO CARDS)
      READ(5,200) (ITITLC(I),I=1,12)
C
C  READ IN CONTROL AND DATA CARDS
C
      READ(5,96) NFLAG1,NFLAGP
      READ(5,99) NTS,MLAG,DT,FBHZ,FEHZ
      READ(5,801) CALX1,CALX2,H,X2
      DHZ=1.0/(2.0*DT*MLAG)
      WRITE(6,811)
```

```
      WRITE(6,200) (ITITEL(I),I=1,12)
      WRITE(6,98) NTS,MLAG,DT,DHZ,FBHZ,FEHZ,CALX1,CALX2,H,X2
C BAND WIDTH FREQUENCIES OF TOTAL ENERGY FLUX- CMIN,CMAX
      CMIN = 0.0
      CMAX = 2.5
      PI=3.14159265
      FB = FBHZ*2.0*PI
      FE = FEHZ*2.0*PI
      DF = DHZ *2.0*PI
      FMIN = 2.0*PI*CMIN
      FMAX = 2.0*PI*CMAX
C CALCULATING PERIOD AND FREQUENCY ARRAYS
      NFREQ=(FE-FB)/DF+0.1
      DO 14 N=1,NFREQ
      XN=N
      FREQ(N)=(XN-1.0)*DF+FB
   14 CYCL(N) = FREQ(N)/(2.0*PI)
      PER(1) = 0.0
      DO 15 N = 2,NFREQ
   15 PER(N) = 1.0/CYCL(N)
C
C COMPUTING POWER SPECTRUM FIRST TIME SERIES.
C
C READING IN FIRST TIME SERIES F1 AND DETRENDING
      REWIND 4
      NREAD=5
      DO 3000 IN=1,NREAD
      READ(4,16) (AX(K),K=1,2048)
      J=0
      DO 100 I=1,2048,8
      J=J+1
      A(J)=AX(I)
  100 CONTINUE
      WRITE(8,18) (A(K),K=1,256)
 3000 CONTINUE
      DO 4322 IM=1,3
 4322 READ(4,16) (GAR(K),K=1,512)
      DO 3001 JN=1,NREAD
      READ(4,16) (BX(K),K=1,2048)
      J=0
      DO 308 I=1,2048,8
      J=J+1
  308 B(J)=BX(I)
 3001 WRITE(9,18) (B(L),L=1,256)
      REWIND 8
      REWIND 9
   18 FORMAT(2(128A4))
   16 FORMAT(4(128A4))
```

```
      INT=1
      DO 19 JJ=1,NREAD
      MINT=INT+255
      READ(8,18) (F1(I),I=INT,MINT)
   19 INT=INT+256
      CALL TREND(F1,NTS,DT,CALX1)
      CALL AVER(F1,NTS,DT)
      WRITE(6,901)(F1(I),I=1,NTS)
C CALCULATING AUTO-CORRELATION FUNCTION
   21 DO 10 M=1,MLAG
      SUM=0.0
      NMAX=NTS-M+1
      DO 8 I=1,NMAX
      NN=M+I-1
    8 SUM=SUM+F1(I)*F1(NN)
      XNMAX=NMAX
      XX=M-1
      TAU(M)=XX*DT
      PHI(M)=SUM/XNMAX
      PHN(M) = PHI(M)/PHI(1)
   10 CONTINUE
      ANORM=PHI(1)
C APPLYING LAG WINDOW
      CALL HAMM(MLAG,PHI)
C FOURIER INTEGRAL TRANSFRMING AUTO-CORRELATION FUNCTION
      MLAGM1=MLAG-1
      XMLAG=MLAG
   46 DO 50 N=1,NFREQ
      SUM=0.5*(PHI(1)+PHI(MLAG)*COS(FREQ(N)*TAU(MLAG)))
      C1=COS(FREQ(N)*DT)
      S1=SIN(FREQ(N)*DT)
      CC=1.0
      SC=0.0
      DO 49 M=2,MLAGM1
      CT=CC*C1-SC*S1
      ST=SC*C1+CC*S1
      CC=CT
      SC=ST
   49 SUM=SUM+PHI(M)*CC
   50 SPEC(N)=SUM*2.0/XMLAG
C     SPECTRAL VALUES -- A*A/DHZ*DHZ ( AMPLITUDE SQUARED/HZ)
C ROUTINE TO CALCULATE THE VARIANCE BY SUMMING THE AREA UNDER THE SPECTRUM
      SUM = 0.0
      DO 650 N=1,NFREQ
  650 SUM = SUM + SPEC(N)
      WRITE(6,651) SUM
      WRITE(6,798) PHI(1)
      IF(NFLAG1) 743,743,744
```

```
  744 CONTINUE
C
C COMPUTING POWER SPECTRUM SECOND TIME SERIES.
C
C READ 2ND TIME SERIES F2 AND DETRENDING
      READ(9,18) (F2(I),I=1,NTS)
      WRITE(6,901)(F2(I),I=1,NTS)
      CALL TREND(F2,NTS,DT,CALX2)
      CALL AVER(F2,NTS,DT)
      WRITE(6,806)
C CALCULATING AUTO-CORRELATION FUNCTION
      DO 70 M=1,MLAG
      SUM=0.0
      NMAX=NTS-M+1
      DO 7 I=1,NMAX
      NN=M+I-1
    7 SUM=SUM+F2(I)*F2(NN)
      XNMAX=NMAX
      XX=M-1
      TAU(M)=XX*DT
      PHI(M)=SUM/XNMAX
      PHN1(M) = PHI(M)/PHI(1)
   70 CONTINUE
      BNORM=PHI(1)
      ABNORM=ANORM*BNORM
C APPLYING LAG WINDOW
      CALL PARZ(MLAG,PHI)
C WRITE AND DRAW AUTO-CORRELATION FUNCTIONS
      WRITE(6,112)
      WRITE(6,107)(TAU(M),PHN(M),PHN1(M),M=1,MLAG)
      CALL DRAW(256,TAU,PHN1,1,0,LABEL4,ITITLA,0.0,0.0,0,0,2,0,5,5,0,
     1LAST)
      CALL DRAW(256,TAU,PHN,3-0,LABEL,ITITLA,0.0,0.0,0,0,2,0,5,5,0,
     1LAST)
C FOURIER INTEGRAL TRANSFRMING AUTO-CORRELATION FUNCTION
      DO 71 N=1,NFREQ
      SUM=0.5*(PHI(1)+PHI(MLAG)*COS(FREQ(N)*TAU(MLAG)))
      C1=COS(FREQ(N)*DT)
      S1=SIN(FREQ(N)*DT)
      CC=1.0
      SC=0.0
      DO 79 M=2,MLAGM1
      CT=CC*C1-SC*S1
      ST=SC*C1+CC*S1
      CC=CT
      SC=ST
   79 SUM=SUM+PHI(M)*CC
   71 SPE2(N)=SUM*2.0/XMLAG
```

```
C ROUTINE TO CALCULATE THE VARIANCE BY SUMMING THE AREA UNDER THE SPECTRUM
      SUM=0.0
      DO 660 N=1,NFREQ
  660 SUM=SUM+SPE2(N)
      WRITE(6,651) SUM
      WRITE(6,798) PHI(1)
C
C
C
C COMPUTING CROSS-CORRELATION FUNCTION.
C
   20 MMT=2*MLAG-1
      DO 5 M=1,MMT
      AB=M-MLAG
      MAB=ABS(AB)
      IT=NTS-MAB
      IF(M-MLAG) 1,1,2
    1 IB1=MLAG-M+1
      IB2=1
      GO TO 3
    2 IB1=1
      IB2=M-MLAG+1
    3 SUM=0.0
      DO 4 I=1,IT
      I1=IB1+I-1
      I2=IB2+I-1
    4 SUM=SUM+F1(I1)*F2(I2)
      XIT=IT
      PHI(M)=SUM/XIT
      PHN2(M)=PHI(M)/SQRT(ABNORM)
      TAU(M)=M-MLAG
    5 TAU(M)=TAU(M)*DT
C     PARZEN FILTER APPLIED TO CORRELLATION FUNCTION
      XMLAG = MLAG
      MLAGH = XMLAG/2.0-0.1
      MLAGH1 = MLAGH + 1
      DO 31 M=1,MLAGH
      MM = M-1
      R = MM
      RM = R/XMLAG
      MA = MLAG+ MM
      MB = MLAG - MM
      UM = 1.0-6.0*RM*RM*(1.0-RM)
      PHI(MA) = PHI(MA)*UM
      PHI(MB) = PHI(MB)*UM
   31 CONTINUE
      DO 32 M = MLAGH1,MLAG
      MM = M-1
```

```
      R = MM
      RM = R/XMLAG
      RM1 = (1.0-RM)
      MA = MLAG+ MM
      MB = MLAG - MM
      UM = 2.0*RM1*RM1*RM1
      PHI(MA) = PHI(MA)*UM
      PHI(MB) = PHI(MB)*UM
   32 CONTINUE
C FOURIER INTEGRAL TRANSFORMING THE CROSS-CORRELATION FUNCTION TO OBTAIN
C           THE CROSS SPECTRUM
   28 DO 30 M=1,MLAG
      MM=M-1
      MA=MLAG+MM
      MB=MLAG-MM
      SPHI(M)=PHI(MA)+PHI(MB)
   30 APHI(M)=PHI(MA)-PHI(MB)
      DO 40 N=1,NFREQ
      SUM1=0.5*(SPHI(1)+SPHI(MLAG)*COS(FREQ(N)*TAU(MLAG)))
      SUM2=0.5*(APHI(1)+APHI(MLAG)*SIN(FREQ(N)*TAU(MLAG)))
      C1=COS(FREQ(N)*DT)
      S1=SIN(FREQ(N)*DT)
      CC=1.0
      SC=0.0
      DO 36 M=2,MLAGM1
      CT=CC*C1-SC*S1
      ST=SC*C1+CC*S1
      CC=CT
      SC=ST
      SUM1=SUM1+SPHI(M)*CC
   36 SUM2=SUM2+APHI(M)*SC
      CSPEC(N)=SUM1/XMLAG
   40 QSPEC(N)=SUM2/XMLAG
      WRITE(6,110)
      WRITE(6,111)(TAU(M),PHN2(M),M=1,MLAG)
      WRITE(6,103)
      WRITE(6,101)
      WRITE(6,104)
C CALCULATING THE PHASE SPECTRUM
      DO 17 I = 1,NFREQ
      PHASE(I) = ATAN( QSPEC(I)/ CSPEC(I))*180.0/3.1416
      IF( CSPEC(I).LT.0.0)PHASE(I) = PHASE(I) + 180.0
      IF(PHASE(I).GT.180.0) PHASE(I) = PHASE(I)-360.0
C CALCULATING THE COHERENCE SPECTRUM
      COHER(I)=(QSPEC(I)*QSPEC(I) + CSPEC(I)*CSPEC(I))/
     1(SQRT(SPEC(I)*SPEC(I)*SPE2(I)*SPE2(I)))
   17 CONTINUE
      IF(NFLAGP) 741,741,742
```

```
  742 CONTINUE
  741 CONTINUE
      MFREQ=2*NFREQ
      DO 13 N=1,MFREQ
      XM=N
   13 DFREQ(N)=(XM-1.0)*DF/(2.0*PI)
C
C WRITING AND DRAWING SPECTRA
C
      DO 51 N=1,NFREQ
      SPEC(N)=10.0*ALOG10(SPEC(N))
   51 SPE2(N)=10.0*ALOG10(SPE2(N))
      WRITE(6,102)(CYCL(M),SPEC(M),SPE2(M),CSPEC(M),QSPEC(M),PER(M),
     1PHASE(M),COHER(M),M=1,NFREQ)
C PLOT SPECTRA AS A FUNCTION OF FREQUENCY.
      CALL DRAW(041,CYCL,SPE2,1,0,LABEL2,IOITLE,0.1,0.000,0,0,0,0,5,4,
     *0,LAST)
      CALL DRAW(041,CYCL,SPEC,3,0,LABLE2,ITITLE,0.1,0.000,0,0,0,0,5,4,
     *0,LAST)
C PLOT PHASE ANGLE AS A FUNCTION OF FREQUENCY.
      CALL DRAW(041,CYCL,PHASE,0,0,LABEL,ITITIL,0.1,200.0,1,0,2,0,5,2,
     *0,LAST)
C PLOT COHERENCE AS A FUNCTION OF FREQUENCY.
      CALL DRAW(041,CYCL,COHER,0,0,LABEL,ITITLI,0.1,1.0,0,0,0,0,5,1,0,
     *LAST)
      CALL DRAW(511,DFREQ,PHN2,0,0,LABEL6,ITITLC,0.0,0.0,0,0,0,0,5,5,0,L
     *AST)
   11 CONTINUE
      GO TO 999
C
  743 CONTINUE
      WRITE(6,107)(TAU(M),PHN(M),M=1,MLAG)
      WRITE(6,105)
      WRITE(6,106)(CYCL(M),SPEC(M)        ,M=1,NFREQ)
      CALL DRAW(435,TAU,PHN,0,0,LABEL,ITITLA,0.0,0.0,2,0,2,0,6,8,1,
     1LAST)
      CALL DRAW(100,CYCL,SPEC,0,0,LABEL,ITITLE,0.1,0.0002,0,0,0,0,6,3,
     10,LAST)
  999 STOP
      END


      SUBROUTINE TREND(FX,NTS,DT,CALXX)
      DIMENSION FX(NTS)
C CALIBRATIONG RECORD
C COMPUTING THE LINEAR TREND
      FNTS = NTS
      SUMF = 0.0
```

```
      DO 101 I=1,NTS
  101 SUMF = SUMF + FX(I)
      SUMF1 = 0.0
      DO 102 I=1,NTS
      XI = I
  102 SUMF1 = SUMF1 + XI*FX(I)
      XNM1 = NTS-1
      XNP1 = NTS+1
      XM = (1.0/DT)*(12.0*SUMF1/(FNTS*XNM1*XNP1)-6.0*SUMF/(XNM1*FNTS))
      B = SUMF/FNTS-XM*XNP1*DT/2.0
      FMEAN = SUMF/FNTS
      WRITE(6,9) FMEAN,XM,B
    9 FORMAT (3X,8H MEAN = ,F10.5,3X,9H SLOPE = ,F10.5,3X,13H INTERCEPT
     1= ,F10.5//)
      DO 103 I=1,NTS
      XI = I
  103 FX(I) = FX(I) - (B+XM*XI*DT)
      RETURN
      END


      SUBROUTINE SMD(MD,X1,X2,NFREQ)
      DIMENSION X1(MD),X2(MD)
      DO 1 N=1,MD
      NA=N+MD
      NN=NFREQ-N+1
      NB=NN-MD
      X2(N) = 0.25*(X1(1)+X1(NA))+0.5*X1(N)
    1 X2(NN)=0.5*(X1(NN)+X1(NB))
    3 MB=MD+1
      ME=NN-1
    5 DO 2 N=MB,ME
      NA=N+MD
      NB=N-MD
    2 X2(N)=0.25*(X1(NA)+X1(NB))+0.5*X1(N)
      RETURN
      END


      SUBROUTINE HAMM(MLAG,PHI)
C    HAMM SUBROUTINE HAMMING LAG WINDOWS THE AUTO-CORRELATION FUNCTION
      DIMENSION PHI(MLAG)
      PI = 3.14159265
      XMLAG = MLAG
      DO 31 M=1,MLAG
      R = M
      UM = 0.54 + 0.46*COS(PI*R/XMLAG)
      PHI(M ) = PHI(M )*UM
```

```
   31 CONTINUE
      RETURN
      END

      SUBROUTINE AVER (FX,NTS,DT)
C
C SUBROUTINE FOR CALCULATING TURBULENT INTENSITY, URMS
C
      DIMENSION FX(NTS)
      U2 = 0.0
      SUMU2 = 0.0
      DO 151  I=1,NTS
      U2 = FX(I)*FX(I)
      SUMU2 = SUMU2 + U2
  151 CONTINUE
      FNTS = NTS
      U2 = SUMU2/FNTS
      URMS = SQRT(U2)
      WRITE(6,152) U2,URMS
  152 FORMAT (3X,6H H2 = ,F10.5,3X,8H HRMS = ,F10.5,5H  M  )
COMPUTING AVERAGE PERIOD, T
COUNTS THE TOTAL ZERO UP-CROSSINGS
      USUM = 0.0
      K = 1
   68 N = K
   69 N = N+1
      IF(FX(N)) 73,69,69
   73 K=N
   71 K = K+1
      IF(FX(K))71,71,80
   80 USUM = USUM + 1.0
      IF(NTS-K) 83,83,68
   83 T = FNTS*DT/USUM
      WRITE(6,82) T
   82 FORMAT (3X,18H AVERAGE PERIOD = ,F10.5,4H SEC//)
      RETURN
      END

      SUBROUTINE PARZ(MLAG,PHI)
C     PARZ SUBROUTINE PARZEN FILTERS AUTO-CORRELLATION FUNCTION
      DIMENSION PHI(MLAG)
      XMLAG = MLAG
      MLAGH = XMLAG/2.0-0.1
      MLAGH1 = MLAGH + 1
      DO 31 M=1,MLAGH
      MM = M-1
```

```
      R = MM
      RM = R/XMLAG
      UM = 1.0-6.0*RM*RM*(1.0-RM)
      PHI(M  ) = PHI(M  )*UM
   31 CONTINUE
      DO 32 M = MLAGH1,MLAG
      MM = M-1
      R = MM
      RM = R/XMLAG
      RM1 = (1.0-RM)
      UM = 2.0*RM1*RM1*RM1
      PHI(M  ) = PHI( M  )*UM
   32 CONTINUE
      RETURN
      END
//GO.FT06F001  DD SYSOUT=A,SPACE=(CYL,(6,1))
//GO.FT04F001 DD DISP=(OLD,KEEP),UNIT=2311,DSNAME=RUFSR2.FILE38,
//             VOLUME=SER=SYS005
//GO.FT08F001  DD  UNIT=SYSDA,DSNAME=F2614.CHAN1A,
//  DCB=(RECFM=FB,LRECL=1024,BLKSIZE=2048),DISP=(NEW,PASS),
//  SPACE=(CYL,(4,1))
//GO.FT09F001  DD  UNIT=SYSDA,DSNAME=F2614.CHAN2A,
//  DCB=(RECFM=FB,LRECL=1024,BLKSIZE=2048),DISP=(NEW,PASS),
//  SPACE=(CYL,(4,1))
//GO.SYSIN DD *
```

BIBLIOGRAPHY

1. Wilson, Wayne D., "Extrapolation of the Equation for the Speed of Sound in Sea Water," Journal of the Acoustical Society of America, v. 34, No. 6, p. 866, June 1962.

2. Leroy, C.C., "Development of Simple Equations for Accurate and More Realistic Calculation of the Speed of Sound in Seawater," Journal of the Acoustical Society of America, v. 46, No. 1, p. 216-226, June 1968.

3. Rautmann, Jurgen, Sound Dispersion and Phase Fluctuations in the Upper Ocean, Thesis, Naval Postgraduate School, Monterey, 1971.

4. Meyer, E. Skudrzyk, Sound Absorption and Sound Absorbers in Water, NAV SHIPS 900.164, v. 1, 1 December 1950.

5. Chernov, Lev A., Wave Propagation in a Random Medium, Dover Publications, Inc., 1967.

6. Enochson, L.D., and Otnes, R.K., Programming and Analysis for Digital Time Series Data, The Shock and Vibration Center, United States Department of Defense, 1968.

7. Bendat, J.S., and Pierson, A.G., Measurement and Analysis of Random Data, John Wiley and Sons, Inc., 1958.

8. Albers, V.M., Underwater Acoustics Handbook, The Pennsylvania State University Press, 1960.

9. Deven, C., Jr., Survey of Thermal, Radiation, and Viscous Damping of Pulsating Air Bubbles in Water, Journal of the Acoustical Society of America, v. 31, December 1959, p. 1654-1667.

10. Glotov, V.P., Kolobaeu, P.A., and Nenimin, G.G., Investigation of the Scattering of Sound by Bubbles Generated by an Artificial Wind in Sea Water and the Statistical Distribution of Bubble Sizes, Soviet Physics-Acoustics, v. 7, Apr. Jun 1962, p. 341-345.

11. Buxcey, S., McNeil, J.E., Marks, R.H., Jr., Acoustic Detection of Microbubbles and Particulate Matter Near the Sea Surface, Thesis, Naval Postgraduate School, Monterey, Calif., 1965.

INITIAL DISTRIBUTION LIST

		No. Copies
1.	Defense Documentation Center Cameron Station Alexandria, Virginia 22314	2
2.	Library, Code 0212 Naval Postgraduate School Monterey, California 93940	2
3.	Commander, Naval Ship Systems Command Attn: Mr. Woodie L. Thompson Department of the Navy, Code PMS 302 Washington, D.C. 20360	1
4.	Commander, Naval Ship Systems Command Attn: Mr. Alfred P. Franceschetti Department of the Navy, Code PMS 302-4 Washington, D.C. 20360	2
5.	Dean of Research Administration Naval Postgraduate School Monterey, California 93940	1
6.	Professor H. Medwin, Code 61Md Department of Physics & Chemistry Naval Postgraduate School Monterey, California 93940	10
7.	Assoc. Professor W.W. Denner, Code 58Dw Department of Oceanography Naval Postgraduate School Monterey, California 93940	1
8.	Asst. Professor E.B. Thornton, Code 58Tm Department of Oceanography Naval Postgraduate School Monterey, California 93940	1
9.	Assoc. Professor N.E. Boston, Code 58Bb Department of Oceanography Naval Postgraduate School Monterey, California 93940	1
10.	Asst. Professor G. Garrettson, Code 61Gr Department of Physics & Chemistry Naval Postgraduate School Monterey, California 93940	1

11. LCDR James R. Fitzgerald 1
Box 1667
Naval Postgraduate School
Monterey, California 93940

12. Professor Peter C.C. Wang, Code 52Wf 1
Department of Mathematics
Naval Postgraduate School
Monterey, California 93940

13. Mr. William Smith 1
Department of Physics & Chemistry
Naval Postgraduate School
Monterey, California 93940

14. Director Acoustic Programs (Code 468) 1
Office of Naval Research
Department of the Navy
Arlington, Virginia 22217

Unclassified
Security Classification

DOCUMENT CONTROL DATA - R & D

(Security classification of title, body of abstract and indexing annotation must be entered when the overall report is classified)

1. ORIGINATING ACTIVITY *(Corporate author)* Naval Postgraduate School Monterey, California 93940	2a. REPORT SECURITY CLASSIFICATION Unclassified 2b. GROUP

3. REPORT TITLE

Statistical Study of Sound Speed in the Inhomogeneous Upper Ocean

4. DESCRIPTIVE NOTES *(Type of report and inclusive dates)*

Master's Thesis; December 1972

5. AUTHOR(S) *(First name, middle initial, last name)*

James R. Fitzgerald

6. REPORT DATE	7a. TOTAL NO. OF PAGES	7b. NO. OF REFS
December 1972	130	11

8a. CONTRACT OR GRANT NO.	9a. ORIGINATOR'S REPORT NUMBER(S)
b. PROJECT NO.	
c.	9b. OTHER REPORT NO(S) *(Any other numbers that may be assigned this report)*
d.	

10. DISTRIBUTION STATEMENT

Approved for public release; distribution unlimited.

11. SUPPLEMENTARY NOTES	12. SPONSORING MILITARY ACTIVITY
	Naval Postgraduate School Monterey, California 93940

13. ABSTRACT

The statistics of the fluctuations of the in-situ speed of sound in the upper ocean have been studied by analyzing the instantaneous phase difference of the output of two hydrophones separated by one meter for sounds of frequency 15 to 151 kHz. The experiment was conducted at 11 ft in water of depth 60 ft in low sea states at night. Comparison of the speed calculated from the time averaged phase difference, with the speed given by velocimeter or empirical relations, yielded differential speeds which deviate by 1 m/sec to 8 m/sec from the accepted values, for frequencies less than 100 kHz. Correlation and spectral analysis of the sound phase and ocean height fluctuations has shown the close relation between these two parameters. There is strong evidence of the presence and importance of bubbles in all of the results, particularly of a large population resonant in the frequency range 56.3 to 71.1 kHz (radius 50 to 60 microns). Evidence is presented to suggest that bubbles appear at the surface during internal wave activity at lower depths and that for sound frequencies near the bubble resonances the sound phase is strongly modulated by, and in phase with, the ocean wave height.

DD FORM 1 NOV 65 1473 (PAGE 1)
S/N 0101-807-6811

Unclassified
Security Classification

A-31408

14. KEY WORDS	LINK A		LINK B		LINK C	
	ROLE	WT	ROLE	WT	ROLE	WT
Speed of sound						
Dispersion						
Phase fluctuations						
Bubbles						
Upper ocean						